eman ta zabal zazu
Universidad del País Vasco
Euskal Herriko Unibertsitatea
The University of the Basque Country

Doctoral Thesis

DLK 1 AND DLK2 CHARACTERIZATION IN MOUSE SALIVARY GLAND DEVELOPMENT

CELL BIOLOGY AND HISTOLOGY DEPARTMENT
ZELULEN BIOLOGIA ETA HISTOLOGIA SAILA

Patricia Garcia Gallastegui

Leioa, 2015

ACKNOWLEDGEMENTS

The present work has been done thanks to the financial support of the research projects given by the Basque Government (Consolidated groups) GIC12/168, by the unit of formation and Research (UFI11/44) and for the Foundation Jesus Gangoiti Barrera. The author of this thesis, Patricia Garcia Gallastegui, has been founded with a grant from the University of the Basque Country, Department of Basque and Multilingualism, grant awarded in 2011.

Después de cinco años parecía que nunca llegaría este momento. Ya ha llegado la hora de defender el trabajo que hemos ido haciendo, el grupo, el departamento, la familia, la cuadrilla… porque sin vosotros este trabajo y el camino andado para llevarlo a cabo no habría sido el mismo.

Firstly, I would like to thank Fernando Unda for giving me the opportunity to join his group and for his guidance and supervision in my project during these years. Thank you for sending me to Matt´s lab, it was an incredible experience. Thank you Matt for your kindness and for accepting me in your lab.

Ostean Gaskon Ibarretxeri eskerrak eman nahiko nioke, bere aholkuak eta animoak emateagatik. Bereziki 2011an euskarako bekaren deialdia agertu zenean nirekin eskatu nahi izanagatik. Eskerrik asko.

Recuerdo los primeros días de laboratorio, como alumna interna sin acabar la carrera, cuando me presente en la puerta del despacho de Fernando, con Maitane y Noemi Jimenez, “esta es la chica nueva” ☺. Gracias Noe y Lucia por haber hecho de conexión aquel día.

Labora egunero joatea ere erraza izan da, tokatu zaidan kide bikainen konpainia dela eta. Barreak, planak, eta zientziako elkarrizketak ere gogoan eramango ditut. Eskerrik asko Fundaei: igor, lutxu, vero, jonlo, olatz eta ikerri. Gracias también a los técnicos en prácticas que han pasado por el de labo: Aroa, Borja, y Erika, veníais a aprender pero también habéis aportado un granito en este trabajo. Gracias a Maitane mi amatxu cientifica, por tus consejos y por los buenos momentos que hemos pasado en los congresos . El tiempo vuela!

También quisiera agradecer al resto de compañeros del Bio Cell, “las Vecinas”: Xandra, Noelia, David, Jairo, Agur“Las Lolas”: Ane, Erika, Roció, Maitane, Arantza, Cris “Los Arechagas” Amaia, Elí, María, Pablo, Miguel, “Las Hilarias” Miren y Olatz. Y algunos más Raquel, Aitor, Fede. Gracias por los cafes en el “refu”, almuerzos, barbacoas, casas rurales, fiestas varias. Espero que mantengamos el contacto sea donde sea que acabemos.

Gracias a los chic@s de microscopía, Alex, Jon, Ricardo e Irene. Gracias a la secretaria del departamento Mari Jose, Asun, Txus, Cristina.

Gracias también a los colaboradores de Albacete, Victor, Pepeja, LaBorda, Maria Luisa, Ana Isabel, sin vosotras colaboración este proyecto de tesis no se habría realizado.

Alor zientifikoa alde batera utzita, nire koadrilako neskei eskertu nahi nieke, eskerrik asko Lideri txi-txikitatik elkarrekin bizi dugunagatik, Iratxeri beti ondoan egoteagatik, eskerrik asko Amaiari, Mailori eta Begori. Beti deskonektatzeko konpainia ezinhobea izateagatik.

Por supuesto sin olvidar eskerik asko a mi familia, Bego, Joseba, Gaizka, Rakel, Neka, Maidertxu, Gaizkatxu, Berezi, Uxu... En especial eskerrik asko a Aita y Ama por haberme animado siempre a sacar el máximo de mí, a pesar de los altibajos. Porque querer es poder y con trabajo todo se consigue!!! A mi Sis, Iru, que aunque en esta última etapa nire alboan ez egon, gertu zentitzen zaitut.

Eta bukatzeko eskerrik asko “romanoei” Pili, Jon, Irantzu eta Txaberri hor egoteagatik. Eta nola ez Etxan, nire abenturen bikotea, eskerrik asko nire laguna izateagatik, eskerrik asko bebe-benetan zertan lan egiten dudan ez ulertu arren beti pazientzia eukitzeagatik.

Bihotz bihotzez, Eskerrik Asko danoi !!!!!

CONTRACTIONS/ABBREVATIONS

ADN: Desoxirribonucleico acid

Agp5: Acupurin 5

AKT: kinase B protein

Alpha SMA: Smooth muscle actin

AMPK: Protein kinasa activated with AMP

ANK: Ankirina

BCA: bicinconinic acid

***B*-CATENIN:**

BHLH: Basic helix loop helix TF

BSA: Bovine serum albumin

CADASIL: Autosomal Dominant arteriopathy with subcortical infarts and leucoencelophaty

CBF1: C Promoter Binding Factor 1 (RBP-JK, LOG 1 =CSL)

CCH: Carbachol

CDNA: Complementary desoxirribonucleic acid

CK 5: Cytokeratin 5

CK 14: Cytokeratin 14

CSL: Proteína de unión al promotor C

DAPI: Nuclear marker

DAPT:N-[N-(3,5-Difluorophenacetyl)-Lalanyl]-S-phenylglycine t-butyl ester

DEPC: diethyl dicarbonate

DLL1, 4: Delta like ligands

DLK: Delta like homolog

DLK1: Delta like 1 (pg2, pref 1, FA1, SCP-1, and zog)

DMEM F12: Dulbecco´s Modified Eagle´s medium F12

CM: Cell membrane

DMSO: Dimetil sulfóxido

DOS: "Delta and OSM-11 like protein" domain

CRD: Cystein rich domain

DSL: Dominio Delta/Serrate/Lag-2

ECM: Extracelular metrix components

EDA: Ectodisplasin

EDAR: Ectodisplasin receptor

EDTA: *Ethylenediaminetetraacetic acid*

EGF: Epidermic growth factor

EGFR: Epidermic growth factor receptor

ERK: extracellular-signal-regulated kinase

ES: Embrionic stem cells

FBS: Fetal bovine serum

FGF: Fibroblast growth factor

GAPDH: Glyceraldehyde 3-phosphate deshidrogenase

GCT: Granular convoluted tubules

GH: Growth hormone

GLI: Transcription factor

hBMSC: Human bone stem cells

HEY: Hairy y Enhancer of Split related with YRPW motif

HES: *Hairy y Enhancer of Split*

HH: Sonic ligand

HS: Heparin sulfate

HSG: Human salivary gland cell line

H&E: Hematoxylin and Eosin

H3P: Histone 3 phosphate mitosis marker

IGF: Insulin like growth factor

IGF-1: Insulin like growth factor

IGFBP1: IGF binding protein

IL: Interleukines

JAGGED 1: Serrate homclys

Ki67: Cell cycle marker

KLF: "Krüppel- like" transcription factor

KO: Knock-out, (-/-)

LNR: LIN/NOTCH repeats

MAPK: Mitogen activated protein kinases

MMPs: Metalloproteinases

mRNA: messenger ribonucleic acid

mTOR: Mammalian Target of Rapamycin

MSC: Mesencimel stemm cells

NaCl: Sodium chloride

NLS: Nuclear localization signal

NFκ β: nuclear transcription factor kappa beta

NICD: NOTCH intracellular domain

NLS: Nuclear localization signal

NOTCH: Receptor signaling

NRR: Negative regulary region

PBS: Phosphate buffer saline

PCR: Polimerase chain reaction

PEST: Proline, glutamine, serine, treonine rich domain

PI3K: Phosphatidylinositol 4,5-bisphosphate 3-kinase

PIP2: Phosphatidylinositol 4,5-bisphosphate

PLC-γ: Phospholipase C-γ

PKC: Protein kinase 3

pGLUCWT: Empy vector

PIP3: Phosphatidylinositol 3,4,5-Triphosphate

pLNCX2: Empy vector

PTC: Patched

PTEN: Proteína homóloga a fosfatasa

pRLTK: Renine expression plasmid

PSG: Parasympathetic ganglia

PG: Parotid salivary gland

RLU: Relative luciferase unit

RAS: Family of GTPases

SDS: Sodium Dodecil sulfate

sDLK1: Soluble recombinant DLK1

Shh: Sonic Hedgehog

SH3: Protein binay comen

SiRNA: Small interfering RNA

SLG: Sublingual salivary gland

SMG: Submandibular salivary gland

SMO: Smoothened

SRC: Family of tyrosine kinases

STAT3: Signal transducer and activator of transcription 3

TAD: Transcription activación domain

TAE: Tris, Acetic, EDTA

TBS: Tris buffer saline

TNF: Tumor necrosis factor

TACE: Tumor Necrosis Factor Alpha Converting Enzyme

TRIS HCl: Tris chloride

VEGF: Factor de crecimiento vascular endotelial

WT: Wild-type (+/+)

ABSTRACT

The organogenesis is a complex process orchestrated by different signaling pathways. The development of different organs is often regulated by the same signaling factors. The study of signaling pathways is not only to understand how organs develop, but also as a clue to investigate cancer and tissue regeneration, since these factors ale also implicated in these processes.

In this work, we studied the salivary gland development. The salivary gland organogenesis occurs by a process called branching morphogenesis. This process also occurs in other organs such as mammary gland, lung and kidney.

One of the most studied signaling pathways in organogenesis of developing tissues is NOTCH, where the non-canonical ligands DLK1 and DLK2 have been recently described.

The main goal of our work was to elucidate the function of DLK1 and DLK2 in terms of NOTCH signaling and their role in the submandibular salivary gland (SMG) development. For this purpose, we used an *in vitro* organotypic culture of SMG rudiments with sDLK1 or DAPT (inhibitor reagent of γ-secretase). For our study, we also performed experiments with null-*Dlk1* mice.

Our results demonstrate that these ligands are highly expressed in the development of the mouse SMG and function as NOTCH signaling inhibitors. In adult mice, DLK1-2 expression decrease, what make us think the possible role of DLK1-2 in the morphogenesis of the SMG.

In SMG cultures, the inhibition of NOTCH signaling pathway, by either sDLK1 or DAPT, reduced SMG branching morphogenesis, impaired innervation and produced apoptosis in the inner epithelial progenitor cells of the developing end buds. As inhibitors of NOTCH disrupted SMG innervation, we employed a cholinergic activation reagent, carbachol (CCh), to rescue the development of the SMG. We found that CCh managed to partially recover the branching of the SMG, but only when the inhibitory effect ceased. In this context, we realized that the impaired SMG branching morphogenesis by NOTCH signaling inhibition was not only a consequence of the reduced innervation, but a DLK1 or DAPT direct effect on the SMG epithelia morphogenesis.

From the analysis of the *Dlk1* (-/-) mice, we concluded that DLK1 absence results in a reduced salivary gland size. As a consequence these mice produced less saliva in time after pilocarpine stimulation. DLK1-KO mice SMG histology and transmission electron microscopy showed a healthy and normal SMG, although the number of epithelial stem/progenitor cells amount increased.

In overall, this work describes the importance and mechanisms of function of NOTCH non-canonical ligands DLK1 and DLK2 in the development of the salivary gland. In conclusion, we propose that the levels of DLK1 in the normal development of the salivary gland need a fine balance between the control mechanisms of inhibiting and promoting stem cells.

INDEX

1. INTRODUCTION

1.1 SALIVARY GLANDS

Salivary glands are organs, associated with the oral cavity, which produce saliva, an essential fluid for normal speech, taste, mastication, swallowing and digestion. Saliva apart from providing lubrication, contributes to the immunity and oral homeostasis and oral tissue repair, because of the growth factors and biological peptides present in the saliva in small quantities.

The salivary system of mice and humans contains three major salivary glands: the submandibular salivary gland (SMG), which produces the majority of secretion of saliva, the sublingual salivary gland (SLG), and the parotids (PG), all of them communicated with the oral cavity through independent excretory ducts (Fig 2.A). In addition, there are numerous (600-1000) minor salivary glands located throughout the oral mucosa and tongue and have short branching tubules (Tucker, 2007).

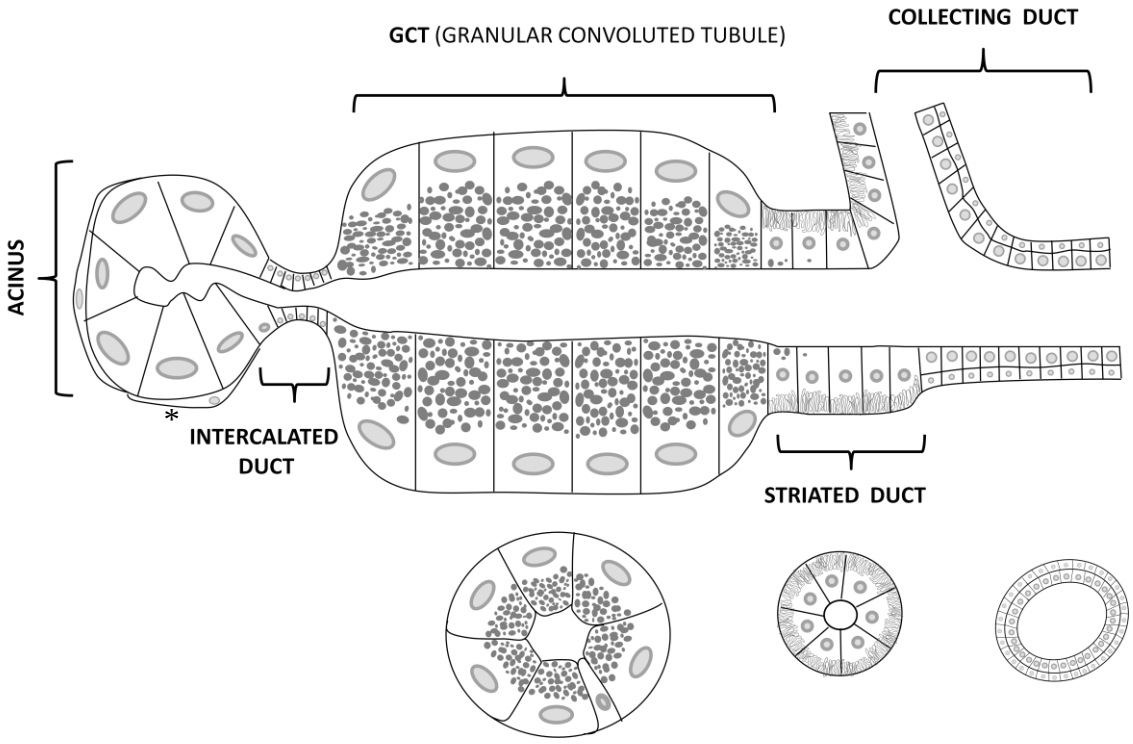

Figure 1. Schematic representation of mice SMG. The main structures are the serous or mucous acinus with their mioepithelial* cells, followed by the intercalated ducts. Then the big granular convoluted ducts with their characteristics vesicles, followed by the striated ducts with their mitochondria in the basal striations of the cells, and finally opening the diameter of the duct the collecting ducts with psedoestratificated epithelia (Adapted from www.pathologyoutlines.com).

The structure of the salivary glands is composed by acini and tubules (Fig 1). The acinus is either serous or mucous, called by the consistency of their secretions, which are watery or viscous, respectively. Mucous cells secrete mucins, which are large glycoproteins with carbohydrate chains. In general, the mucins are negatively charged which contributes to the viscosity of the saliva. Serous acinar cells secrete a large number of proteins, such as amylase, but lack mucins. In addition some acini are termed seromucous, and produce both mucins and serous proteins. The saliva is secreted in each acinous whose composition is modified across it travels through the tubules.

The acini drain into intercalated ducts that later lead to the striated ducts. In rodents the SMGs had the intercalated and striated ducts separated by the granular convoluted ducts (GCT) that display sexual dimorphism being more abundant in males (Osamu Amano *et al*., 2012). In the mouse the SLG (Fig 2.B) is mostly mucous what made it dye weaker with the hematoxylin. In contrast SMG (Fig 2.C) is a mixed gland with both serous and mucous cells. The PSG (Fig 2.D) is mainly serous that is why the Hematoxylin-Eosin (H/E) is highly basophile.

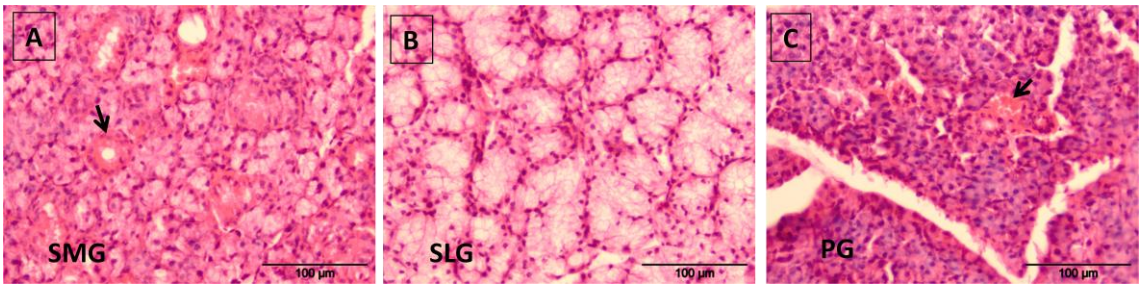

Figure 2. Salivary gland histology. (B) H/E of the adult SMG with the characteristic mixed acini (arrow = GCT). (B) H/E of the SLG, acini are mucous. (C) H/E of the serous PG (arrow=striated duct).

The stellate mioepithelial cells surround the acini and intercalated ducts, the contraction of these cells directs saliva out of the acini into the ducts and results from stimulation by the parasympathetic and sympathetic nervous system. In the mouse, the activity of the three glands differs between males and females. Aminotransferase activity for example, is comparable in males and females for the parotid and sublingual glands, but the male submandibular gland has around 10 fold more activity than the female (Hosoi *et al*., 1978). The morphological similarities of these glands, therefore, show very real differences in how they operate in the adult.

1.2 SALIVARY GLAND DEVELOPMENT

The three pairs of major salivary glands arise from the oral epithelium, while it is known to be between the oral ectoderm with the foregut endoderm, a point that separates the stomodeum from the cavity of the primordial pharynx (Dudek *et al.,* 1998), the exact position where is initiate is unknown.

First, it was suggested that the parotid glands were ectodermal, whereas the SMG and SLG were endodermal (Avery, 2002). The endodermal origin was supported by data showing that adult salivary gland progenitors can differentiate into pancreatic cells and hepatocytes when transplanted into hepatectomized liver (Hisatomi *et al*., 2004). However, while it is clear that salivary gland progenitors can differentiate into these cell types in the appropriate extracellular microenvironment it is not proof that *in vivo* the salivary epithelium is derived from the endoderm.

The employment of genetic lineage tracing using lineage-specific Cre drivers has helped toclarify the lineage of some cell types within the glands. The mesenchyme and nerves in the gland are neural crest in origin as shown by lineage tracing with Wnt1-cre (Jaskoll, *et al*., 2002). Recent genetic lineage tracing experiments using the Sox17-2A-iCre/R26R mouse, which marks endodermal cells, showed that the epithelia of all three major salivary glands are not of endoderm origin, suggesting an ectodermal lineage (Jaskoll *et al.*, 2003).

Besides, animal models and human mutations that cause ectodermal dysplasia, developmental syndromes that specifically affect ectodermal organs, point to the idea that the major salivary glands arise from common multipotent precursors residing in the embryonic ectoderm. All this data are not concluding and the ectodermal origin of the epithelium need to be confirmed (Patel and Hoffman, 2014).

The submandibular is the first major salivary gland to develop in the embryo, followed by the neighboring sublingual and then the parotid. Mammalian salivary glands are generated during embryonic development by the process of branching morphogenesis, which plays a critical role in the development of many other related organs, including the lung, kidney, and mammary gland (Tucker, 2007).

Salivary gland initiation and formation occur by a coordinated cell proliferation and clefting. While spherical epithelial structures, called end buds, which invade the surrounding mesenchyme branches and increases the size, in parallel cell migration, apoptosis and interactions between epithelial mesenchymal neuronal and endothelial cells take place.

Development of the mouse SMG (Fig 3), is first visible as a thickening of the epithelium next to the tongue around stage E11.5 (embryonic day 11.5, prebud stage). The epithelium invaginates and forms an epithelial salivary bud, linked to the oral surface by the primitive main duct at E12.5. At E13.5 the epithelium forms some branches with approximately 3-5 buds (pseudoglandular stage), these correspond to major lobules of the gland.

At E15.5, the majority of the ducts, which initially contained a solid core of epithelial cells, develop lumen spaces by polarization of the cells located at their center (canalicular stage).

At E17.5, the branches form the excretory ducts and the terminal buds develop the secretory acini (terminal bud stage). Development of the rodent salivary gland continues after birth and the final differentiation of acini and granular tubules concludes at the sexual maturation stage (Gresik, 1994; Tucker, 2007).

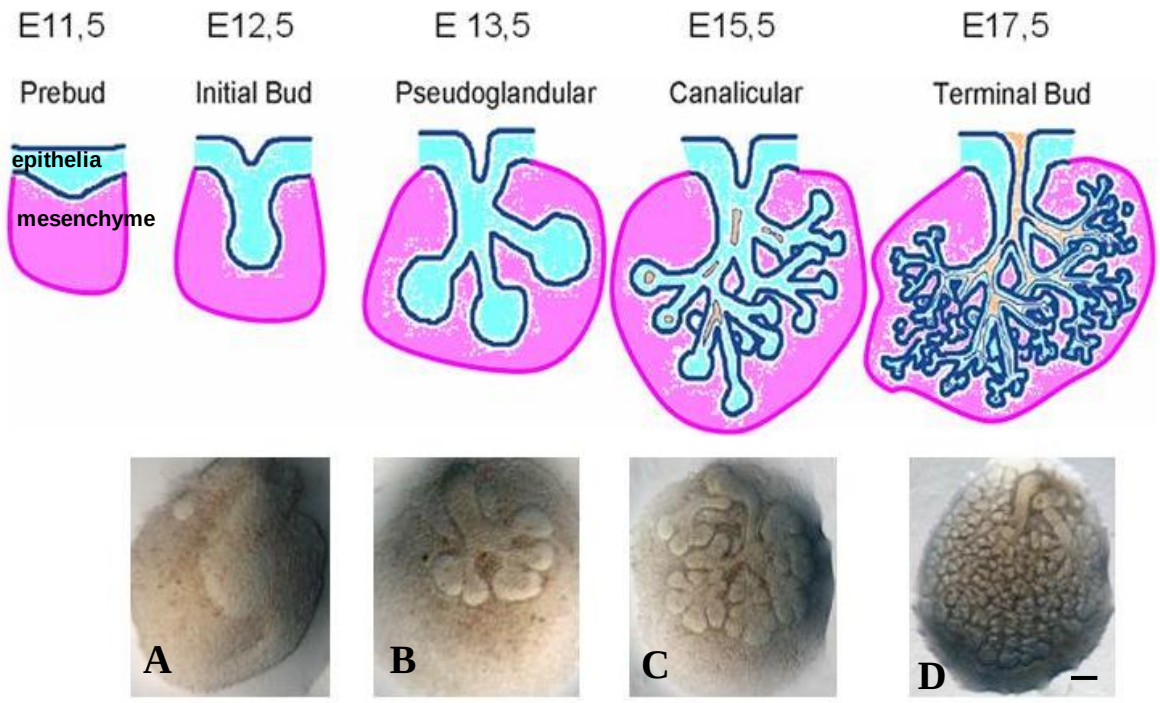

Figure 3. SMG developmental stages. Salivary gland morphogenesis implies complex epithelial-mesenchymal interactions. Initially the epithelia invaginates to the mesenchyme and form the initial bud (A), then this bud starts to branch in the pseudoglandular stage increasing rapidly the number of end buds (B), meanwhile the epithelial cells start to polarize and reorganize to form a lumen called the canalicular stage (C), and finally in the terminal stage the epithelial cells are differentiated and the ducts are formed (D). The salivary gland acquires the final differentiation after birth at the sexual maturation stage. Scale bar: 150 µm.

1.3 SIGNALING PATHWAYS OF THE SMG ORGANOGENESIS

Salivary glands are currently the focus of intense research on tissue engineering (Ogawa *et al*. 2013; Liu & Wang, 2014). Considering the similarities between morphogenesis and regeneration in many other organs, the potentials of using molecular cues in salivary gland development to promote salivary regeneration are worth careful exploration. To begin to understand the complex interactions within this dynamic signaling network, firstly we must determine the contribution of individual pathways and identify those which are important and necessary for SMG development. Techniques like knock-out, transgenic and mutant mice, siRNA transfection or function blocking antibodies have provided insights into which signaling pathways present in the developing SMG play essential morphogenetic roles.

One of the most studied and essential pathway for SMG development is the **fibroblast growth factor** (FGF) signaling. The FGF family includes at least 23 members which have been shown to have diverse biological functions, including cell proliferation, epithelial branching and histodifferentiation (Szebenyi *et al*., 1999). Ligand binding to the appropriate receptor results in receptor dimerization, activation of intrinsic tyrosine kinase activity and autophosphorilation which activates several intracellular cascades. Among others, Ras pathway, Src family of tyrosine kinases, PI3K/AKT, the PLC-γ/PKC and the STAT3 pathway. FGF signaling has variable pleiotropic effects according to a cells need. In terms of its implication on SMG morphogenesis Fgfr2-IIIB-/-, Fgf10-/- and Fgf8 conditional mutant mice presented SMG aplasia showing up the importance of this pathway (Jaskoll and Melnick, 1999).

Another important pathway in SMG development is **Sonic Hedgehog** (Shh). This protein belongs to family of signaling molecules that induces cell survival, proliferation, differentiation and pattern formation in various embryonic tissues (McMahon, 2003). The cellular response to Hh (ligand) is controlled by two transmembrane proteins Patched (Ptc) and Smoothened (Smo), a positive and a negative regulator of Hh, respectively. Hh binding to Ptc relieves the inhibition of Smo, a G protein, which initiate a signaling cascade that results in the activation of target genes via Gli family of transcription factors. Ptc and Smo are localized in the epithelia which suggested that Shh may act within the epithelium in a juxtacrine manner to promote proliferation and differentiation of epithelial cells. In fact branching morphogenesis of the SMG is promoted by Hh activation *ex vivo*, and is impaired by Hh inhibition *in vivo* and *ex vivo* (Jaskoll *et al*., 2004b). Additionally, Shh -/- mice shows SMG developmental delay.

Ectodisplasin (Eda) and its receptor (Edar) are members of the TNF superfamily, which is important for balancing mitogenesis and apoptosis during embryonic development. Eda signaling is downstream of Wnt signaling and upstream of Hh in salivary gland development (Haara *et al*., 2011). Eda signaling is critical for branching morphogenesis. Eda mutations in mouse and human are associated with absence or hypoplasty of ectodermic derivates, all exocrine glands including salivary glands (Jaskoll *et al*., 2003).

Apart from these signaling pathways, the **extracellular matrix components** (ECM) play an important role in SMG branching morphogenesis. For instance, laminin-111 (Fig 4.B) and its receptor integrin α6β1 are required for mouse SMG morphogenesis *ex vivo* (Kadoya *et al*., 1998). Mutation in integrin α3 leads to defects in the apical basal polarity, and its lost resulted in a similar phenotype to that of laminin α knockout. Cell mobility within the epithelia end buds and cell matrix interactions contribute to different processes during branching morphogenesis. Moreover, remodeling of the ECM and cell surface by metalloproteinases (MMPs) generates bioactive cleavage products and releases growth factors stored in the basement membrane (Catalan *et al*., 2009). However, most of the single MMP null mice have slight phenotypes due to compensations or overlapping functions.

Salivary glands are richly innervated by both **sympathetic and parasympathetic nerves**. The parasympathetic (Fig 4.A) nerves release acetylcholine, which activates the muscarinic receptors to stimulate fluid secretion, sympathetic nerves control salivation through the activation of α and β adrenoreceptors (stimulate fluid rich and protein rich secretion, respectively). Recent research has focused on the role that plays the innervation on the SMG development, since parasympathetic ganglia (PSG) removal reduces the expression of epithelial progenitor markers such us cytokeratin 5 (CK5). In addition, the CK5 positive cells in the epithelium decrease (Knox SM *et al*., 2010). Moreover, parasympathetic innervation has also been described to regulate tubulogenesis and lumen formation during salivary gland development (Nedvetsky *et al*., 2014).

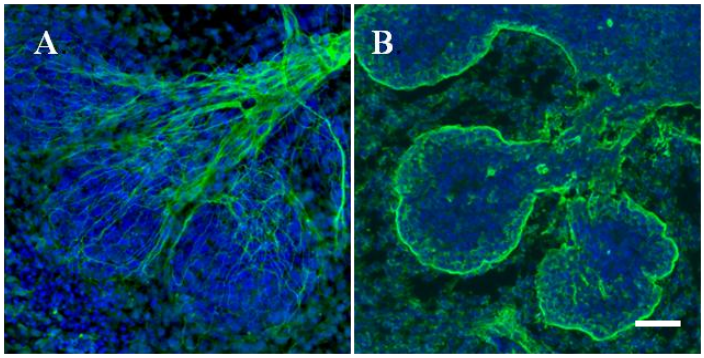

Figure 4. Parasympathetic innervation and ECM laminin. Reciprocal interaction between epithelium (nuclei in blue) and (A) β-III tubulin (green) of stained PSG axons and (B) Laminin (green) an ECM component that regulate branching morphogenesis during SMG development. Scale bar: 50 µm.

1.4 NOTCH SIGNALING PATHWAY

1.4.1. NOTCH RECEPTORS

The NOTCH gene was initially sequenced in the 1980s. However, it was named for the first time in 1919 due to the phenotype of a mutant *Drosophila* with an indentation (*notched*) in the wings (Mohr O, 1919). NOTCH homologues have since then been identified in numerous other organisms including mammals (Fleming *et al*., 1998). NOTCH orthologs are very well conserved from the nematode to humans. Interistingly, *Drosophila* NOTCH mutants (Hartenstein *et al*., 1992; Lammel and Saumweber, 2000) did not form salivary glands (Fleming *et al*., 1997; Hukriede *et al*., 1997).

Mammalian NOTCH receptor family consists of four members from NOTCH1 to NOTCH4. Notch receptors are single-pass transmembrane proteins that form a heterodimer comprised of two noncovalently bound subunits. NOTCH proteins are initially synthesized as full-length unprocessed proteins, following transport through the secretory pathway to the trans-Golgi network. NOTCH is cleaved at a site referred to as the S1 cleavage site to generate two NOTCH subunits, one monomer with the extracellular domain and the other with a short fragment of the domain and the complete transmembrane, and intracellular domains (Fiuza and Arias, 2007; Hansson *et al*., 2004).

The NOTCH receptors encode approximately 300kD single-pass transmembrane proteins (Fig 5). The extracellular region of the NOTCH receptor has a variable number of EGF-like repeats, epidermal growth factor (EGF-like: 36 repetitions in NOTCH1 and 2, 34 repeats NOTCH3, and 29 in NOTCH4) and three replicates LIN/NOTCH (LNR), which are essential for ligand binding and subsequent activation (Fig 5, yellow). Below, there is a hydrophobic region, which mediates heterodimerization. Together, the LNR and the hydrophobic region form the negative regulatory region (NRR) located adjacent to the cell membrane. This region prevents the ligand independent activation of NOTCH receptors (Sanchez-Irizarry *et al*., 2004).

The intracellular region of NOTCH receptors (NICD Notch Intracellular Domain) includes seven replicates of ankyrin (ANK domain), a RAM domain, two nuclear localization sequences (NLS) flanking the ANK domain and a domain rich in proline-glutamate-serine-threonine (PEST). The ankyrin repetitions are the most conserved regions and are essential for signal transduction. The RAM domain contains the primary binding site for the repressor CBF1 (C Promoter Factor Binding 1)/RBP-JK/Suppressor of Hairless/Lag-1, a transcription cofactor (Chillakuri *et al*., 2012) (Fig 5).

NOTCH proteins do not have enzymatic activity, but generate signals via direct molecular interactions. The region that extends from the C-terminal until the ankyrin regions has been related to various protein interactions and transactivations of transcription factors. The C-terminal domain PEST is involved in the degradation of NICD by proteolysis. Mutations that cause deletions in this region are associated with T cell leukemia, which emphasize the importance of degradation the NICD and its regulation (Chillakuri *et al*., 2012).

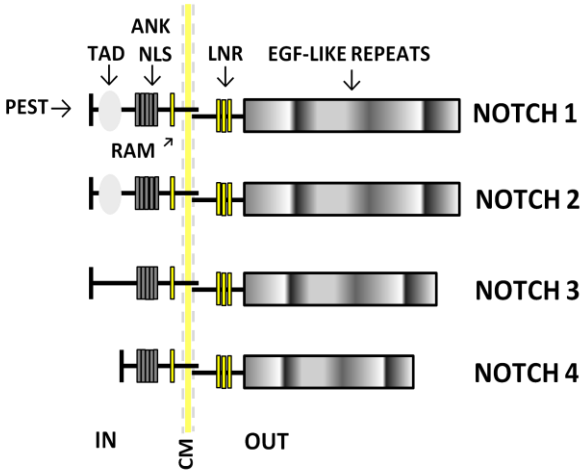

Figure 5. Structure of NOTCH receptors. The extracellular region of NOTCH1-4 receptors have a variable number of EGF-like repeats and three LNR repeats near the hydrophobic region, responsible of heterodimerization close to the cell membrane (CM). Right after the transmembrane motif in the inner side of the cell there is the RAM motif, then the 7 ankyrin repeats (ANK), two nuclear localization signals (NLS), , and in the C-terminal the PEST domain. Besides, NOTCH1 and NOTCH2 have transcriptional activation domains (TAD).

In all animal models tested, mutations in the NOTCH receptors result in developmental abnormalities and thus, not surprisingly, human pathologies. For instance, the cerebral autosomal dominant arteriopathy with subcortical infarcts and leukoencephalopathy (CADASIL) syndrome is an inherited disease associated with point mutations in the extracellular domain of the human NOTCH3 receptor (Joutel *et al.*, 1996).

Furthermore, the Alagille syndrome is associated with human NOTCH ligand JAGGED1 mutations that predict truncated extracellular fragments of the ligand (Li *et al.*, 1997; Artavanis-Tsakonas, 1999). In each case, it is not clear whether the associated mutations reflect a loss or gain of function. Nonetheless, it is likely that the mutant activity could be influenced by extracellular soluble molecules.

1.4.2. NOTCH LIGANDS:

Similar to NOTCH receptor, their ligands are single-pass transmembrane proteins expressing on neighboring cell surfaces. In mammals, there are three ligands with high homology to the ligand Delta of NOTCH in *Drosophila*, called Delta-like, DLL1, DLL3 and DLL4 (Katsube and Sakamoto, 2005; Blanpain *et al.*, 2006). The DLL2 name was not used to avoid confusion with other known Delta2 genes not belonging to the family NOTCH ligands. There are also two Serrate homologs, the second Drosophila Notch ligand, called JAGGED1 and JAGGED2.

DSL domain (Fig 6. red) preceding the module at the N-terminal of NOTCH ligands is an unknown structure, but functionally important because it is responsible of Alagille Syndrome. Below the DSL is located the DOS domain (Delta and OSM-11-like), which is composed by a tandem of EGF repeats specialized in the interaction with EGF-like repeats 11 and 12 of NOTCH receptors. Both domains DSL and DOS are involved in receptor binding. The ligands DLL3 and DLL4 lack the domain DOS. After EGF-like repeats a cysteine rich domain (CRD) is found close to the cell membrane. This domain distinguishes DELTA and JAGGED ligands (Fig 6, green). In the cytosolic region of the proteins lies a PDZL domain, which facilitates adjacent interaction with proteins and multimerization of the ligands (Fig 6. purple) (Chillakuri *et al.*, 2012).

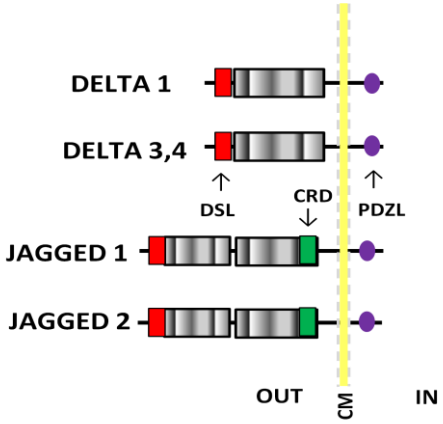

Figure 6. NOTCH ligands structure. The Notch ligands have N-terminal region in the extracellular space with a DSL domain (Delta / Serrate / Lag-2), a DOS domain (Delta and OSM-11-like), a variable number of EGF-like repeats, and a region rich in cysteine (CRD) close to the cell membrane (CM). In the intracellular space there is a PDZL domain in C-terminal.

1.4.3. SIGNAL TRANSDUCTION:

The canonical NOTCH signaling starts with the interaction of NOTCH receptor with their ligands, triggering a cascade of proteolytic cleavages by extracellular metalloproteases and membrane γ-secretases (Fig 7). First cleavage of Notch receptor occurs during receptor membrane anchoring. Afterwards, ADM endopeptidase 17, also called TACE (tumor necrosis factor alpha-converting enzyme) is responsible of the next cut in the site 2 (S2) of NOTCH receptor. S2 is located in the short region of the extracellular subunit near the membrane, allowing the extracellular EGF-like of NOTCH ligand subtracting the extracellular region, and leaving free the receptor subunit containing the transmembrane and intracellular regions (NICD).

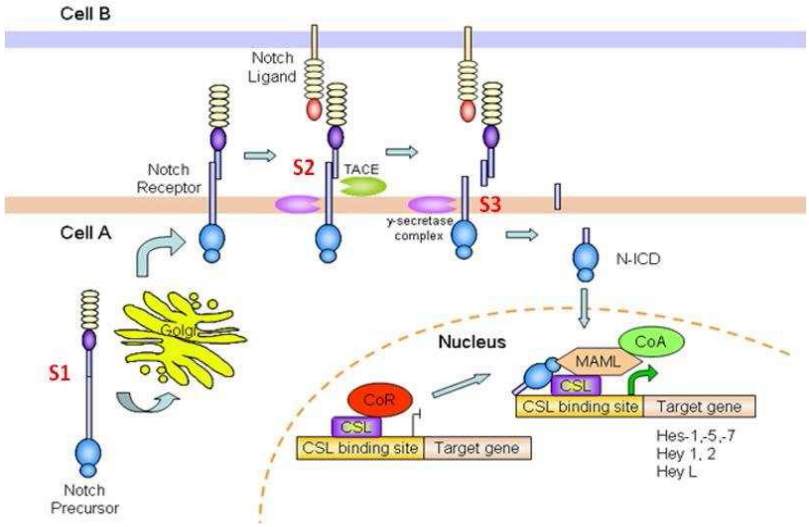

Figure 7. NOTCH receptor cleavage points. Processing in the S1 before anchoring to the membrane, S2 by TACE and S3 by γ-secretase lead to NICD that translocates to the nucleus. (Wu *et al*., 2007)

This protein resultant from the second cut is going to be at the same time a substrate for the third cleavage at a point called proteolytic site 3 (S3), which is located in the intracellular region. On this occasion, the cut is made by the complex γ-secretase formed by four integral membrane proteins: presenilin (responsible for the protease activity), nicastrin, Pen-2 and Aph-1. The third cut results in the release and translocation to the nucleus of the Notch intracellular domain (NICD) (Mumm & Kopan, 2000).

Once in the nucleus, NICD binds to the transcription factor CSL/RBP-Jk/CBF-1, which is a repressor when NICD is not present, but in presence of NICD, this transcription factor is an activator. CSL/RBP-Jk/CBF-1 binds to a specific sequence in the DNA (GTGGGAA) in the promoter region of the inducible target genes of NOTCH signaling.

The most typical downstream target genes activated by the NICD-CSL/RBP-Jk/CBF-1 complex are HES and HEY, basic Helix-Loop-Helix (bHLH) transcription factors. HES family contains 7 members, but only HES1, HES5 and HES7 are NOTCH targets. The HEY family have three genes identified in mammals (HEY 1, 2, L) and all of them can be induced by NOTCH receptors. NOTCH signaling can also be independent of CSL. In this context it has been described that NICD can interact with other proteins and modulate NOTCH pathway positively (Deltex, Mastermind) or negatively (Numb) (Frise *et al.*, 1996).

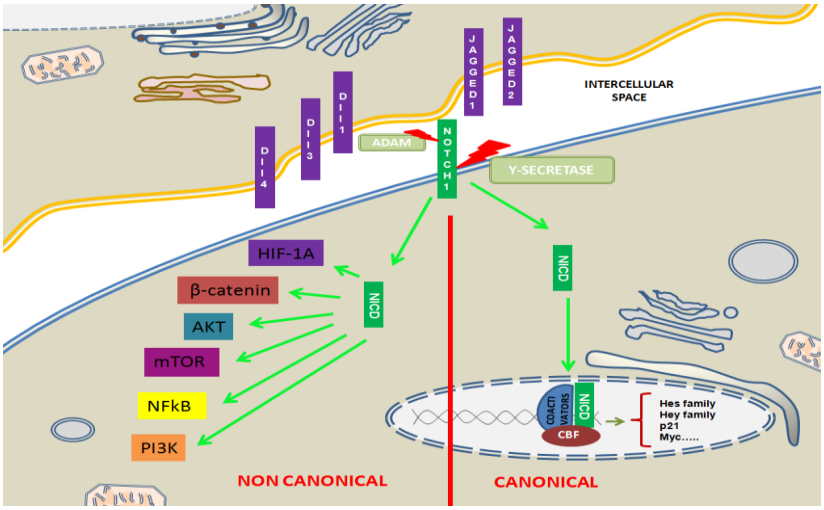

Figure 8. NOTCH signaling transduction. Schematic representation of the canonical and non canonical NOTCH signaling.

Recent studies describe three types of non-canonical NOTCH signaling: 1) γ-secretase regulated activation of the NOTCH pathway that occurs independently of ligand interaction; 2) NICD activity independent of CSL/RBP-Jk/CBF-1 and 3) membrane bound NOTCH signaling in the absence of cleavage by the γ-secretase complex, in some cases independent of ligand interaction. There are many signaling pathways involved in non-canonical NOTCH signaling, executed by cross-talk of NICD with other molecules, such as NFkB, PI3K, AKT, mTOR, HIF-1a, and β-catenin (Fig 8) (Ayaz and Osborne, 2014; Sanalkumar R *et al.*, 2010).

1.5 NOTCH AND DEVELOPMENT

Phenotypic analyses in both vertebrate and invertebrate systems indicate that the fundamental role of Notch during development is to control cell fate choices. This process occurs as a rule between adjacent cells. Lateral specification events are often responsible for the segregation of specific lineages from clusters of precursor cells as well as for defining borders between groups of cells (Greenwald, 1998). As embryo development take place, differences between neighbors caused by stochastic events and intrinsic or extrinsic factors are amplified through signals of NOTCH and their ligands, guiding distinct biochemical events that will dictate final cell fates. NOTCH mediated cell communication depends on the differential expression of ligand and receptor in neighboring cells, giving rise to a balance, that will determine a specific cell fate (Artavanis-Tsakonas *et al*.,1999).

The juxtaposition of cells expressing differing amounts of ligand and receptor suggest that a cell can adopt a "signaling" mode simply by expressing more ligand relative to its neighbor (Heitzler and Simpson, 1991). Thus, among apparently equivalent neighbor cell expressing both DELTA and NOTCH, a small increase in ligand in one cell could favor its adopting the signaling role.

In this way, NOTCH signaling plays a central role in diverse cellular tasks such as embryonic development (Iso *et al*., 2003), stem cell maintenance (Yamamoto *et al*., 2003; Chiba, 2006), adult tissue homeostasis (Schwanbeck *et al*., 2008), and fate-specific differentiation (Apelqvist *et al*., 1999; Zhu *et al*., 2006). In addition to the role in development and homeostasis, deregulations of NOTCH components are widely and directly implicated in various human disorders (Talora *et al*., 2008). These disorders include developmental syndromes (Gridley, 2003; Louvi *et al*., 2006), and the initiation, progression and maintenance of pancreatic (Mysliwiec & Boucher, 2009) and other cancers (Pierfelice *et al*., 2011; Rose, 2009). Notch signaling has also emerged as a specific therapeutic target for T-cell acute lymphoblastic leukemia (Weng & Aster, 2004) and colon cancer (van&Clevers, 2005).

1.6 DLK1 AND DLK2 PROTEINS

DLK 1 (Delta-like1, also named pG2, Pref1, FA-1, SCP-1 and ZOG) is a transmembrane and secreted protein belonging to the EGF-like repeat containing family, where NOTCH receptor and their ligands belong. In humans, DLK1 is located in the 14q32 chromosomic band (Gubina *et al*., 1999). Mature human DLK1 has 383 aminoacids and shares 85 % aminoacid sequence identity with mouse and rat homologs.

The aminoacid sequence, deduced from the cDNA sequence, suggests that DLK1 has a short intracellular, a transmembrane and an extracellular region (Fig 9). The extracellular region has six EGF-like repeats and a signal peptide in N terminal (Laborda *et al*., 1993). Two of the EGF-like, EGF1 and EGF2 specifically, constitute in tandem the DOS domain (Delta and OSM-11-like proteins), involved with the interaction of the receptor (Falix *et al*., 2012). In C-terminal of the extracellular domain there is a region recognized by the protease TACE, which is able to release the EGF-like region into the extracellular medium.

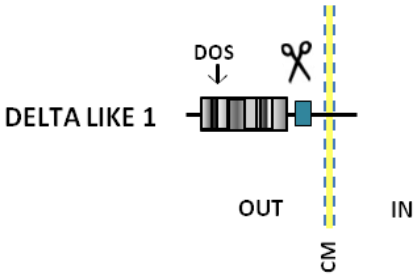

Figure 9. DLK1 protein graphic representation. DLK1 consists on an extracellular region with six EGF-like repeats, a transmembrane region, and a intracellular region. The EGF-like 1 and 2 are known as DOS domain. TACE domain protease cleavage point (in blue).

The alternative processing of DLK1 mRNA produces polymorphic variants of the protein. Additionally to the full-length DLK1A, alternative splicing generates other three major short forms, DLK1B, 1C and 1D (Smas *et al*., 1994; Lee *et al*, 1995; Smas *et al*., 1997). The most common produced variants correspond to, fristly an mRNA encoding a wholae protein called variant DLK1A, and secondly an mRNA encoding a protein lacking amino acids from the third cysteine of the sixth EGF to the start of the transmembrane region, called variant DLK1C, and where the TACE region is absent. Thus, DLK1 can function as a transmembrane protein or as a secreted protein, depending on alternative splicing of its mRNA and TACE protease activity (Wang and Sul 2006), which can bring wider implications to its function.

In 2007, a protein whose structural features were virtually identical to those of DLK1, and very similar to the NOTCH ligand DLL1 was described (Nueda *et al*., 2007b; Nueda *et al*., 2008). It was named as DLK2. Obviously, DLK2 it also belongs to the EGF-like family. The human gene of this protein is located in chromosome 6p21.1 and has six exons, one more than DLK1. The first exon is not coding and the sixth is the longest. The striking structural similarities between DLK1 and DLK2 point to a genetic duplication of the genes (Nueda *et al*., 2007a).

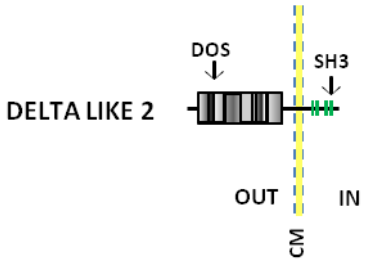

Figure 10. DLK2 protein graphic representation. DLK2 consists on an extracellular region with six EGF-like repeats, a transmembrane region, and a region intracellular. The EGF-like 1 and 2 are known as DOS domain. The intracellular region has two SH3 protein binding domains (green).

The analysis of the cDNA sequence indicated that DLK2 (Fig 10) , encodes a transmembrane protein that has six EGF-like repeat domains of identical structure to those of DLK1, a transmembrane region and a short intracellular region, which keeps very low homology with DLK1 intracellular region. Despite DLK2 lacks the TACE protease cleavage site, the greatest differences between DLK1 and DLK2 find the intracellular regions. DLK2 has in its intracellular region four potential sites for binding SH3 domains, absent in DLK1 (Pawson and Nash, 2003).

This indicates that the intracellular region of DLK2 may be involved in interactions with proteins with SH3 domains, among which several are involved in intracellular signaling, which could have important functional implications.

Furthermore, in humans, the two proteins have in their extracellular region consensus sequences for calcium binding. DLK2 has two binding sites for this element, located in EGFs 5 and 6, and DLK1 has a single calcium binding site, located in the EGF 5. In addition, both DLK1 as DLK2 possess consensus sequences for glycosylation, which are more numerous in DLK1.

1.6.1. *Dlk1* AND *Dlk2* EXPRESSION

In the mouse embryo, *Dlk1* can be detected since the 8.5 day of gestation (Smas *et al*., 1994) and then it can be detected both in developmental and in adult tissues. In the development of mice, at E12.5, *Dlk1* is expressed in high levels in different parts of the embryo. *Dlk1* is in the developing pituitary, pancreas, adrenal gland, many mesodermally derived tissues, and in organs that develop doing branching morphogenesis, such as lung and salivary gland. At E16.5, *Dlk1* expression is down-regulated in most tissues but remains in the pituitary, the adrenal gland, and in skeletal muscle (Yevtodiyenco and Schemidt, 2006). Regarding *Dlk2* less is known, but at 16.5 (Fig 11) the mRNA labeling suggest that *Dlk2* has a similar pattern of *Dlk1* but is also in the brain.

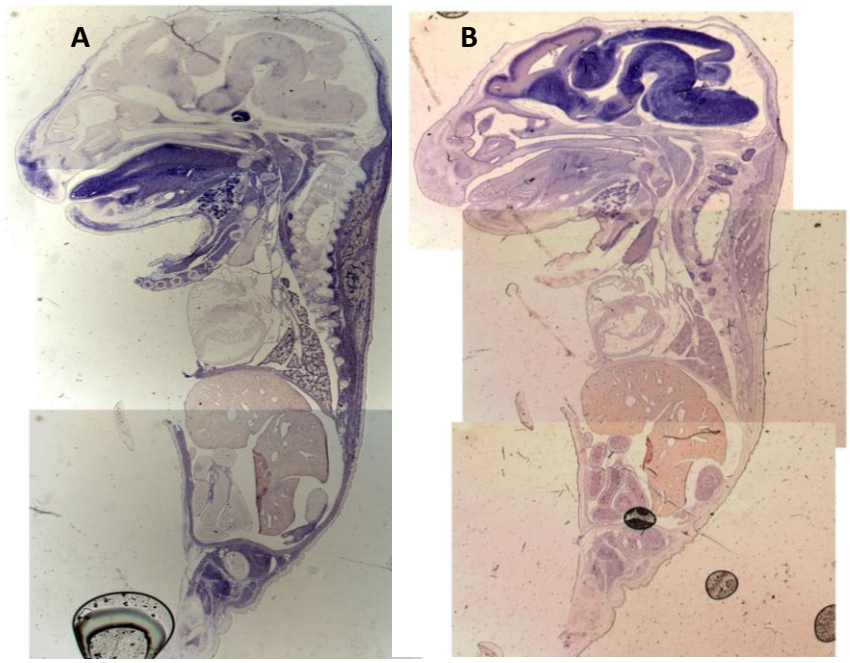

Figure 11. *Dlk1* and *Dlk2* expression pattern in E16.5 mouse embryo sections. (A) Dlk1 (B) Dlk2 mRNA labeling by *in situ* hybridization (images kindly provided by JJ Ramirez, Universidad de Castilla La Mancha).

In the adult (Fig 12) *Dlk1* is highly expressed in fetal liver, placenta and adrenal glands, brain, testicles, and ovaries, and in less proportion, in the kidneys, muscles, thymus and heart. However, all the tissues, except for fetal liver and adult spleen, muscle and heart, express *Dlk2*. Both genes are expressed at different levels by placenta and adult adrenal glands, brain, testicles, kidneys, ovaries and thymus.

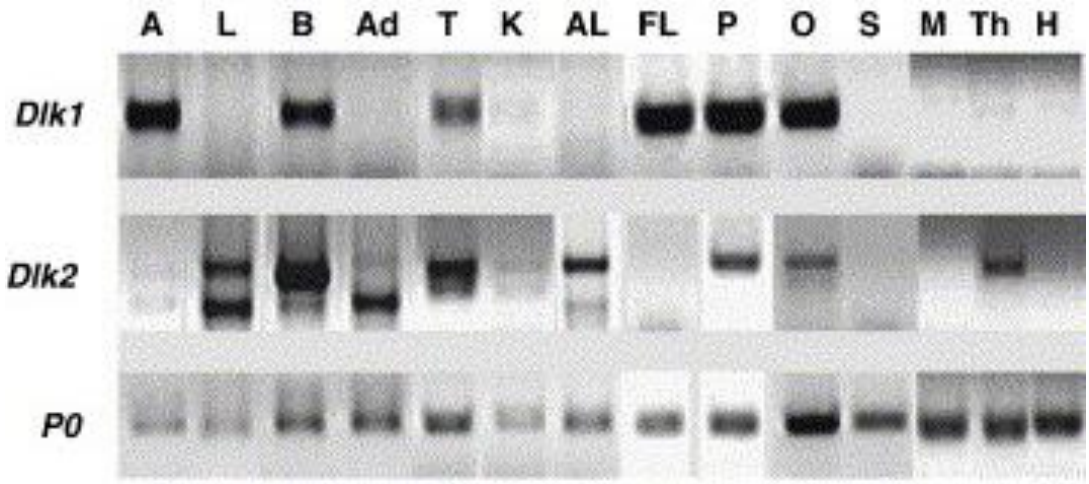

Figure 12. *Dlk1* and *Dlk2* gene expression in adult mouse tissues. RT-PCR analysis of the expression of genes *Dlk1* and *Dlk2* mouse tissue: A: Adrenal Gland, L: Lung, B: Brain, Ad: Adipose tissue, T: Testis, K: Kidney, AL: Adult Liver, FL: Fetal Liver, P: Placenta, O: Ovaries, S: Spleen, M: Muscle, Th: Timo, H: Heart. P0 is the constitutive gene (Nueda *et al.,* 2007b).

1.6.2. DLK1 AND DLK2 FUNCTION AND MECHANISM OF ACTION

DLK1 is a member of a cluster of imprinted genes which is only expressed from the paternally-inherited chromosome (Schmidt *et al*., 2000; Takada *et al*., 2000). Genes with genomic imprinting have an important role in the control of fetal growth and development (Murphy & Jirtle, 2003; Rand & Cedar, 2003; Wilkins & Haig, 2003) and DLK1 is not an exception. Indeed, mice lacking DLK1 show growth retardation at birth and in the first days of life (Moon *et al*., 2002; Raghunandan *et al*., 2008). Furthermore, genetically modified mouse embryos to express a double dose of DLK1, which mimic the condition of loss of imprinting on the locus DLK1, did not thrive after birth despite the advantage that it could be assume for fetal and perinatal growth (da Rocha *et al*., 2009).

The role of DLK1 has been more studied than that of DLK2. DLK1 function is pleiotropic. Accumulating evidence suggests that DLK1 is involved in differentiation processes, including neuroendocrine differentiation (Floridon, 2000), differentiation of hepatocytes and biliary epithelial cells (Tanimizu *et al*., 2003), neurogenesis (Sacri R Ferrón *et al*., 2012), hematopoiesis (Moore *et al*., 1997; Mirshekar-Syahkal B *et al*., 2013), osteogenesis (Abdallah BM *et al*., 2004), muscle differentiation (Andersen *et al*., 2013), chondrogenic differentiation (Chen *et al*., 2011) and adipogenesis (Smas & Sul,

1997b). It has also been found that DLK1 inhibits growth hormone secretion in pituitary GH3 cells (Ansell *et al*., 2007). Moreover, recent data show that DLK1 may also be involved in the regulation of cell growth and cancer (Kim *et al*., 2009, Yanai *et al*., 2010).

At this time, no researchers has identified a master or a unique receptor for DLK1. However, a number of binding partners have been identified. The first evidences about DLK1 function demonstrated, employing the yeast-two-hybrid systems, that NOTCH1 tandem EGF-like repeats 12/13 interact with the extracellular DLK1 EGF-like repeat region (Nueda *et al*., 2007b). The interaction of DLK1 with NOTCH1 resulted in an inhibition of basal NOTCH signaling and its downstream target HES-1 expression and subsequently inhibition of adipogenesis (Sanchez-Solana *et al*., 2011).

More recently, using mice models of DLK1 loss and gain of function, DLK1 has been reported to inhibit angiogenesis via interaction with NOTCH receptors (Rodriguez *et al*., 2012). Thus, DLK1 and DLK2 are considered as non canonical NOTCH ligands.

On the other hand, an interaction between DLK1 and the C-terminal region of fibronectin was also reported to mediate the anti-adipogenic effect of DLK1 via activation of integrin signaling and MEK/ERK activation (Wang *et al*., 2010). Additionally, the membrane bound DLK1 binds to insulin-like growth factor IGF-I and IGF binding protein 1 (IGFBP1) complex leading to the release of IGF-1 and enhancing IGF receptor signaling (Nueda *et al*., 2008). Mitogen activated protein kinase (MAPK) and the MEK/ERK pathways are activated in the presence of DLK1 and mediate the inhibition of adipogenesis (Kim *et al*., 2007). In addition, DLK1 inhibitory effects on chondrogenesis are associated with the inhibition of PI3K/AKT signaling (Chen *et al*., 2011).

Other authors demonstrated the activation of NF-kB signaling as a potential mechanism underlying the inhibitory effect of DLK1 on MSC differentiation (Abdallah *et al*., 2007). Constitutive expression of DLK1 or direct addition of FA1 to human bone stem cells (hBMSC) cultures, activate the NF-kB pathway leading to increased production of a number of cytokines and immune-related factors including IL-1α, IL-1β, IL-6, IL-8, CCL20 and COX-2 with known inhibitory effects on osteoblast and adipocyte differentiation (Chang *et al*., 2013). A similar mechanism has been identified for DLK1 stimulated bone resorption in DLK1 transgenic mice. The association between DLK1 expression and the inflammatory response has been reported in other studies that demonstrate the presence of a relationship between DLK1 and pro-inflammatory cytokine production by adipose tissue (Chacon *et al*., 2008) and by human skeletal muscle myotubes (Abdallah *et al*., 2007).

2. GOALS

Salivary gland function may be compromised by multiple diseases and conditions, such as the side effects of radiation therapy against multiple head and neck cancers. Salivary gland alterations may lead to xerostomia ('dry mouth syndrome') which brings high discomfort to patients, negatively affecting their quality of life. (Bouma *et al*., 2003; Vissink *et al.*, 2010). Thus, these last few years research groups are doing big efforts to develop regeneration strategies, where a deep knowledge on salivary stem cell biology (Lombaert *et al*., 2008), salivary innervation (Knox *et al.,* 2013) and cell-signaling pathways governing salivary gland morphogenesis will all be fundamental (Jaskoll *et al.,* 2004a; 2004b; Dang *et al*., 2009; Rebustini and Hoffman, 2009; Patel *et al.,* 2011).

Our thesis is centered on NOTCH signaling as a crucial pathway for salivary gland development. The non canonical NOTCH ligands, DLK proteins, could act as inhibitory ligands of NOTCH receptor in salivary gland cells and could play an important role in the morphogenesis (epithelium and mesenchyme growing and differentiation) and innervation of the mouse salivary gland.

To know the importance of DLK1-2 during salivary gland development, we proposed to investigate the following objectives:

1- To study the expression pattern of DLK1 and DLK2 throughout the development of the mouse salivary glands.

2- To analyze the mechanism of action of DLK1 in terms of NOTCH pathway by using a human salivary gland cell line.

3- To evaluate the effect of the inhibition of NOTCH signaling in the development of mouse submandibular salivary glands (SMG) and in the isolated salivary epithelia.

4- To investigate the effect of the absence of the protein DLK1 in the adult and in the development of the mouse salivary gland, through the characterization of the *Dlk1* (-/-) mice.

3. MATERIAL AND METHODS

3.1 MICE STRAINS

Two different strains of mice were used for the experiments of this project:

- Anisogenic albino-swiss mice, OF1 strain (Oncis France strain 1) from IFA CREDO.
- Backcross of 129XI/SVJ and C57Bl/6 strains, to generate *Dlk1* (+/+) and *Dlk1* (-/-). These mice were kindly provided from the Faculty of Medicine from the University of Castilla La Mancha (UCLM).

DLK1 knock-out (KO) mice was performed targeting a construct that was assembled and electroporated into SVJ129 embryonic stem (ES) cells. The construct had a neomycin-resistance cassette replaced 3.8 kbp of the endogenous allele, including the promoter and first three exons of *Dlk1*. Chimeric animals were bred to establish *Dlk1* KO mice. Genotype analysis was done by Southern blot or PCR amplification using the following primers: 5´dlk, CCAAATTGTCTATAGTCTCCCTC; 5 Neo,CATCTGCACGAGACTAGTG; and 3´ SCR (screen), CTGTATGAAGAGGACCAAGG (from *Dlk1* intron 3). Analysis of phenotype was done after three backcrosses to C57Bl/6, and then intercrosses of heterozygotes were used to generate homozygote, heterozygote, and wild-type (WT) mice. For all experiments, age-matched wild-type littermates from heterozygous intercrosses were bred and used as controls (Raghundan *et al*., 2008).

Both mice strains, Swiss and DLK1 WT and KO, were breed in the animal facilities of the University of the Basque Country (UPV/EHU), under standard conditions of cleanness, *ad libitum* nourishment and a light cycle from 8 am to 8 pm.

3.2 MICE GENOTYPING

Dlk1 (+/+) and *Dlk1* (-/-) genotyping was made by conventional Polymerase Chain Reaction, described as following.

The genomic DNA was obtained from a piece of the tail of a DLK1 +/+ and DLK1 -/- mouse and was digested over-night at 55°C in salting-out buffer with 30 µl Proteinase K (Roche, 10 mg/ml).

SALTING- OUT BUFFER:	40 mM Tris-HCl pH 8.0	0.5% SDS
	2 mM EDTA	200 mM NaCl

The next day we added 250 µl of NaCl 6M, we shook the sample upside down five times and incubated in ice for 10 minutes. Then we centrifuged at 16000 g at 4°C and added 500 µl of the supernanant in a new tube with 1 ml of cold ethanol 95%, to precipitate the DNA. We shook the tube and centrifuged. Afterwards, we washed the pellet with ethanol 70% and centrifuge again. Finally, we carefully dried the pellet and reconstituted in miliQ water to a concentration of 20 ng/µl.

Once we had the DNA we carried out a PCR with the MyTaq™ Red Mix (BioLine), that contains the polymerase and the nucleotides necessary for the reaction. We just added the following to the reaction:

- 5 µl MyTaq
- 0.8 µl Primers
- 0.8 µl cDNA
- 4 µl DEPC water

The conditions used for the PCR, made in iCycler MyiQ™ Single Color Real-Time PCR Detection System (BioRad), were denaturation at 95°C for 30 seconds, annealing at 55°C for 30 seconds and extension at 72°C for 1 minute, repeated for 35 cycles for Neo gene; and repeated for 40 cycles for DLK1 gene.

The primers used to recognize the *Dlk1* (-/-) mice were:

Neo Forward: 5´TTGAACAAGATGGATTGCACGCAGG3´
Neo Reverse: 5´GGCTGGCGCGAGCCCCTGATGCTCT3´

The primers used to recognize the DLK1 WT/WT mice were:

Dlk1 Forward: 5´TGTGACCCCGAATATGGATTCTGCGAGG3´
Dlk1 Reverse: 5´CATGGTTCCTTGCAGACTCCATTGACACACAGC3´

The analysis of the PCR amplified products was made by electrophoresis in a 2% agarose/TAE buffer with GelRed Nucleic Acid Stain (Biotium) gel. The samples were runned in Run One Electrophoresis Cell (EmbiTech) at 100 mA voltage, for 20 min. The first lane of a gel always had a molecular weight marker (100-bp DNA Ladder Pluss, BioChain). To visualize bands, the gel was exposed to UV light (High Perfomance Ultraviolet Transiluminator, UVP) and we captured an image.

3.3 SUBMANDIBULAR SALIVARY GLAND CULTURE

Thirteen days-old Swiss mouse embryos (E13, vaginal plug = day 0) were collected and SMGs primordia were isolated by microsurgery under stereoscopic microscope. Salivary glands were cultured on Millicells (Millipore, PICMORG50) nitrocellulose made filters, containing DMEM-F12 medium supplemented with vitamin C (180 µg/ml) and transferrin (5mg/ml). Pictures of SMG cultures were taken at 0, 24 and 48 hours.

We added different treatments to the organotypic cultures, 1) DAPT (gamma-secretase inhibitor; N-[N-(3, 5-difluorophenacetyl-L-alanyl]-S-phenylglycine t-butyl ester, Calbiochem) 20 µM, 2)human recombinant soluble DLK1 protein, sDLK1 (R&D Systems) at 2.5 µg/ml, 3) Carbacoylcholine Chloride (CCh), an analogue of acetylcholine, 10nM (TOCRIS bioscience), used as a stimulator of cholinergic activity in the SMG (Knox et al., 2013).

After culture treatments, the percentage of spooner branch ratios was determined for each explant (Jaskoll et al. 2004a). The spooner ratio is the relative number of epithelial end buds for 0h, 24h, 48h normalized with respect to the control SMG at 48h, (which constitutes the 100% value). Each experiment was repeated at least three times.

3.4 EPITHELIAL MESENCHYMAL DISSECTION AND CULTURE

SMG mesenchyme-free epithelia were cultured as previously described (Morita & Nogawa, 1999), with some modifications. Thirteen days-old Swiss mouse embryos (E13, vaginal plug = day 0) were collected (Fig 13.A) as described above and incubated in Dispase (Gibco) for 14 minutes at 37°C. Then, the glands were rinse twice with 10% BSA/DMEM-F12 to wash the Dispase. SMG epithelia with up to five buds were separated from the mesenchyme with fine forceps in BSA/DMEM-F12 solution containing 10% BSA/DMEM-F12 (Fig 13.B).

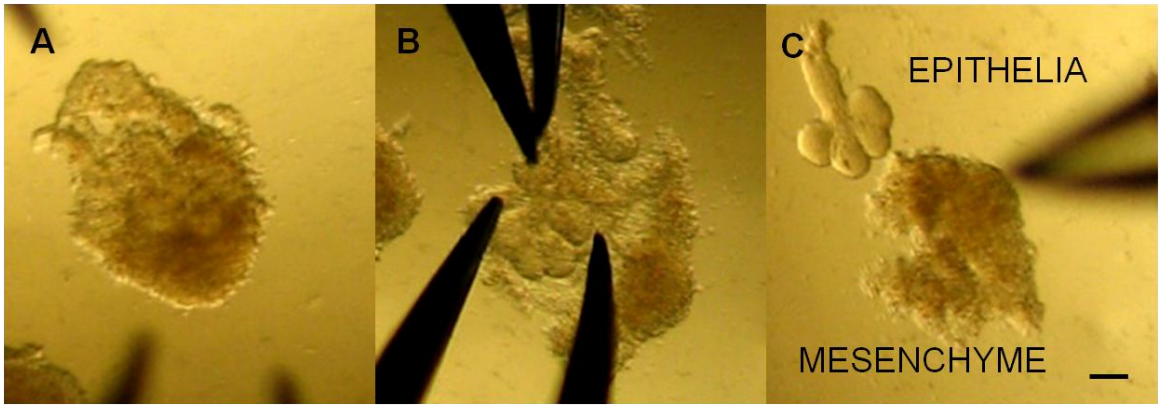

Figure 13. Mouse embryo SMG isolation and epithelial-mesenchymal dissection. (A) E13 SMG with five epithelial end buds and the mesenchyme. (B) SMG after Dispase treatment and removing mesenchyme with the forceps. (C) Separated epithelial rudiment and the mesenchyme. Scale bar: 150 µm.

The epithelial rudiments (Fig 13.C) were placed on Whatman Nuclepore Track-etch polycarbonate made filters (13 mm, 0.1 µm pore size; VWR, Buffalo Grove, IL) at the air/medium interface. The filters were floated on 200 µl of DMEM-F12 in 50 mm glass-bottom microwell dishes (MatTek, Ashland, MA). The medium, DMEM-F12 was supplemented with 100 U/ml penicillin, 100 µg/ml streptomycin, 150 µg/ml vitamin C and 50 µg/ml transferrin.

The epithelia rudiments were covered with 15 µl of 3D laminin-1 (1 mg/ml; Trevigen, Gaithersburg, MD) diluted 1:1 in medium (5 mg/ml; BD Biosciences, San Jose, CA), and the filter was floated on top of 200 µl of medium.

Fibroblast Growth Factor 10 (FGF10) was added to the cultures at 800 ng/ml concentration (R&D Systems, Minneapolis, MN) always in combination with Heparan Sulfate (HS) at a concentration of 100 ng/ml (Sigma-Aldrich, MO). FGF10/HS was our control treatment and was analyzed either alone or in combination with sDLK1 (R&D Systems) at 2.5 µg/ml.

Five gland rudiments were cultured on each filter at 37°C in a humidified 5% CO_2 and 95% humidity air atmosphere. Samples were photographed at 2, 24 and 48 hours. Each experiment was repeated at least three times.

3.5 STAINING

3.5.1 HEMATOXYLIN AND EOSIN (H/E)

Adult salivary glands were fixed in paraphormaldehyde in PBS 4% over-night, then dehydrated (Shandon Citadel 1000) and embedded in paraffin (Shandon Histo Center 2). Once we had the paraffin with the sample inside we made sections (cutting thickness 5 µm) with the microtome (Shandon Finesse 325). The slides were kept over-night at 65°C. The next day the samples where desparaffinized with citrosol 10 minutes, rehydrated with ethanol 100%, 96%, 70% each 5 minutes, consecutively. Then the samples were stained with hematoxylin 30 seconds, washed with water the eosin 1 minute and rinsed in H_2O. Finally, we dehydrated with growing ethanol 70%, 96%, 100% to finish with citrosol and the samples were mounted with DPX Mounting for histology (Sigma). Images were captured in an Olympus optical microscope BX50FO, runned with CellA software.

3.5.2 INMUNOFLUORESCENCE

Mouse E12, 14, 17, 19 SMGs and explants cultured in the presence or the absence of drugs were fixed for 1 h in paraformaldehyde 4% (depending on the size of the tissue), embedded in O.C.T. Compound (Tissue-Teck®, Sakura) and frozen in dry ice. Sections (10 µm thickness) of every sample were obtained by cryostat (Leica CM3050S) and incubated overnight with the primary antibodies. **Rabbit to DLK1** and **DLK2** antibodies were donated by Prof. Laborda (University of Castilla-La Mancha) and obtained as previously described by Hermida *et al.*, 2008 and Rivero *et al.*, de 2012, respectively. Both DLK antibodies recognize intracellular epitopes of the protein, and were used at a 1:1000 working dilution. To compare DLK1 expression in the adult SMG with the location of the myoepithelial cells, we made a double immunohistochemistry with the **mouse monoclonal to α-Smooth Muscle Actin** (SMA) antibody (A2547, Sigma, 1:250 dilution) and anti-DLK1, followed by two secondary antibodies Alexa Fluor 594 (red) goat anti-mouse IgG (A11005, Invitrogene) and Alexa Fluor 488 (green) goat anti-rabbit IgG (A11008, Invitrogene), respectively.

To detect the active soluble form of the NOTCH1 receptor, we used **rabbit to NOTCH 1 intracellular domain** (N1ICD) antibody (ab8925, Abcam 1:250 dilution). Thereafter, sections were incubated with Alexa Fluor 488 goat anti-rabbit IgG (A11008, Invitrogene).

E13 SMGs were cultured for 48 h in presence or absence of DAPT and sDLK1 and immunolabeled with **rabbit to Ki67** antibody (ab15580, Abcam, 1:500 dilution) to detect cell proliferation. **Rabit to Phospho Histone H3** (H3P) antibody (06-570, Millipore 1:500 dilution) to detect mitotic cells. Apoptotic cells were found by **rabit to cleaved Caspase 3** antibody (9661, Cell Signalling 1:200 dilution).

Progenitor salivary stem/progenitor epithelial cells were immunolabeled by **rabbit to cytokeratin 5** (CK5) antibody (ab53121, Abcam 1:400 dilution) and **mouse to cytokeratin14** (ab49747, Abcam 1:200 dilution), respectively. Then, sections were incubated with Alexa Fluor 488 goat anti-rabbit IgG antibody (A11008, Invitrogene) or with Alexa Fluor 594 goat anti-mouse IgG (A11005, Invitrogene).

Whole mount immunofluorescence of some E13 SMGs cultured for 48 h in the presence or the absence of DAPT and sDLK1 were prepared for immunolabeling with **rabbit to βIII tubulin** antibody (specific neuron marker, ab18207, Abcam 1:500 dilution) to visualize the cell bodies and axons of the PSG neurons. High magnification images were captured in an extended focus acquired in XYZ to scan the whole section (around 40 µm) and then stacked in a single 3D image. Nuclei of the cells were counterstained with DAPI.

Transiently transfected HSG cells were cultured for two days to increase the levels of DLK1 and DLK2 proteins. Immunofluorescence and image acquisition were performed as described previously, using **rabbit to Hes1** primary antibody (ab71559, Abcam 1:200 dilution) and antibody Alexa Fluor 594 goat anti-rabbit IgG (A11012, Invitrogene).

In all the preparations we used **DAPI** (1:1000, Invitrogin D3571) for nuclear counterstaining.

Confocal images were recorded by using confocal Olympus FV500 Fluoview microscope runned with the software package Nikon DS-Qi1Mc. Epiflourencence Images were captured with the microscope Zeiss Axioscop, runned by Nikon NIS-Elements. Quantification of immunolabeling density in images was performed by using Image J software, and it was always normalized to cell surface area. The experiment was repeated and measured three times.

3.6 TRANSMISSION ELECTRON MICROSCOPY

SMG samples were fixed overnight in 2% glutaraldehyde diluted in 0.1 M cacodylate buffer (pH 7.4), washed in isosmolar cacodylate/sucrose buffer and post-fixed in 1% osmium tetroxide. After repeated washing, samples were dehydrated with 30% to 100% of ethanol, washed in propylene oxide and embedded in Epon Polarbed resin. Ultrathin sections (70 nm) were deposited onto 150 mesh copper grids, post-stained with uranyl acetate and lead citrate, and visualized in a Philips EM208S transmission electron microscope. Digital images were acquired with an Olympus SIS Morada digital camera.

3.7 CELL CULTURE

We used the human ductal submandibular salivary gland cell line HSG (Shirasuna K, 1981). Cells were harvested in standard DMEM-F12 culture medium (Gibco), supplemented with 10 % fetal bovine serum (Biochrom) and 10 µg/ml of penicillin/streptomycin (Sigma).

3.8 LUCCYFERASE ASSAY

The NOTCH transcriptional activity was analyzed by luciferase assays in HSG cell line. Cells were transfected with pGLucWT, a plasmid expressing luciferase reporter gene under the control of a promoter that contains four copies of a CSL/ RBP-Jk/CBF-1 binding site, which binds N1ICD active form of NOTCH (Baladrón *et al.*, 2005).

To normalize our data, cells were also transfected with pRLTK (renilla expresion plasmid, Promega, Madison, WI, USA). As a positive control of these assays, HSG cells were co-transfected with pGLucWT and pN1ICD-2500 (expresses an active N1ICD protein) plasmids or with pGLucWT plasmid and pLNCX2-myc (empty vector).

We used the Green Fluorescence Protein (GFP) expression construct pEGFP-N1 (Clontech, Mountain View, California) to determine transfection efficiency. Transient transfections were performed in 50% confluence cells with 0.75-1 µg of different plasmids by using Superfect reagent (Qiagen INC., Hilden, Germany) following the recommendations of the manufacturer. We cultured transfected HSG cells at 37ºC and 5% CO_2 in complete medium. After 24 to 48 hours of transfection, cells were lysed and processed using the dual Luciferase Kit (Dual-Luciferase Reporter Assay System, Promega, Madison, WI, USA). This kit has the substrate that the luciferase enzyme is catalizes to a colored product; however the negative control renilla is not able to make this reaction. The luminometer measures this colored product correlatively to luciferase enzyme quantity. As a result, the transfection background is eliminated. Experiments were repeated at least three times.

The potential effects of DLK1 or DLK2 on NOTCH activation and signaling were analyzed also by co-transfecting HSG cells with pGlucWT plasmid and HDLK1S and/or HDLK2S expression plasmids. Additionally, HSG cells were treated with DAPT 10 µM.

The plasmid HDLK1S contains the entire human DLK1 cDNA from plasmid HDLK1-AG1 (Lee *et al*., 1995). HDLK1-AG1 was digested with *Hind*III-*Not*I restriction enzymes and the purified cDNA-containing fragment was cloned into the *Hind*III-*Not*I restriction sites of the pLNCX2 expression vector (Clontech, Palo Alto, CA, USA). Plasmid HDLK2S contains the entire human *DLK2* cDNA (MGC Full-Length clone IMAGE ID 54954558). *HDLK2* cDNA from the MGC clone was isolated by digestion with *Hind*III-*Not*I restriction enzymes and subsequently cloned into the *Hind*III-*Not*I restriction sites of pLNCX.

On another set of experiments, subconfluent human HSG cell lines were transiently transfected by Trans LT1 (Mirus) with human expression plasmids for DLK1S, DLK2S or PCLNX2 (empty vector, used vector as control). Transfected HSG cells were cultured for two days to increase the levels of DLK1 and DLK2 proteins and then studied downstream targets regulation.

3.9 QUANTITATIVE POLIMERASE CHAIN REACTION

The RNA extraction from embryonic glands or epithelial rudiments was extracted with RNA miniKiT Ambion (Cat nº.AM1931). When the tissue was bigger (adult salivary gland) the extraction was made with RNeasy kit Qiagen (Cat nº.74104). Both kits use a solution of fenol and thiocyanate of guanidine to lysate the cells and inhibit the RNAses. Then a system of columns made by gel of silica is used, where the RNA was attached. Afterwards the column is washed and finally eluted. The amount of RNA is quantified and the integrity of the RNA checked with the ratio 260/280, considered optimum around 2 (Synergy HT, Bioteq). RNA was stored in -80°C, until use.

Reverse transcriptase reaction we used the iScript™ cDNA Synthesis kit (BioRad) following the manufacturer's instructions. To performe cDNA we started with 1 µg of RNA, 4 µl of 5x iScript Reaction Mix (Bio-Rad, 170-8890) and 1 µl of iScript Reverse

Transcriptase, the volume of the reaction was 20 µl, supplemented with DEPC water. The reaction is produced through the following steps: priming at 25°C for 5 min, synthesis at 32°C for 30 min, and finally elongation at 85°C for 5 min. cDNA was stored at -20° until its use.

qPCR was carried out in iCycler MyiQ™ Single-Color Real-Time PCR Detection System (BioRad) with 5 µl Power SYBR® Green PCR Master Mix (Life technologies), which contains fluorescent enzyme and nucleotides, 8 µl of DEPC water, 0.5 µl of forward and reverse primers at a concentration of 6,25 µM (Isogen) and 0.5 nl of cDNA per well, in triplicates of each sample in a 96 well plate with a adhesive cover. The steps followed were: 95°C for 10 min, followed by 45 cycle of 95°C for 30 sec for DNA denaturalization, 51-61°C depending on the primers for 30 sec for the binding and 75°C for elongation. Finally, there is a cycle of 95°C for 1 min and another of 65°C for 1 min and the melting curve between 65°C and 95°C in 60 cycles increasing the temperature 0.5°C each cycle. The qPCR products were stored at 4°C.

Quantification of the data obtained from the termocycler, Ct values, was normalized to a house keeping gene, calculated as ΔCt. The different conditions were compared as ΔΔCt, and transformed to be logarithmic. The final value was the fold change (Schmittgen TD & Livak KJ, 2008). The differences between the compared conditions were considered statistically significance with a confidence interval of 95%.

The employed primers were:

Ck14 Forward: 5´ACCGCCAGATCCGCACCAAG3´
Ck14 Reverse: 5´TCCTAAGCCTGAGCAGCATGTAGC3´

Ck5 Forward: 5´ TCCTGTTGAACGCCGCTGAC3´
Ck5 Reverse: 5´CGGAAGGACACACTGGACTGG3´

Aqp5 Forward: 5´TCTACTTCTACTTGCTTTTCCCCTCCTC3´
Aqp5 Reverse: 5´ CGATGGTCTTCTTCCGCTCCTCTC3´

Fgf10 Forward: 5´ TCTTCCTCCTCCTCGTCCTTCTCCTCTCCTTCC3´

Fgf10 Reverse: 5´ CCGCTGACCTTGCCGTTCTTCTCAATCG3´

Dlk2. Forward: 5´GGCCAGTGTGTGTATGACGG3´,

Dlk2 Reverse: 5´CGGCATGTGAAGTTGAGGG3´

Gapdh. Forward: 5´ACGGCACAGTCAAGGCCGAG3´,

Gapdh Reverse: 5´CACCCTTCAAGTGGGCCCCG3´

3.10 WESTERN BLOT

Embryonic SMGs were isolated from E13 littermates and cultured in the presence or the absence of DLK1, 2.5 µg/ml, for 48 h. Samples were collected, washed in PBS and a pulse of centrifugation in PBS was given. Pellets were dissolved in RIPA lysis buffer (80 mM Tris-HCl [pH 8], 150 mM NaCl, 0.5% sodium deoxycholate, 1% Nonidet P-40 [NP-40], 0.1% SDS) on ice for 15 min and clarified by brief spinning in a microcentrifuge. Protein content was determined by bicinchoninic acid method. Forty micrograms of proteins were loaded per lane in a SDS-polyacrylamide gel, electrophoresed and then electroblotted onto Nitrocellulose Transfer membranes (Whatman).

For immunodetection of proteins, membranes were blocked for 1 h at room temperature in 5% nonfat dry milk–0.1% Tween20 in PBS. Subsequent incubations and washes were conducted with 10% TBS (145 mM NaCl ,50 mMTris-HCl [pH 7.4]). The membranes were incubated overnight at 4ºC with anti-rabbit N1ICD antibody (ab 8925, Abcam, 1:500 dilution) and the housekeeping monoclonal anti-α-tubulin antibody (T5168 Sigma-Aldrich, 1:4,000). Detection of the antigen-antibody complexes was accomplished via goat polyclonal secondary antibody to rabbit IgG-H&L (HRP) (ab6721, Abcam 1:3,000 dilution) or goat polyclonal secondary antibody to mouse IgG-H&L (HRP) (ab97046, Abcam 1:3,000 dilution). Labeled bands were visualized by enhanced chemiluminescence (ECL) (GE Healthcare) following manufacturer's instructions.

3.11 SALIVA MEASSUREMENT

Dlk1 (-/-) and *Dlk1* (+/+) male and female mice (8 months of age) were anesthetized by 1 % isoflurane inhalation in air. Afterwards, saliva secretion was modulated by intraperitoneal injection of pilocarpine (0.05 mg/100 g body weight). Policarpine is a stimulator of the parasympathetic innervation of the SMG. This reagent has a β adrenergic activity and it is a muscarinic agonist.

The secreted saliva was then absorbed onto paper plugs inserted into the oral cavity. The saliva-saturated plugs were weighed and corrected for the original weight of the paper plug. The volume of secreted saliva was calculated as the increase in weight of the paper plug per unit of body weight.

3.12 STATISTICAL TREATMENT

Data were collected and normalized to the control. Before statistical analysis, all data distributions were subjected to a normality test. For non-parametric data, statistical differences among groups were assessed using the Kruskal-Wallis test, and for parametric distributions we used ANOVA with post-hoc test. The minimum level for statistical significance was set to $p<0.05$. Data were processed using IBM SPSS statistic 19 software. Bar graphs show the mean ±SEM.

.

4. RESULTS

4.1 ANALYSIS OF DLK1, DLK2 AND N1ICD DISTRIBUTION DURING MOUSE SMG DEVELOPMENT

To investigate the role of DLK1 and DLK2 in mice SMG development, we first compared the expression levels of *Dlk1* and *Dlk2* during the different stages of the developing and adult SMG (Fig 14).

By qPCR we found that *Dlk1* and *Dlk2* were expressed since early in the development of the SMG E12 (12 day-old embryos), when the morphogenesis of the gland starts and the expansion of the progenitor cells occur. Then *Dlk1* decreases gradually through E14, E17 and E19. In P2 (2 days after birth) and in the adult SMG *Dlk1* is very little expressed, whereas *Dlk2* is equally expressed through E12, E14, E17 and E19 until the SMG is differentiated at P2 where the level of Dlk2 decreased as in the adult.

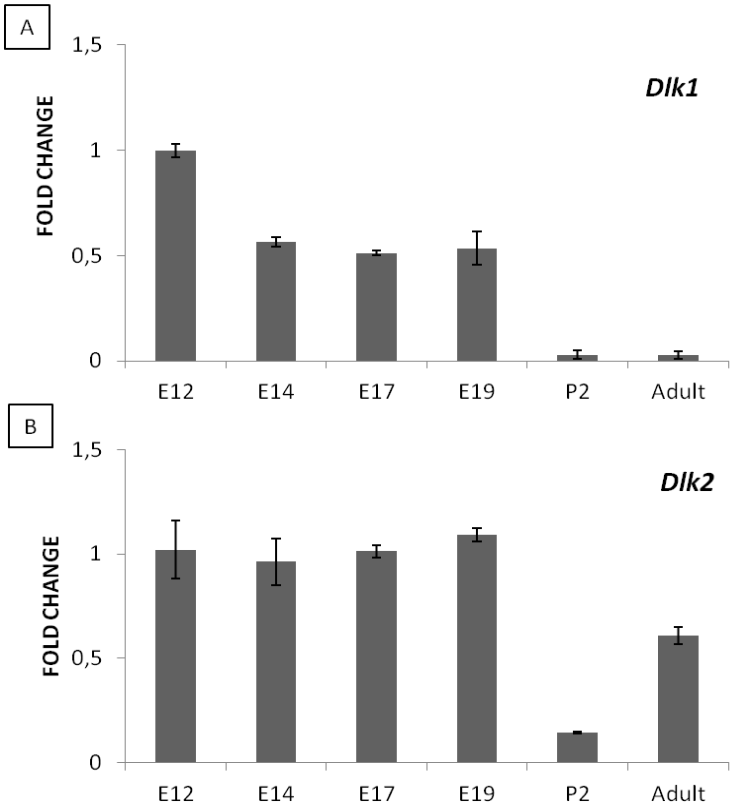

Figure 14. Expression levels of *Dlk1* and *Dlk2* during salivary gland development and adult salivary gland. (A) qPCR *Dlk1* expression level normalized to E12 (B) qPCR *Dlk2* expression level normalized to E12.

Then, we compared the cellular and tissue distribution of DLK1, DLK2 and N1ICD (activated NOTCH receptor) by inmunofluorescence on SMG sections from E12 to E19 (Fig 15.A-H). A clear difference in the patterns of DLK1 and DLK2 expression was observed.

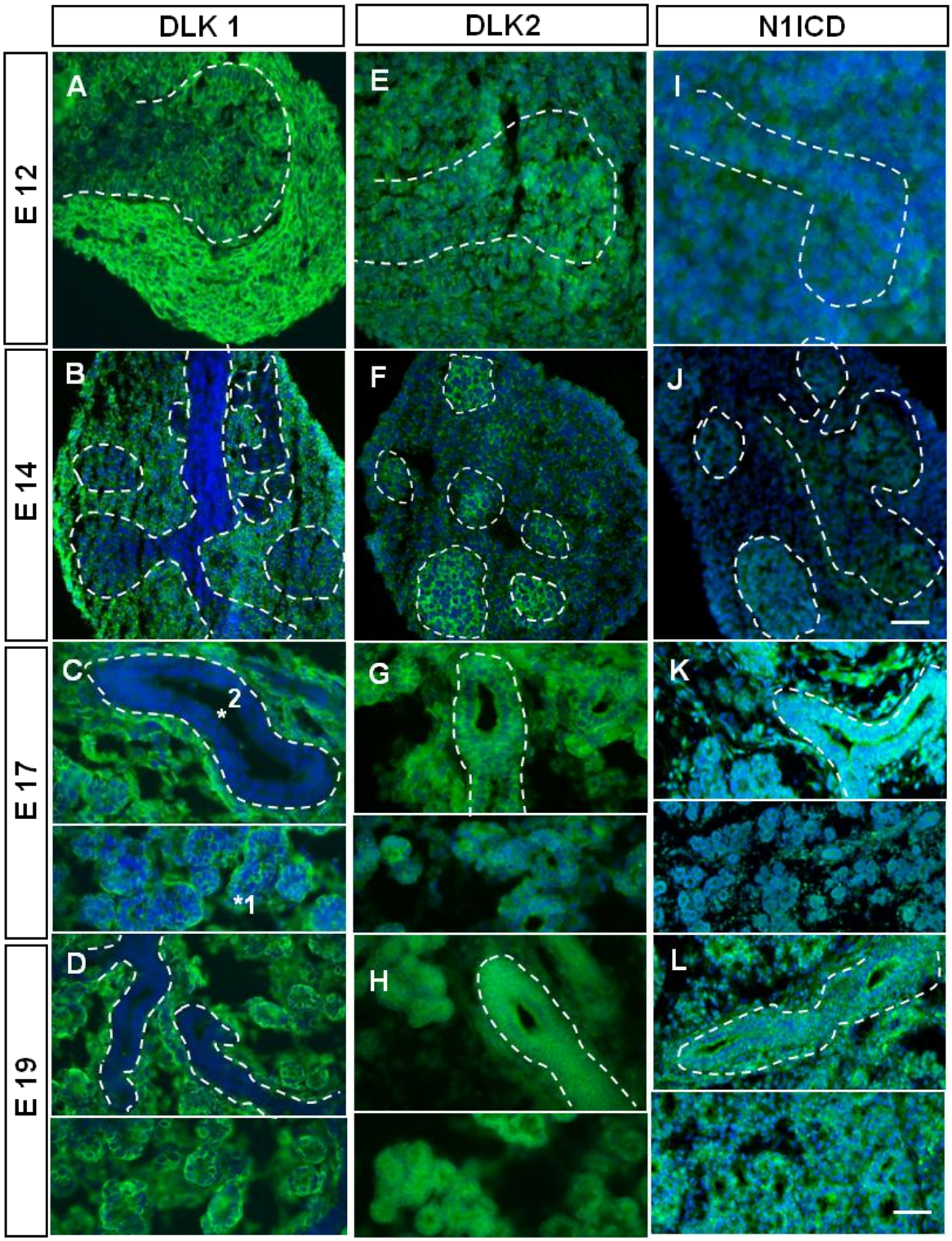

Figure 15. **Expression patterns of DLK1, DLK2 and NICD1 during salivary gland development.** E12 day-old mouse embryo SMG representing the initial bud stage is positive for DLK1 (A) DLK2 (E) and NICD1 (I). The E14 SMG, between the pseudoglandular and the canalicular stages, shows a differential expression for DLK1 (B, mainly in the mesenchyme) and DLK2 (F, mainly in the epithelium); (I, J) NICD1 expression at E12-14; (A, B, E, F, I, J) Scale bar: 150µm. At the terminal bud stage, E17 to E19, this expression pattern continues, being both the acinar and the ductal epithelia negative for DLK1 (C, D), but positive for DLK2 (G, H) and NICD1 (K, L) Scale bar: 50µm.

In bud stage SMGs (E12), we detected a strong DLK1 expression in the mesenchyme. Distal bud epithelial cells were also labeled, but less intensely (Fig 15.A). DLK2, in turn, was diffusely distributed both in the epithelial and mesenchymal compartments (Fig 15.E).

By the pseudoglandular stage (E14), DLK1 expression was high in the undifferentiated mesenchyme and in the distal bud epithelial cells, but the proximal epithelial cells of the forming ducts remained negative (Fig 15.B). In contrast, DLK2 labeling appeared concentrated in epithelia, but the signal in the mesenchyme was very weak (Fig 15.F).

At E17 (canalicular stage), the expression of DLK1 was found in the mesenchyme and in the distal acinar and myoepithelial cells, whereas lumenized ducts were devoid of DLK1 immunoreactivity (Fig 15.C). To corroborate the DLK1 labeling of myoepithelial cells, we carried out a double immuhistochemistry against DLK1 and α smoth muscle actin (αSMA), a marker of myoepithelial cells. We found a colocalization of DLK1 and αSMA in cells surrounding serous and mucous acini, and identified as myoepithelial by their αSMA labeling and their stellate morphology (Fig 16 C, C´).

Regarding DLK2 expression in E17 SMG, the signal appeared to be abundant on ductal cells and somewhat weaker in the acinar cells (Fig 15.G). At the terminal bud stage (E19), DLK1 remained in the mesenchyme and it was clearly localized in myoepithelial cells surrounding the acinar structures, but less intensely in acinar cells (Fig 15.D). However, DLK2 expression, this was detected in both ductal and acinar cells (Fig 15.H), in a pattern similar to that found for E17 SMGs.

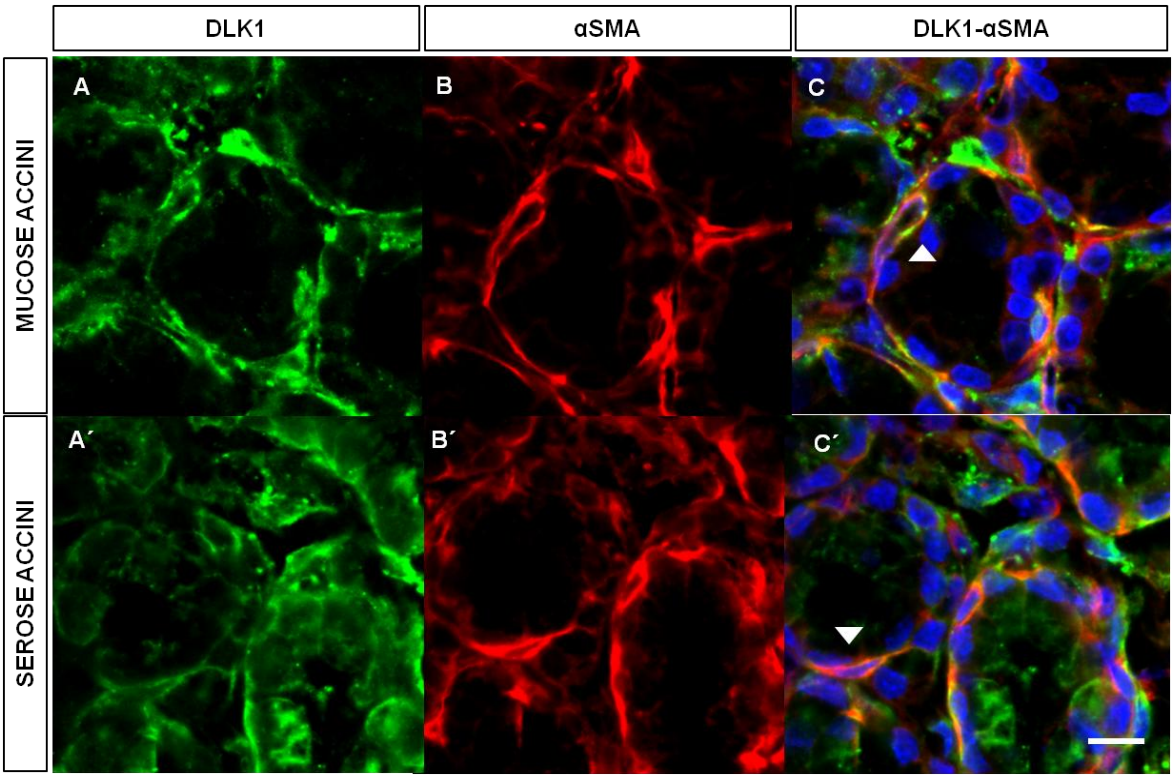

Figure 16. DLK1 and αSMA immunofluorescence of E17 SMGs. (A, A´) DLK1 expression (green) is positive for serous and mucous acini. (B, B´) αSMA labeling (red) and (C, C´) merged images for both markers showing a colocalization signal (arrows) corresponding to DLK1 labeling of myoepithelial cells. DLK1 is also present in cells of the serous acini. Scale bar: 20 µm.

In summary, DLK1 and DLK2 showed an apparently opposite expression pattern during the different stages of salivary gland development: DLK1 was poorly present in the epithelium of the SMG development; DLK2 was highly present in that tissue. Conversely, the salivary gland mesenchyme is strongly positive for DLK1 and less positive for DLK2. This inverse correlation of DLK1 and DLK2 expression levels has also been observed in other cell types (Nueda *et al*., 2007b). However, it is important to note that our antibodies only recognize intracellular epitopes of DLK1 and DLK2, and at least in the case of DLK1, it is known that the full protein can be cleaved and released as a soluble biologically active form (Wang & Sul., 2006; Mei *et al*., 2002). It is yet unknown whether DLK2 may undergo a similar proteolytic processing.

We compared the expression patterns of DLK1 and DLK2, with NOTCH signaling activity in the SMG, assessed by immunofluorescence against the NOTCH1 Intracellular Domain (N1ICD) fragment, which is the cleaved, nucleus-targeted, transcriptionally active form of the NOTCH1 receptor.

Thus, cells that activate NOTCH1 signaling presented higher levels of N1ICD immunoreactivity. N1ICD was intensely detected in SMGs from E17 to E19, both in the nuclei and in the cytoplasm of ductal and acinar cells (Fig 15.K-L). In the other stages of SMG development analyzed, N1ICD labeling showed a similar intensity for cells in the salivary mesenchyme and epithelium.

To assess whether NOTCH signaling was also active in the PSG neurons, we carried out a double immunolabeling with βIII tubulin and N1ICD. The result was a colocalization of these two markers, although the N1ICD signal was overall less intense in the PSG than in the adjacent salivary gland duct epithelia (Fig 17). Taken together, our results suggest that the NOTCH1 pathway is active in both the acinar and ductal epithelia as well as in the PSG, and this may have an important role in the regulation of the development of the SMG.

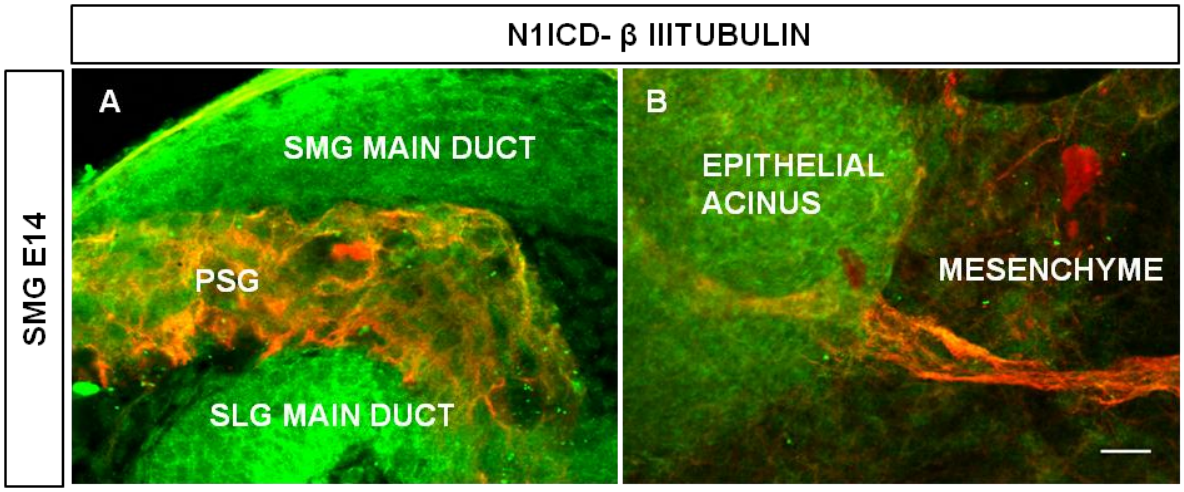

Figure 17. NOTCH signaling activity in the PSG. E14 SMG confocal immunofluorescence images showing a merge between N1ICD in green and β-III tubulin (PSG neuron marker) in red. Both the PSG (A) and the axonal bundles innervating the epithelial acini (B) appear labeled in yellow-orange, indicative of colocalization of these two markers. The main excretory ducts of the submandibular (SMG) and sublingual (SLG) glands are also intensely labeled for N1ICD. Scale bar: 20 μm.

4.2 DLK1 AND DLK2 PROTEINS INHIBIT NOTCH1 SIGNALING IN EPITHELIAL HSG CELLS

In preadipocyte and mesenchymal cells, DLK1 and DLK2 act as inhibitors of the NOTCH signaling pathway (Sánchez-Solana *et al*., 2011; Nueda *et al*., 2007a). To address whether DLK1 and DLK2 could also regulate NOTCH signaling in salivary gland cells we used a Human Salivary Gland (HSG) epithelial cell line to perform a luciferase assay, in which we measured the transcriptional activity of the NOTCH pathway.

To study whether DLK1 or DLK2 were implicated in NOTCH transcriptional activity, we co-transfected the HSG salivary gland cell line with pGLucWT/pRLT and HDLK1S or HDLK2S expression plasmids. Transfection with both HDLK1S and HDLK2S induced a significant reduction of luciferase activity (Fig 18.B), suggesting that both DLK1 and DLK2 act as inhibitory non-canonical ligands of NOTCH1 in HSG cells, as previously described in other cell types (Baladrón *et al*., 2005; Nueda *et al*., 2007b; Sánchez-Solana *et al*,. 2011). HSG cells treated with 10 µM DAPT (NOTCH inhibitory reagent) also presented decreased luciferase activity, to similar levels as those of transfected cells.

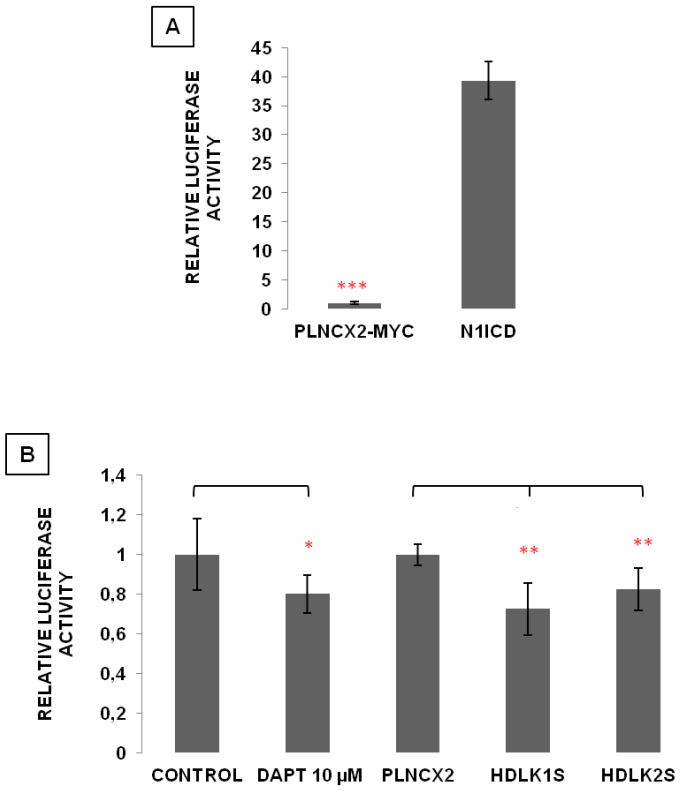

Figure 18. DLK1 and DLK2 inhibit endogenous NOTCH1 receptor-mediated signaling. (A, B) Luciferase/NOTCH activity measurements. (A) HSG cells were transfected with pGLucWT/pRLT plasmids, and with N1ICD expression plasmid as a positive control. (B) Luciferase activity of HSG cells transfected with pLPCX2 (as control) or HDLK1 or HDLK2 expression constructs, or treated with 10 µM DAPT. Mean ±SEM of three independent experiments. Analysis of variance (ANOVA) with post hoc Tukey test; *p ≤0.05,**p≤0.01,***p≤0.001.

To corroborate these results, we transiently transfected HSG cells with human DLK1S and DLK2S expression plasmids, and we assessed the expression of the NOTCH signaling target HES1 by immunolabeling and Image J quantification of the labeling density. We observed a significant reduction in the nuclear HES1 signal, which reinforced the inhibition of the pathway with both HDLK1S and HDLK2S transfection (Fig 19).

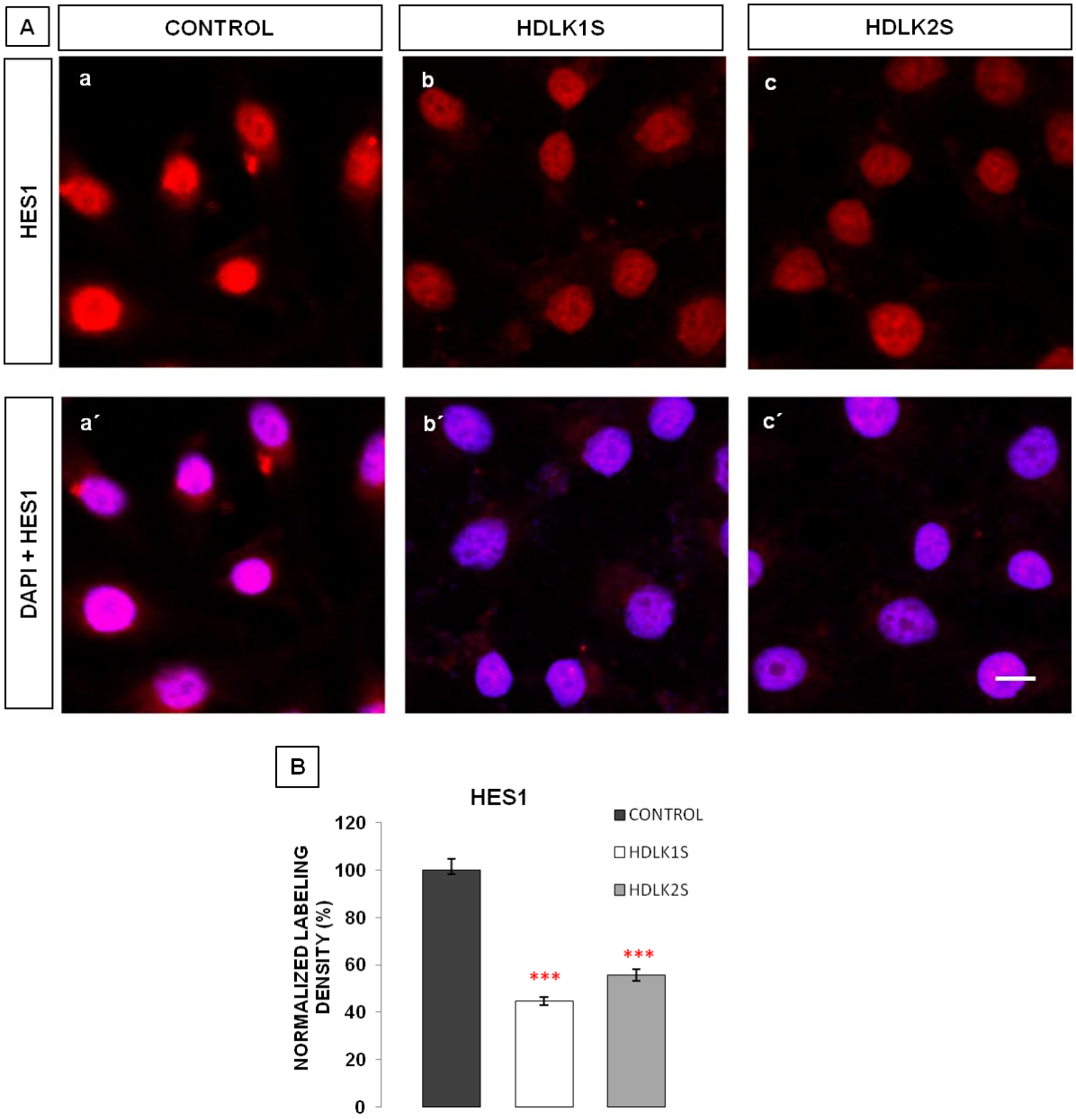

Figure 19. DLK1 and DLK2 reduce the specific NOTCH signaling target HES1. (A) Immunocytochemistry against HES1 after transient transfection of the HSG cell line with human DLK1 or DLK2 expression plasmids. (a) Control HSG cells (transfected with the control empty vector). HES1 protein localization is mainly nuclear. (b, c, b´, c´) Merged image of HSG cells transiently transfected (with plasmids HDLK1S or HDLK2S) and immunostained after 2 days. The cell nuclei were stained in blue with DAPI. Scale bar: 50 µm. (B) Quantification of the relative nuclear HES1 average fluorescence of HSG cells transfected with HDLK1S or HDLK2S plasmids, as compared to cells transfected with the empty vector. Mean ±SEM of three independent experiments. Analysis of variance (ANOVA) with post hoc Tukey test; ***p ≤0.001.

4.3 NOTCH SIGNALING INHIBITION DECREASES SMG BRANCHING MORPHOGENESIS AND INNERVATION

Previous studies showed that abrogation of NOTCH signaling by gamma-secretase inhibitors, like DAPT, inhibited the expression of differentiation markers in HSG cell lines, which suggested the importance of the NOTCH signaling pathway for salivary gland cell growth and differentiation (Dang *et al*., 2009). To evaluate whether blocking NOTCH signaling pathway could affect organ development and branching morphogenesis of the SMG, E13 SMG embryo primordia were cultured in the presence or absence of 2.5 µg/ml sDLK1 or 20 µM DAPT, for 2 days (Fig 20).

Firstly, we assessed whether exposure to sDLK1 effectively abrogated NOTCH1 signaling in SMG organ cultures, by immunofluorescence and immunoblotting against N1ICD. We found that sDLK1 induced a virtual disappearance of the N1ICD immunolabeling and N1ICD western-blot band (Fig 21.J). Therefore, similarly to the results obtained with the HSG cell line, sDLK1 inhibited NOTCH1 in the whole SMG (Fig 21.A,B).

Next, we evaluated whether the reduction in NOTCH1 activity affected branching morphogenesis of the cultured SMGs, by means of counting the number of acini, and calculating the percent spooner ratios at 24 h and 48 h of treatment (Fig 26).

A significant reduction in branching morphogenesis was found on SMGs exposed to a disruptive treatment of NOTCH signaling, either with sDLK1 or DAPT, as compared with the controls (Fig 20.B, C). The effect on branching was more evident after 48 h of culture, measured by spooner ratio (Fig 26).

The presumptive acini showed an abnormal morphology, including the appearance of darker areas in their center, when examined by transmitted light (Fig 20. arrows). In addition, the acini were wider and did not seem to form clefts, indicative of reduced branching ability.

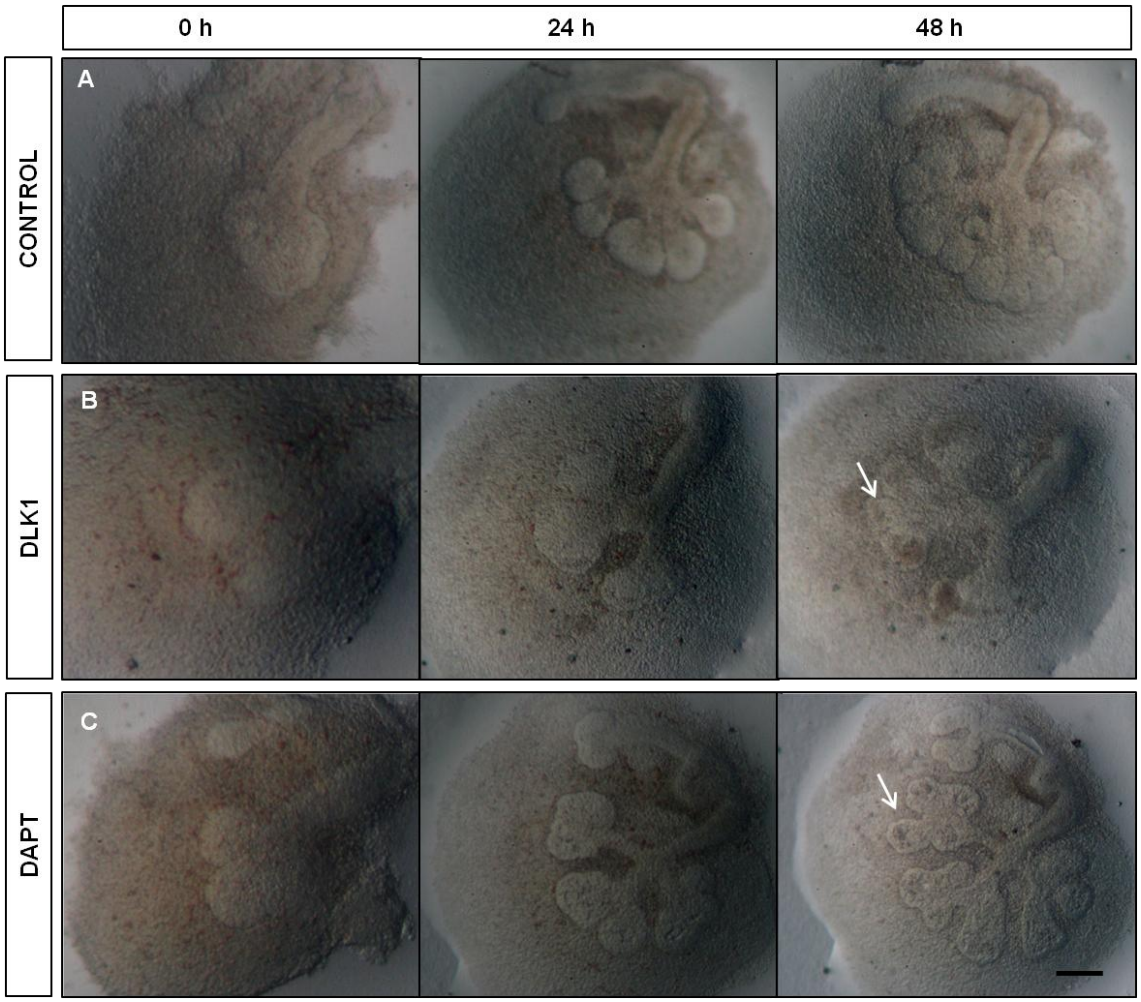

Figure 20. Inhibition of NOTCH signaling reduces branching morphogenesis and causes irregular morphology. (A) The natural morphological appearance of control E13 SMG at 0 h is that of a single end bud that branches exponentially and rapidly increased the number of end buds at 24 and 48 h *in vitro*. (B) 2.5 µg/ml sDLK1-treated SMGs showed a decreased branching and widened end buds (arrow) after 48 h in culture. (C) 20 µM DAPT-treated SMG for 48 h showed a similar abnormal morphology to that shown by sDLK1-treated SMGs. Scale bar: 150µm

To explore the cause of this reduction in branching morphogenesis, we analyzed cell proliferation in sDLK1 or DAPT-treated and control SMG cultures. Interestingly, either sDLK1 or DAPT-treated SMGs showed a rate of cell proliferation similar to that of control SMGs after 2 days in culture (Fig 21.E-F, H, I), as assessed by immunofluorescence against the cell cycle marker Ki67 and the cell mitosis marker Histone3-phosphate (H3P).

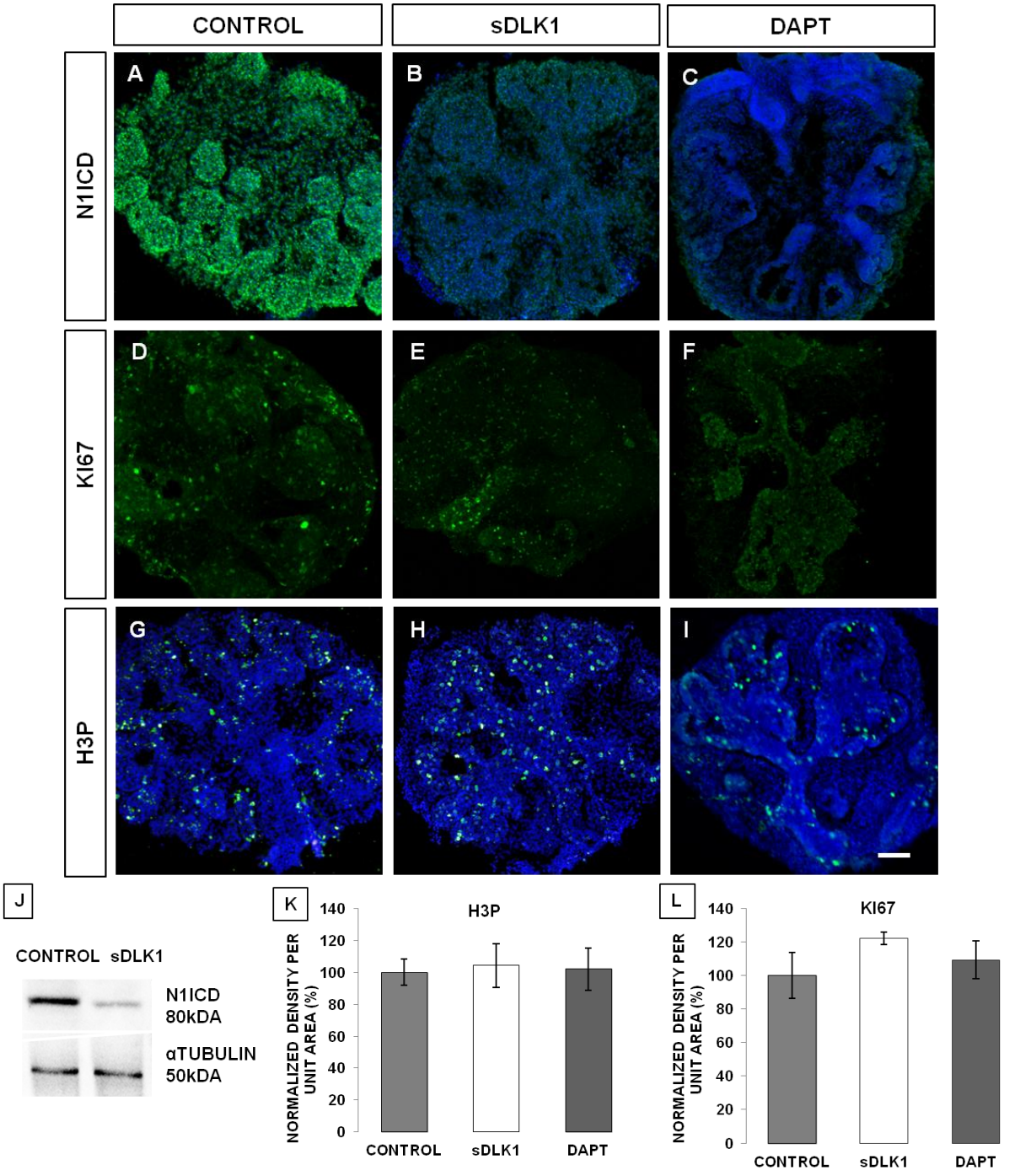

Figure 21. NOTCH signaling inhibition by DLK1 does not affect cell proliferation in SMGs. (A) Control SMGs E13 cultured for 48 h and immunostained with N1ICD (nuclei counterstained with DAPI) to evaluate the state of NOTCH1 activation. (B, C) SMGs E13 treated with 2.5 µg/ml sDLK1 and 20 µM DAPT for 48 h show far less N1ICD immunoreactivity. (D) Control SMGs E13 cultured for 48 h and immunostained with Ki67. (E, F) E13 SMGs treated for 48 h with sDLK1 and DAPT show a number of Ki67+ cells similar to that of controls. (G) Control E13 SMGs cultured for 48 h and immunostained with H3P. E13 SMGs treated for 48 h with sDLK1 (H) and DAPT (I) show a number of H3P+ cells similar to that of controls. Scale bar: 150 µm. (K, L) Graphics show quantification of the relative integrated labeling density per unit area of Ki67+ and H3P+ cells. The comparison of the control SMGs and SMGs treated with sDLK1 shows no significant difference by ANOVA. Mean ±SEM of three independent experiments. (J) Western blot assay showing a decrease in the intensity of the N1ICD band in E13 SMGs cultured for 48 h in the presence of sDLK1.

None of these assays unveiled a significant difference in the number of either Ki67^{+} or H3P^{+} labeled cells, suggesting cell proliferation in the SMG was unaffected by sDLK1 or DAPT. Considering that NOTCH signaling pathway is critical for the maintenance and survival of epithelial stem/progenitor cells during development (Banplain *et al*., 2006), we wondered whether decreased branching was related to an increase in epithelial apoptosis caused by NOTCH signaling inhibition.

Thus, we treated E13 SMG with DAPT and studied the rate of apoptotic cell death, by immunofluorescence against the active cleaved form of caspase3. Treatment with DAPT increased the number of caspase3^{+} cells in the lumens of presumptive acini. These clumps of apoptotic cells corresponded to a subpopulation of dying epithelial cells. Therefore, NOTCH signaling inhibition by DAPT caused an increase in acinar cell apoptosis (Fig 22.B). This apoptosis induction caused a disorganization of the distal acinar epithelia, as detected by transmission electron microscopy (Fig 22.B´). This apoptotic cells colocalized with the darker areas inside the acini of the SMG cultured 48h with the inhibitors of NOTCH signaling sDLK1 and DAPT as is showed in Fig. 20.B-C.

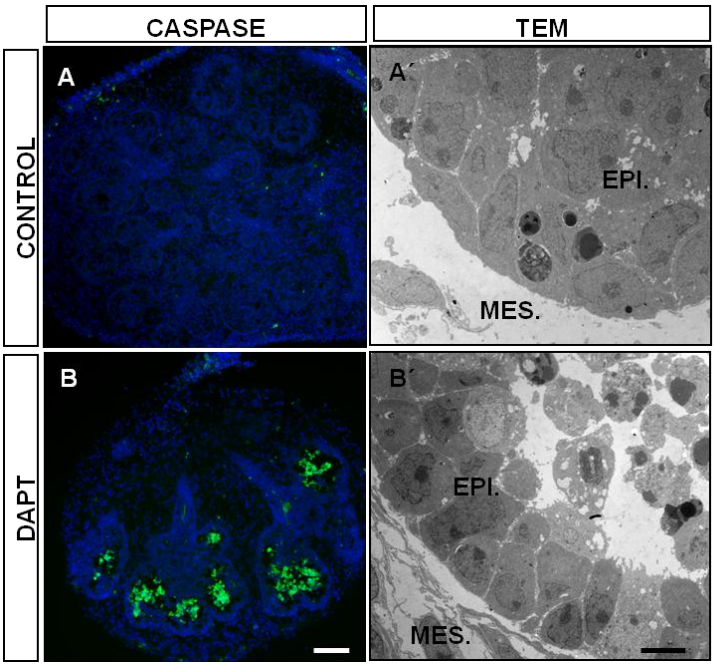

Figure 22. Inhibition of NOTCH signaling induces apoptosis of the epithelial cells inside the forming acini of cultured SMGs. Immunostaining against active caspase3 (green) of E13 SMGs cultured for 48 h (A, control) or treated with 20 µM DAPT (B). Caspase3^{+} cells accumulated inside the acini. Scale bar: 150 µm. TEM micrograph of E13 SMGs end bud control (A´) or treated with DAPT (B´) for 48 h, showing cells with apoptotic morphology inside the disorganized epithelium. Normal epithelium (EPI.) and the mesenchyme (MES.) are shown. Scale bar: 5 µm.

Recent reports point to parasympathetic innervation as a crucial factor modulating branching morphogenesis of the developing salivary gland. Thus, the presences of parasympathetic ganglia in the SMG, together with the cholinergic innervation of salivary epithelia by the resident neuronal cells, are two fundamental factors for the correct SMG organogenesis (Knox *et al.,* 2010). The development of peripheral nerve ganglia is also sensitive to NOTCH signaling (Taylor *et al*., 2007). In this context, we hypothesized that exposure to NOTCH inhibitors sDLK1 and DAPT could negatively impact on PSG neuronal development and innervation, which would affect SMG morphogenesis.

To assess whether the salivary epithelium-nerve interactions were well conserved after sDLK1 or DAPT treatments, we immunostained the cell body and axons of PSG neurons for βIII-tubulin**,** a cytoskeletal protein normally present in these cells.

In normal conditions, the PSG is extracted together with the SMG, and the axons thoroughly innervate the salivary epithelia (Fig 23.A, A') extending across and around the end of the initial buds. The axonal bundles tend to converge on the area of ductal epithelium from which lobular outgrowth occurs following a branching pattern. However, when we treated E13 SMGs with sDLK1 (Fig 23.B, B') or DAPT (Fig 23.C, C') for 48h, the innervation showed an abnormal pattern: βIII tubulin^{+} axons concentrated near to the PSG and in proximal ductal epithelia, and did never reach the end of the buds.

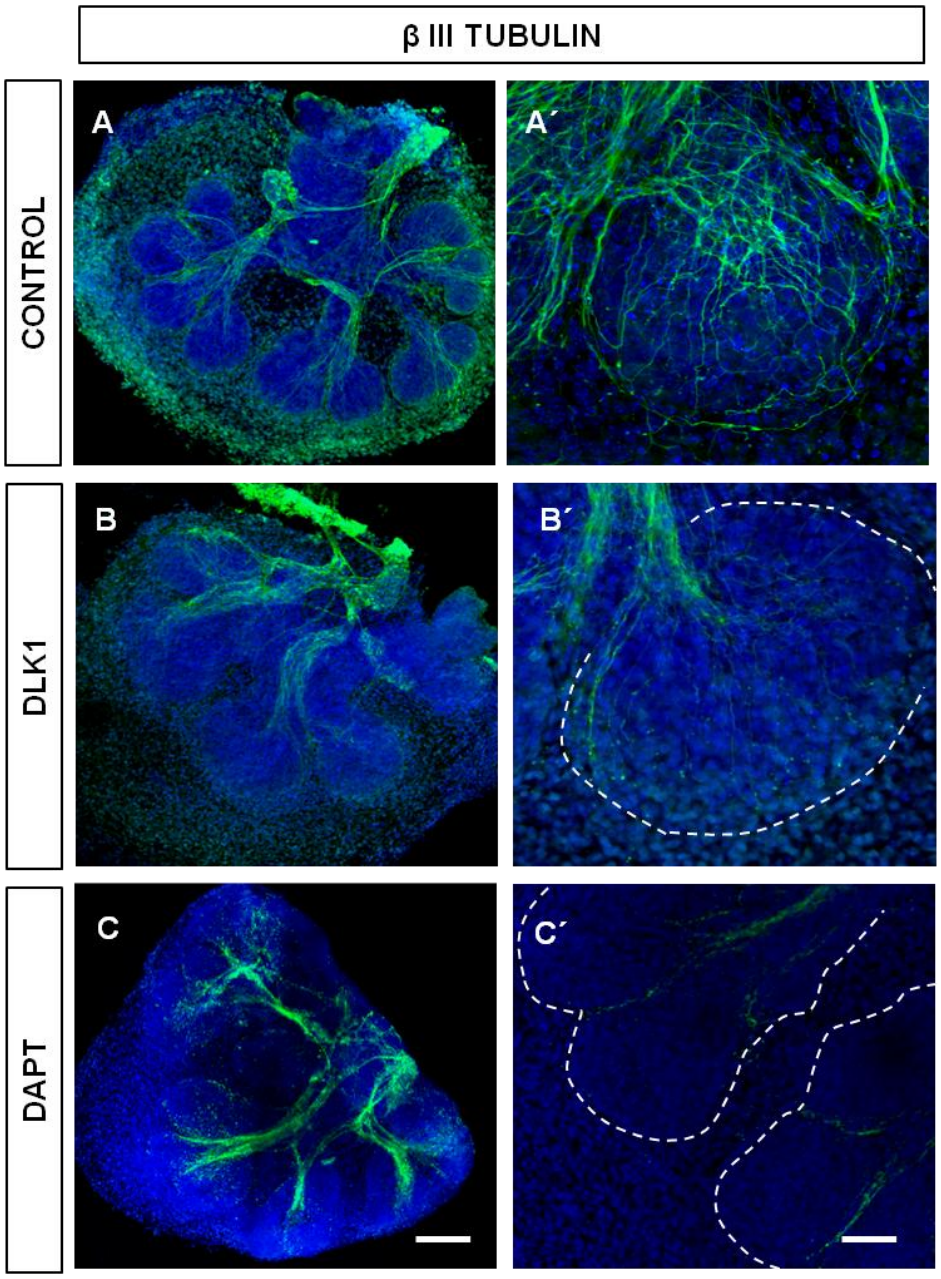

Figure 23. Salivary gland innervation is reduced when NOTCH is inhibited cultured SMG. (A-A´) Whole-mount image showing innervation (green; immunostaining for β III Tubulin) of control SMG E13 cultured for 48 h. High magnification (A) and extended focus (A´) on one of the end buds from A, innervation of a control SMG.(B) Innervation in sDLK1-treated SMG for 48 h. (B´) An end bud from B, showing less axonal density. (C) Innervation after DAPT treatment for 48 h. (C´) axons do not reach the end buds. (A-C): Scale bar: 150 µm. (A´-C´): Scale bar: 50 µm.

4.4 CHOLINERGIC ACTIVATION DOES NOT RESCUE NORMAL SMG BRANCHING MORPHOGENESIS, BUT RESTORES PSG INNERVATION IN sDLK1 OR DAPT-TREATED SMGs

When resident submandibular PSG were physically removed from the SMG in organ culture, a strong reduction in epithelial branching morphogenesis ensued (Knox *et al*., 2010). This effect was reported to be associated with a reduction in the number of cytokeratin 5^+ epithelial cell progenitors and was reversed by the addition of the acetylcholine analog Carbachol (CCh) to the culture media, thus compensating the loss of cholinergic nerve fibers. Since in our experiments we also observed a dramatic decrease in the axonal density innervating SMG acini after exposure to sDLK1 or DAPT, we wondered whether the loss of cholinergic input may be a reason why SMGs showed reduced branching morphogenesis when they were exposed to NOTCH signaling inhibitory treatments.

Taking this into consideration, we cultured E13 SMGs with 10 nM CCh alone and CCh in the presence of sDLK1 or DAPT, for 48h. Then, we studied branching morphogenesis (Fig 24.A, B, C) and innervation (Fig 25.A, B, C), as before. We found that CCh did not rescue normal SMG epithelial branching (Fig 26), but interestingly, innervation was completely restored with sDLK1+CCh or DAPT+CCh treatments(Fig 25.B, C), to levels quantitatively comparable (Fig 25.A) to those of control non-treated SMGs and CCh alone. The axonal density, as assessed by βIII tubulin whole-mount immunostaining, was clearly higher than that of sDLK1 or DAPT-treated SMGs that had not received CCh and only slightly lower compared to the control. However, despite the recovery of innervation by CCh treatment, the branching morphology of the SMGs was the same as those of SMGs treated with sDLK1 or DAPT and cultured in the absence of CCh.

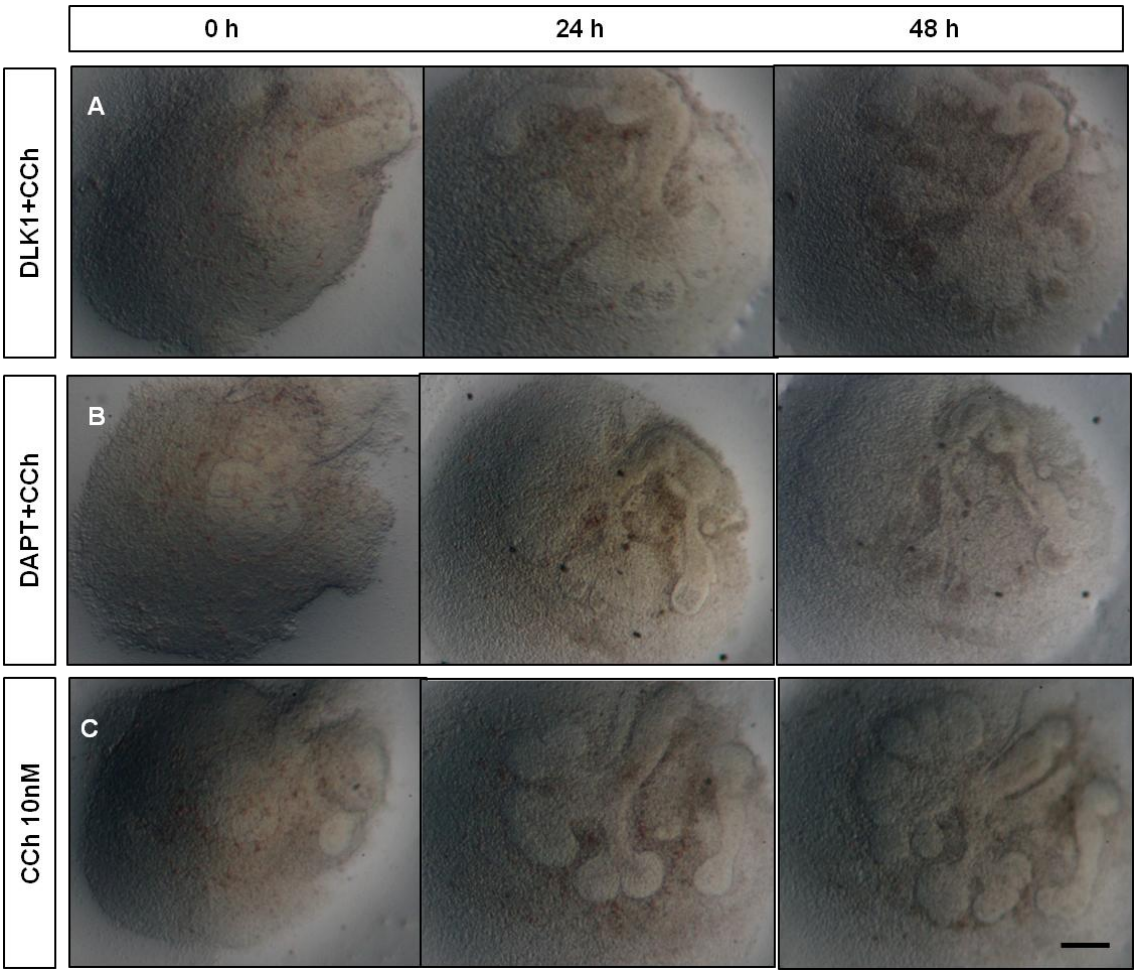

Figure 24. CCh addition does not restore branching morphogenesis (A) Morphology of sDLK1- and CCh-treated SMGs during 48 h. Normal morphology is not rescued by CCh addition (B) E13 SMGs treated with DAPT and CCh showing no rescue of normal morphology. (C) SMGs treated with 10 nM CCh for 48h (A-C) Scale bar: 150µm

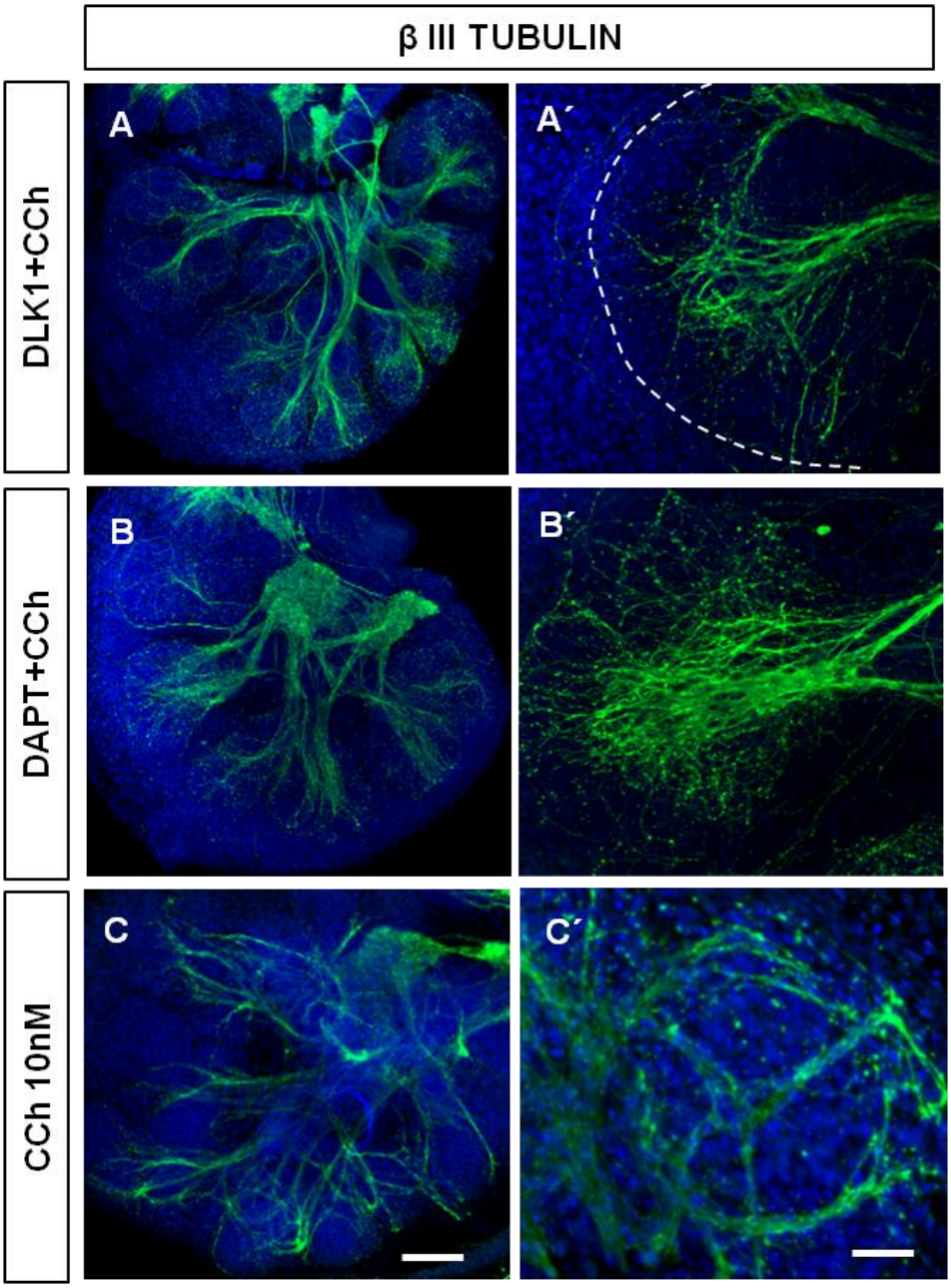

Figure 25. CCh increases the axonal density in the end buds. (A) Innervation of a sDLK1 and CCh treated SMGs for 48 h. (A´) Increased magnification showing restored axonal density after treatment with CCh. (B) Restored innervation of a DAPT- and CCh-treated SMG for 48 h. (B´) Magnification and expanded focus from J. (C) SMGs treated with 10 nM CCh for 48h and immunostained for β III tubulin showing innervation similar to control samples (C´) higher magnification. (A-C) Scale bar: 150µm. (A´-C´): Scale bar: 50 µm.

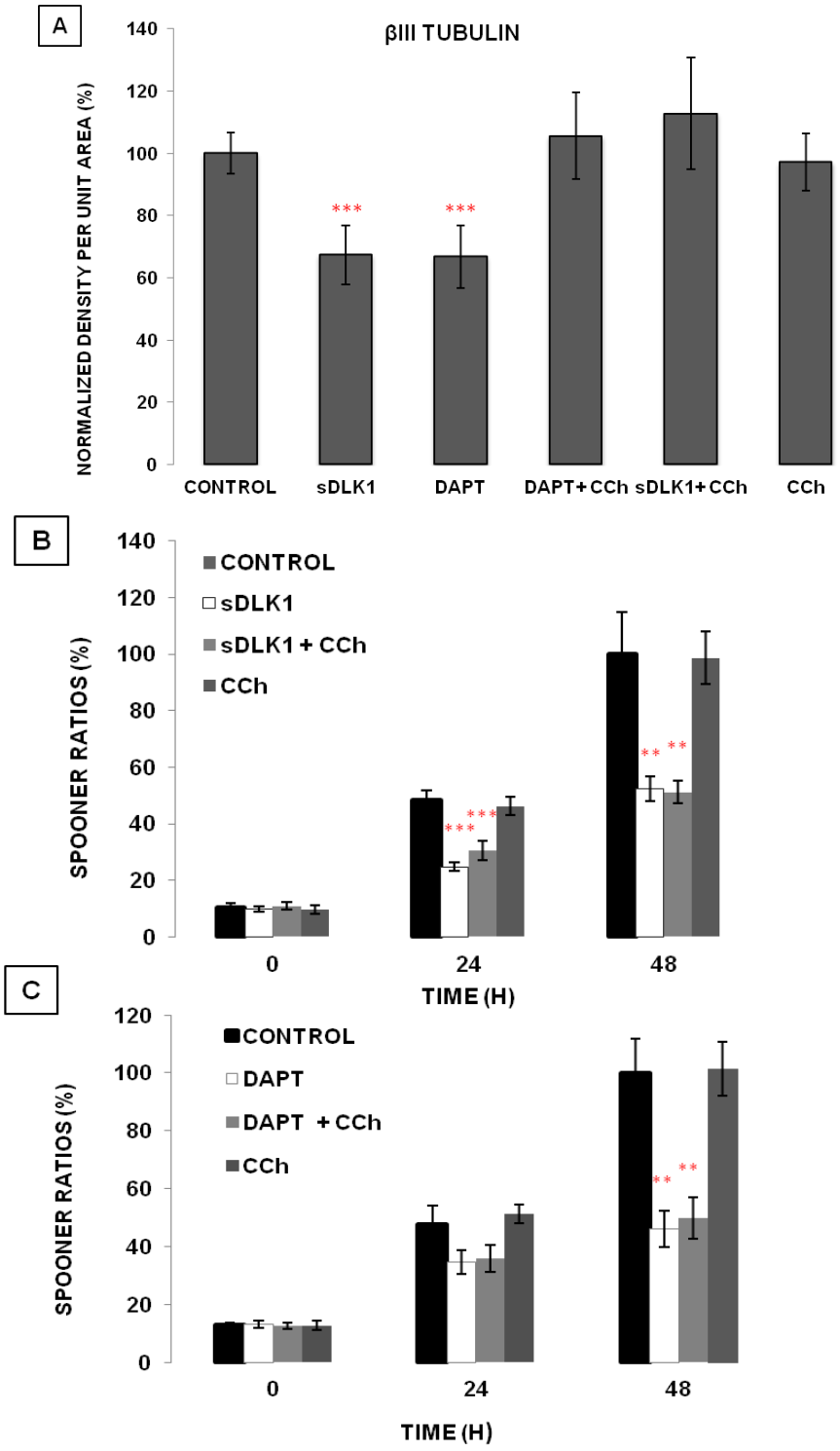

Figure 26. **Quantification of SMG branching morphogenesis after treatment with the NOTCH signaling inhibitors.** (A) Quantification of the innervation (βIII tubulin labeling density) of end buds for each treatment. Mean ±SEM (n=4). ANOVA with post hoc Tukey test; ***p ≤0.001. (B) sDLK1 and (C)DAPT, and with or without CCh. Acinar end buds were counted and the relative spooner ratios were represented for each SMG, with respect to control SMGs cultured for 48 h. Mean ±SEM of 10 SMGs from three independent experiments. Kruskal-Wallis test; **p≤0.01,***p ≤0.001.

Given that cholinergic activation was previously associated with an increase in cytokeratin 5^+ epithelial progenitor cells in SMGs (Knox *et al*., 2010), we wondered whether CCh treatment would increase the number of cytokeratin 5^+ cells in SMGs cultured in control conditions, or treated with sDLK1.

To this end, we performed whole-mount immunofluorescence of E13 SMGs cultured for 48h against cytokeratin 5 (Fig 27). SMGs in control conditions showed a majority of cytokeratin 5^+ cells located in the ductal proximal areas, roughly corresponding with the places where the PSG were present. A smaller population of cytokeratin 5^+ cells were scattered along the acinar epithelia. However, we found that the treatment with sDLK1 for 48 h induced a decrease in cytokeratin 5^+ cells, both in the ducts and the acini, which could be almost completely reversed by addition of 10 nM CCh (Fig 27). Therefore, the pool of cytokeratin 5^+ progenitor epithelial cells was preserved in SMGs treated with sDLK1 and CCh, although as mentioned before, this did not result in a rescue of normal SMG branching morphology.

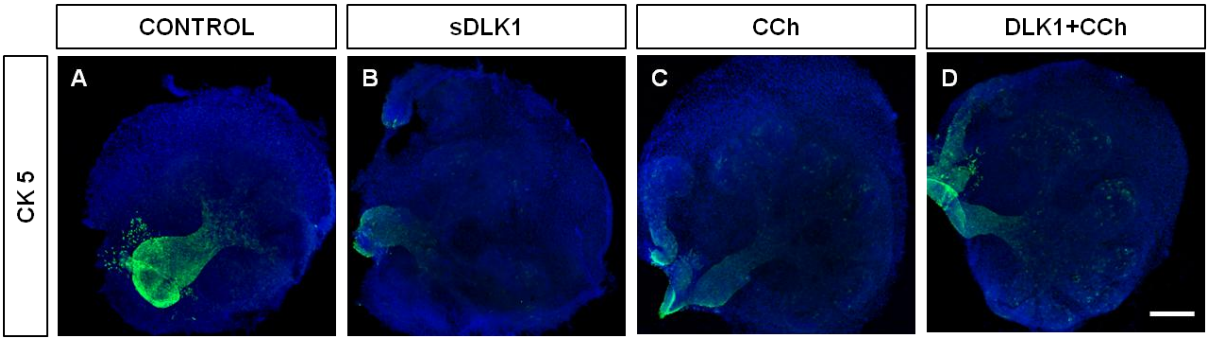

Figure 27. In vitro inhibition of NOTCH signaling with DLK1 reduces the number epithelial progenitor cells, which is reverted by CCh. (A) Whole-mount of control E13 SMGs cultured for 48 h showing $CK5^+$ (green) cells, mainly in the ducts and some in the acini. Nuclei were counterstained with DAPI. E13 SMGs cultured for 48 h in the presence of DLK1 (B) or CCh (C). Whole-mount immunofluorescence of E13 SMGs cultured for 48 h in the presence of DLK1 and CCh (D). Scale bar: 150 µm.

4.5 CHOLINERGIC ACTIVATION ENHANCES SMG BRANCHING MORPHOGENESIS RECOVERY AFTER WITHDRAWAL OF sDLK1 OR DAPT

Pharmacological cholinergic activation by CCh rescued salivary innervation and epithelial progenitor cell pools after treatment with sDLK1 for 48 h, but this did not suffice to rescue normal branching morphogenesis of the SMG.

As mentioned above, when SMG cultures were exposed to DAPT, apoptosis of a subpopulation of epithelial cells occurred. Maintaining innervation and the number of salivary progenitor cells may not be sufficient to restore normal branching morphology, if the new epithelial cells died shortly upon formation, failing to complete their differentiation. When a terminally-committed cell fails to differentiate properly, this usually leads to its rapid elimination by apoptosis; then, the epithelial cell loss would obviously hamper salivary branching restoration. Thus, we studied whether cholinergic activation would lead to a recovery of normal salivary morphogenesis, once the primary cause of the epithelial apoptosis (i.e: NOTCH signaling inhibition by sDLK1 or DAPT) was removed.

To assess this, we cultured E13 SMGs as before, for 96 h. In this context, SMGs were subjected to a NOTCH inhibitory treatment with sDLK1 or DAPT, for 48 h. Then, SMGs were allowed to recover in medium supplemented or not (control) with CCh, for another 48h. Recovery of a normal salivary branching morphogenetic pattern was enhanced in the presence of CCh, once sDLK1 or DAPT were removed from the culture media (Fig 28.B,D), as compared to controls (Fig 28.A, C). After 96 h in culture, SMGs exposed to CCh showed better branching spooner ratios than control SMGs, during the same time. Recovery under these conditions was stronger in the case of treatment with sDLK1. Interestingly, some of the acini presented a rod-like appearance.

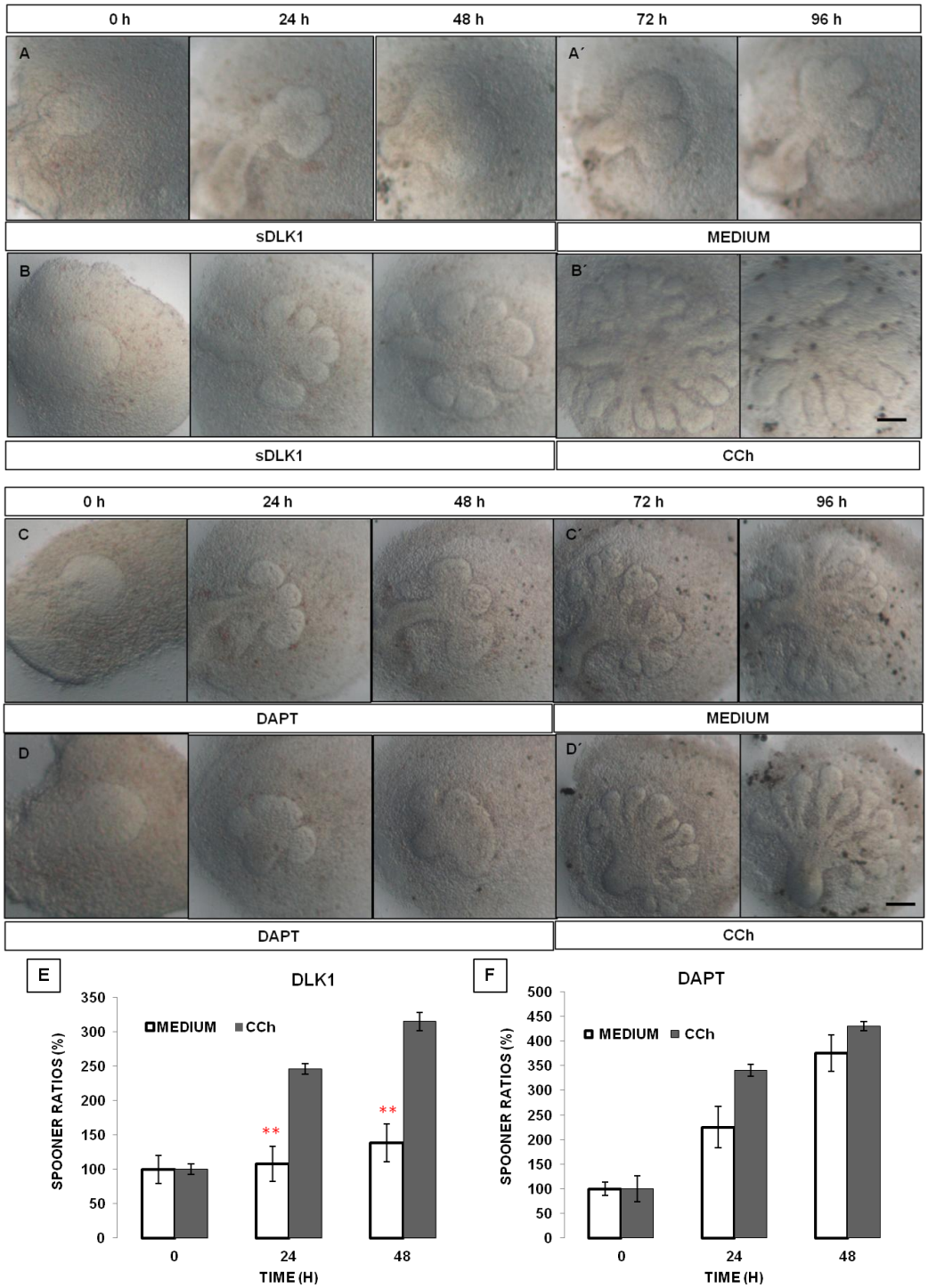

Figure 28. Carbachol (CCh) stimulates the recovery of branching morphogenesis in E13 SMGs treated with sDLK1 or DAPT during 48 h in vitro. E13 SMGs treated with 2.5 µg/ml sDLK1 or 20 µM DAPT for 48 h, were separated and a half was cultured in medium with 10 nM CCh for additional 48 h. SMGs cultured for 48 h with sDLK1 (A, B) and for additional 48 h with control medium (A´) or CCh (B´). SMGs cultured for 48 h with DAPT (C, D) and for additional 48 h with control medium (C´) or CCh (D´). The acini at 96 h in culture acquired a rod-like elongated shape after CCh treatment (*).Scale bar: 150 µm. Quantification of SMG branching morphogenesis after treatment with inhibitors sDLK1 (E) or DAPT (F) for 48h (time = 0) and additional 0, 24 or 48 h with medium alone or medium + CCh. Relative spooner ratios for each SMG were normalized and represented with respect to each control, mean ±SEM of three independent experiments (n=7). Kruskal-Wallis test; **p≤0.01.

4.6 INHIBITION OF NOTCH SIGNALING AFFECTS ISOLATED SALIVARY GLAND EPITHELIAL BRANCHING CULTURED *IN VITRO*

As demonstrated above, the inhibition of NOTCH signaling affects epithelial branching morphogenesis of the developing salivary gland. However, we did not know whether the branching inhibition was only a consequence of the reduced PSG arborization or if the NOTCH signaling inhibition was having any direct effect in the epithelia.

To answer this question we cultured *in vitro* isolated epithelia during 48h. Epithelia from E13 SMGs were separated from the mesenchyme, embedded in laminin and cultured for 48h in DEMEM F12 supplemented with fibroblast growth factor 10 (FGF10) and heparan sulphate (HS) as control or FGF10.HS with sDLK1 2.5 µg/ml. The control condition needs FGF10 to grow, and the HS in order to let the FGF10 accessible to its receptor in the epithelium (Patel *et al*., 2008, Makarenkova *et al*., 2009).

The initial control epithelia (Fig 29.A) had around 4-5 end buds. At 24 h of culture the end buds enlarge and the number increased to an average of 7. At 48 h, the number of end buds is not increased and they were thinner and longer. Though, when we add sDLK1 2.5 µg/ml (Fig 29.B), the morphology of the epithelia dramatically changed. More than the 50% of the epithelia decreased the number of end buds extensions to 3. The remaining loses all the end buds and had a round shape even at 24 h and at 48 h of treatment. These result showed that the inhibition of Notch signaling has a direct effect on the epithelial branching morphogenesis of the SMG.

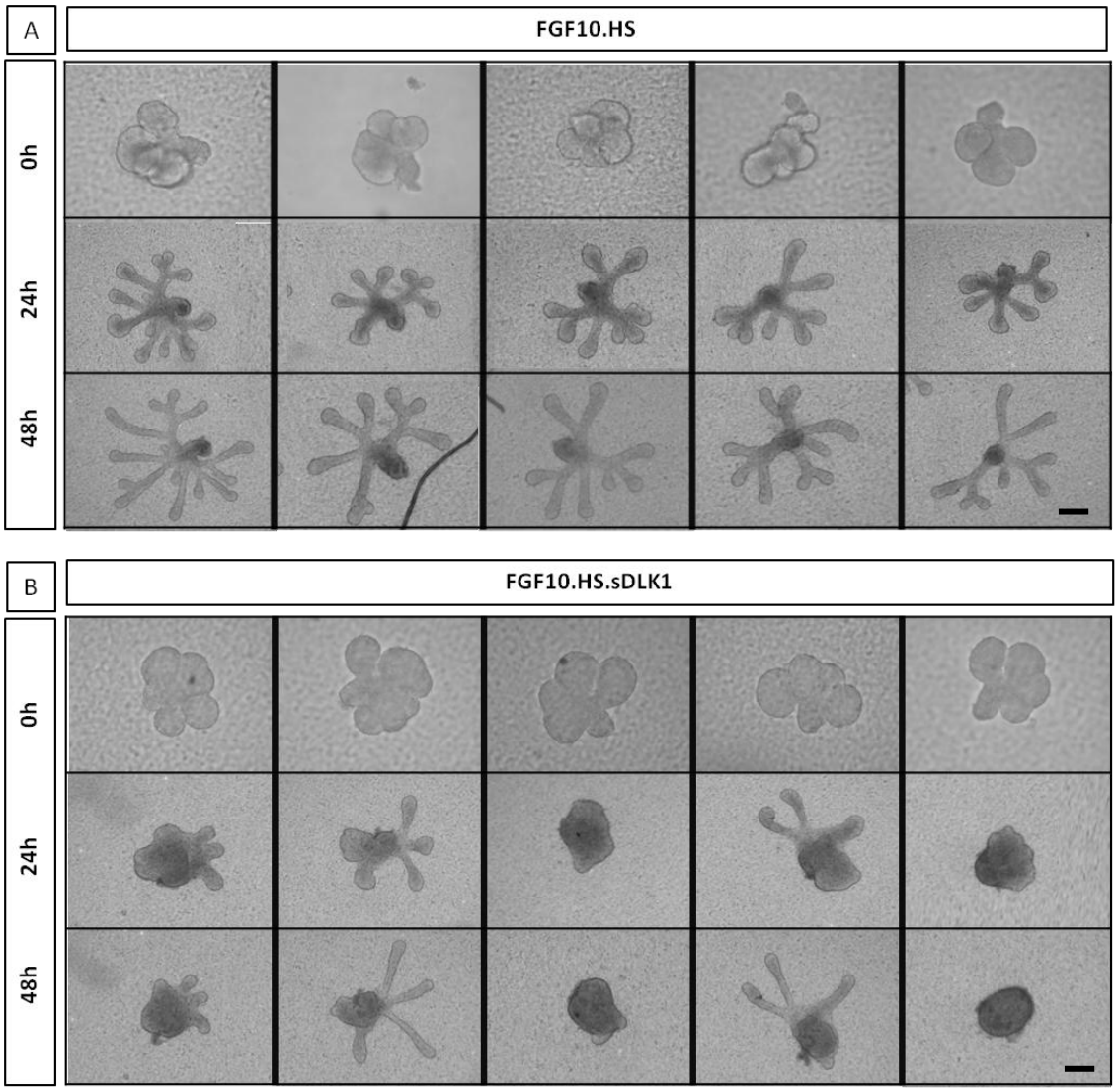

Figure 29. sDLK1 abolish end bud formation in SMG epithelia isolated culture. (A) Control epithelia (n=5) organotypic culture with FGF10.HS for 0h, 24h and 48h. (B) Epithelia (n=5) cultured with sDLK1 2.5 µg/ml has a reduced number of buds and loss the characteristic morphology of a developing epithelia. Scale bar: 100 µm.

4.7 *Dlk1* KNOCK OUT MICE FEATURES

Knockout (KO) mice are particularly useful tools that let study the specific effect of the inactivation of a gene. In or work mice were produced by a cassette containing *Neo* gene in *Dlk1* gene. For that reason, when we analyze mice genotype, we detected *Neo* gene in *Dlk1* (-/-), but not in the *Dlk1* (+/+) (Fig 30). Additionally, we found *Dlk1* gene in WT male and female mice, but not in *Dlk1* (-/-) mice.

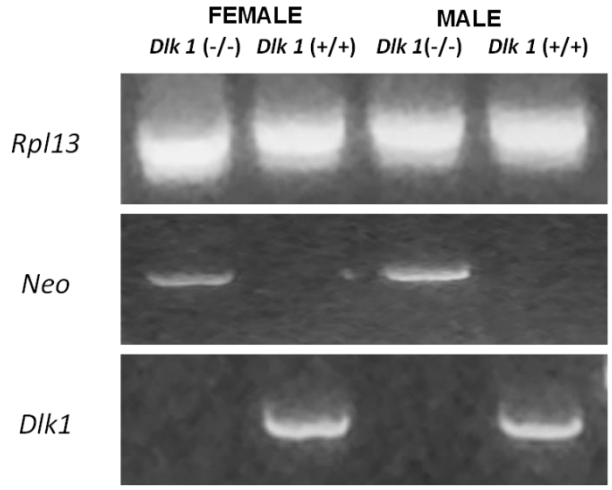

Figure 30. WT and KO *Dlk1* mice genotyping. DNA from the tail of a female and a male *Dlk1 (+/+)* and *Dlk1* (-/-) was amplified for a constitutive gene *Rlp13*, *Neo* and *Dlk1*. The WT mice express *Dlk1* and the *Dlk1 (-/-)* miceexpress *Neo* gene.

First studies on the phenotype of global *Dlk1*-null mice reported that these animals presented growth retardation, skeletal abnormalities and accelerated adiposity (Moon *et al*., 2002). Indeed, mice lacking *Dlk1* showed a reduced weight at birth and during the first weeks of life. Then, strains of mice generated on a BALB/CJ genetic background were eventually able to recover and gain a normal weight compared to wild type littermates (Moon *et al*., 2002), whereas the ones made on either a 129/SvJ or C57BL/6 background remained smaller throughout adult life (Cheung *et al*., 2013; Raghunandan *et al*., 2008).

To corroborate these findings we compared the body size for both strains (n=10). As suggested before, the *Dlk1* (-/-) mice were smaller and their bodies weighted less. The *Dlk1* (-/-) male body weight (25.6g±sd) was significantly smaller compared to *Dlk1* (+/+) male (34g±sd). The *Dlk1* (-/-) female body (22.3g±sd) also weighted less than the *Dlk1* (+/+) body (26.3g±sd). This body weight difference was stronger for the male mice than for the female (Fig 31).

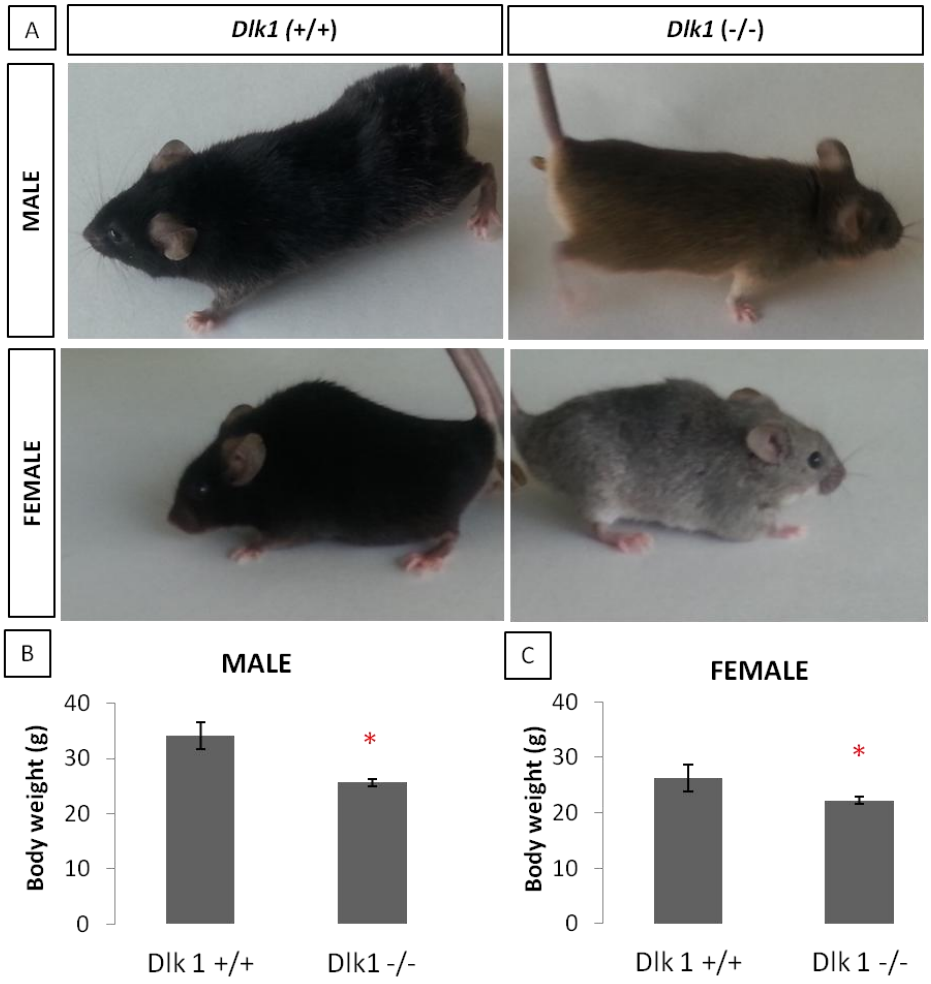

Figure 31. *Dlk1 -/-* male and female mice are smaller and weight less than *Dlk1 (+/+)* mice. (A) Images of appearance and size of mice. Male and female *Dlk1 (-/-)* mice are smaller in size that *Dlk1 (+/+)* mice. Above a graphic representation of the body weight for (B) male and (C) female, n=10 mice. Student test; *p≤0.05.

4.7.1 *Dlk1* KNOCK OUT SALIVARY GLAND PHENOTYPE

Since *Dlk1* is expressed during SMG development and has a role in salivary gland branching morphogenesis, we decided to look up the glands of the *Dlk1 (-/-)* mice and compared with the WT ones. We compared the anatomy and morphology of adult male and female *Dlk1* (-/-) and (+/+) mouse submandibular (SMG), sublingual (SLG) and parotid (PG) salivary glands. We exposed the glands of the mice after perfusion to be photographed (Fig 32.A), and we weighed them after careful dissection. The *Dlk1* (-/-) glands resulted to be smaller than the *Dlk1* (+/+) ones. In addition, the glands of the females were smaller than the ones of the males.

Thereafter, we weighed dissected glands of *Dlk1* (-/-) and *Dlk1* (+/+) mice, of n=6 males and females, and represented their relative weight with respect to the total body weight of the mice (Fig 32.B, C). Salivary glands of knock-out mice were smaller and weighed significantly less, both for males and females, than those of wild type mice. Moreover, the glands of the females weight less than the ones of the males. We attribute this size difference between males and females to the sexual dimorphism characteristic of the rodent salivary gland (Atkinson *et al*., 1959; Gresik E, 1980).

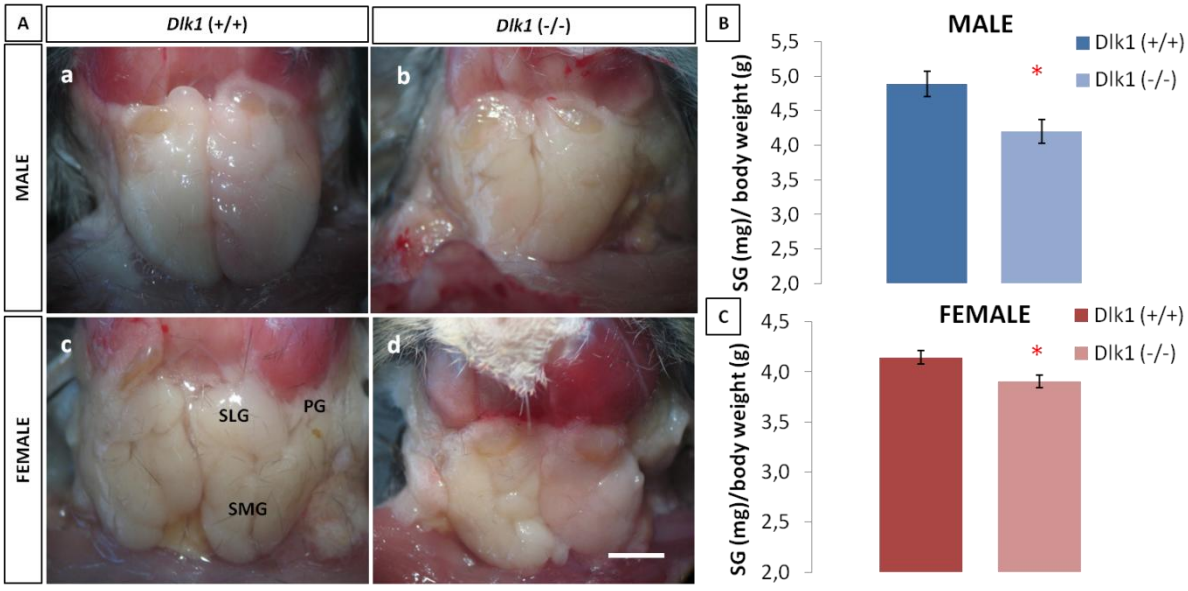

Figure 32. *Dlk1* (+/+) and *Dlk1* (-/-) adult salivary gland anatomy and weight. (A) SMG, SLG, and PG photographed at both sides of the neck after perfusion: (a) *Dlk1* (+/+) male (b) *Dlk1* (-/-) male (c) *Dlk1* (+/+) female (d) *Dlk1* (-/-) female. Scale bar: 5 mm. (B) Graphic representation of the weight (mg) of the salivary gland complex for male and (C) female of *Dlk1* (+/+) and *Dlk1* (-/-) mice in respect to total body weight (g).. Data are represented as mean ± SEM (n=10 of each group). Unpaired t Test, *p≤0.05.

As *Dlk1(-/-)* glands were smaller we decided to check out the histology of the adult salivary glands SMG, SLG and PG (Fig 33.A) and salivary glands through representative developmental stages (Fig 33.B). We wanted to assess if there were salivary gland malformations at the tissue-level.

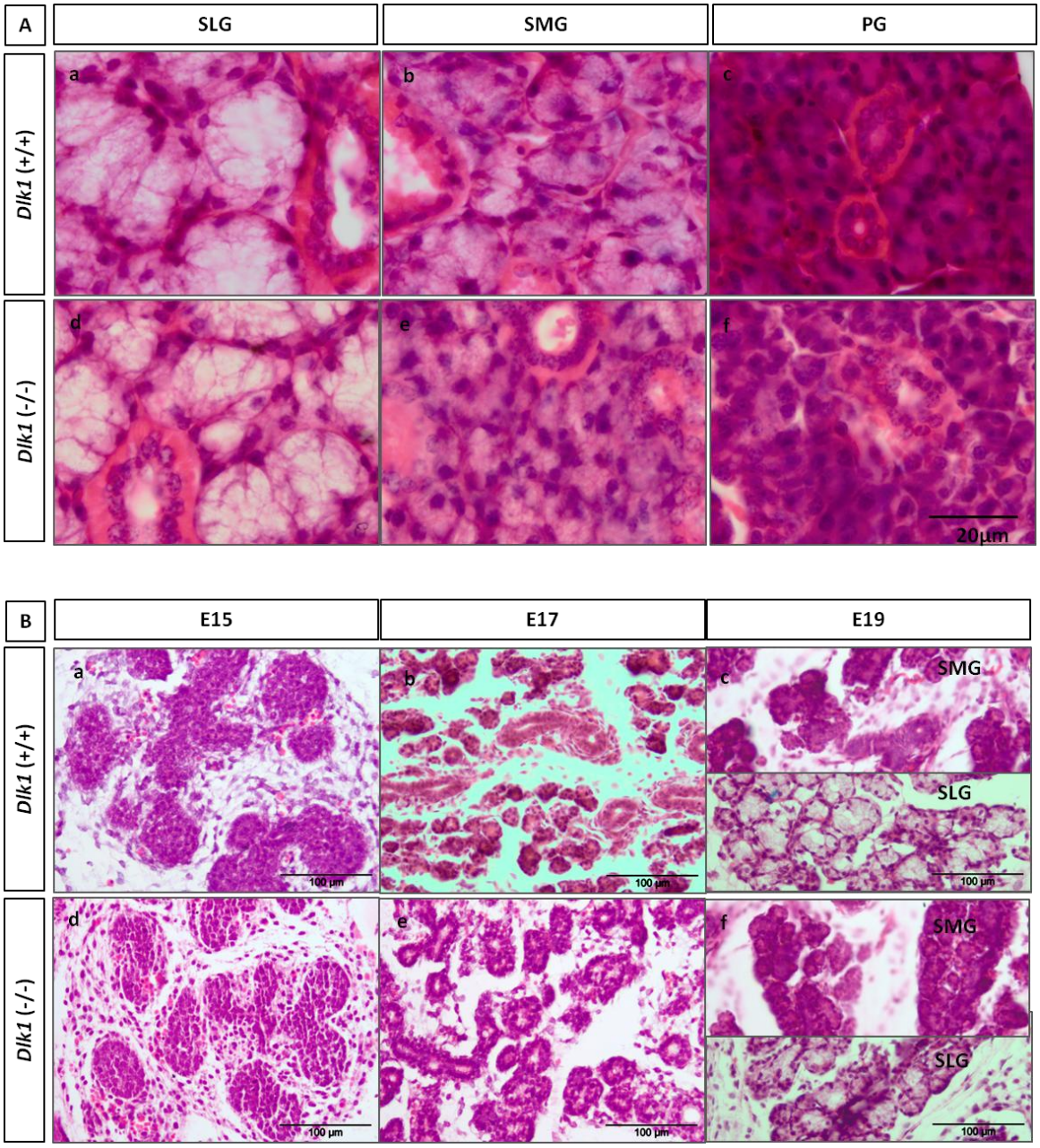

Figure 33. Hisltology of *Dlk1* (+/+) and *Dlk1* (-/-) salivary glands. (A) H/E staining on adult SLG, SMG and Parotid glands. Sacle bar: 20 µm. (B) H&E staining on E15 and E17 SMG , and E19 SMG and SLG. Scale bar: 100 µm.

The adult H/E was also similar for *Dlk1 (+/+)* and *Dlk1* (-/-) SLG, SMG and PG (Fig 33.A). In both mice, the SLG have the acini with high pyramidal cells with a pale basophilic cytoplasm and basal nuclei. The intercalated ducts are short and narrow and are lined by low cubical epithelium with the nuclei apical. The SMG, that produce seromucous saliva, are characterized by the granular convoluted tubules (GCT), which are among the intercalated and striated ducts. The acini contain high pyramidal cells with pale basophilic cytoplasm and central nuclei. Finally, the PG, mainly serous has in *Dlk1 (+/+)* and *Dlk1*(-/-) both very small acini. This are made up of pyramidal cells with strongly basophilic cytoplasm and large spherical nuclei at the base. The intercalated ducts are short and narrow and are lined by low cubical cells with large nuclei. A detailed histological examination did not reveal any difference between *Dlk1* (+/+) and (-/-) salivary glands.

Since *Dlk1* expression in the salivary gland takes place almost exclusively during embryonic development, we wondered if we would detect some kind of histological alteration in salivary glands at different stages of organogenesis (Fig 30.B). Thus, we stained sections of *Dlk1* (+/+) and (-/-) salivary glands at E15 (canalicular stage), E17 (terminal bud stage) and E19 (differentiation stage) with H/E. Progressive differentiation of SMG and SLG acini and tubuli was observed in this time sequence. At E15 the morphology of the glands is the tipical canalicular stage with the epithelia more coloured with eosin (pink) and the mesenchyme with less condensed cells more pale. At E17 the apearence of the *Dlk1* (+/+) and (-/-) SMGs are almost the same, and we start to see the ducts in transverse. At E19 we can celarly diferentiate the SMG more serous and the SLG mostly mucous (less pink becouse of it citoplasmic mucous containings), and there was not any noticeable difference between *Dlk1* (+/+) and *Dlk1* (-/-). However, again, no histological differences could be observed between *Dlk1* (+/+) and *Dlk1* (-/-) mice.

As there was no difference in the H/E, we stained paraffin samples for alcian blue in order to visualize the mucins contents of the glands (Fig. 34).

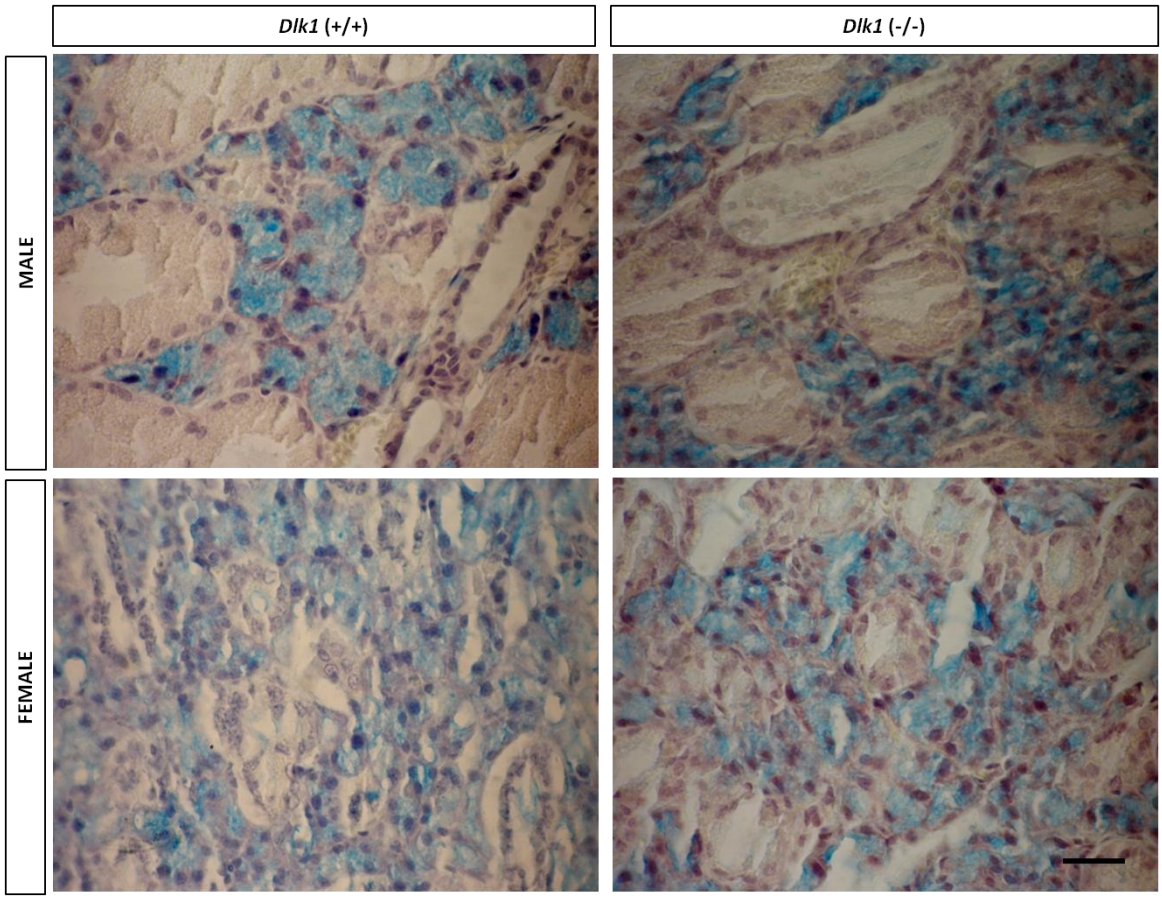

Figure 34. Similarities in the amount of mucins in the *Dlk1 (-/-)* and *Dlk1 (+/+)* male and female. SMG visualized by alcian blue staining. Scale bar: 20 µm.

However, the mucins, stained in blue, seem to be in very similar quantities between *Dlk1 (-/-)* and *Dlk1 (+/+)* despite the concentration seem to be different between males and females because males SMG show superior GCT.

Thereafter, the most likely explanation for the lack of a strong salivary phenotype in *Dlk1* (-/-) mice is some kind of genetic compensation. We have alreddy described that the related protein DLK2, structurally and functionally homologous to DLK1, was also present during salivary gland development. For this reason, we wanted to evaluate if a DLK2 upregulation could somehow account for a compensatory effect in the absence of DLK1 in knock-out mice.

Thus, we performed both a RT-PCR (Fig 35.B) and qPCR (Fig 35.C) to check *Dlk2* mRNA expresion of E14 and P1 SMG, and a immunocytochemical analysis of DLK2 protein expression in E13 and P1 SMG samples, but we found no difference between *Dlk1* (+/+) and (-/-) mice (Fig 35.A). Therefore, *Dlk2* expression upregulation does not occur in *Dlk1* (-/-) salivary glands, making this an unlikely mechanism for genetic compensation in this context.

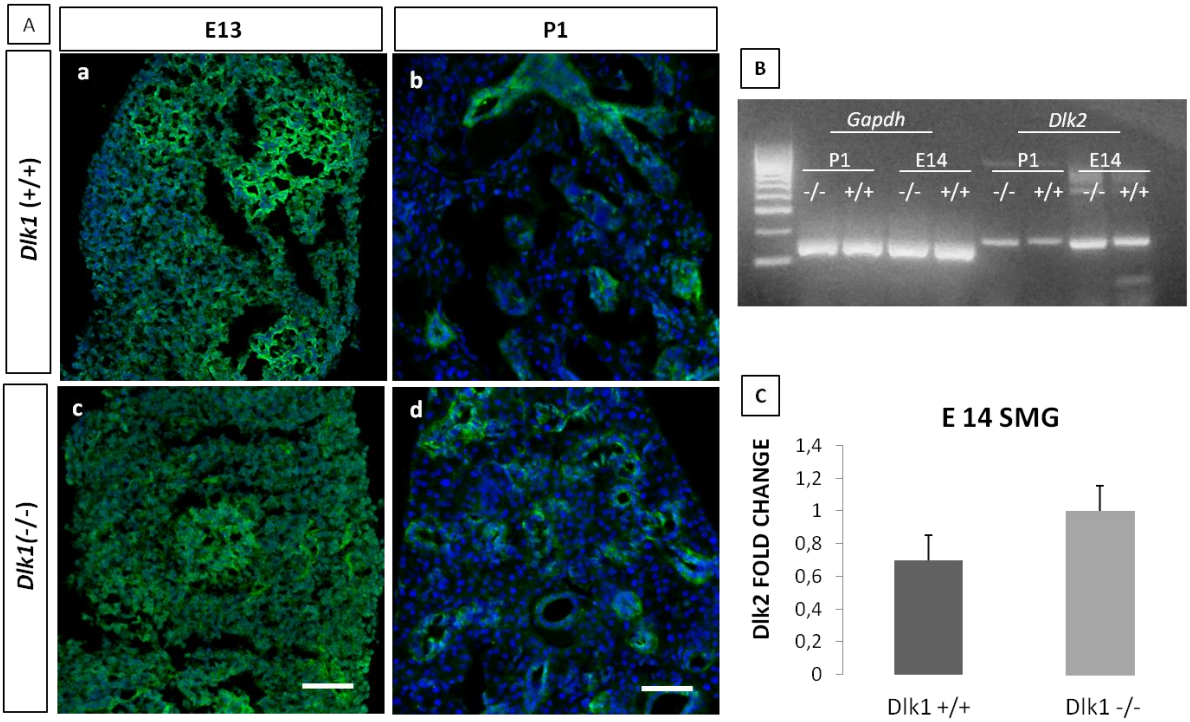

Figure 35. DLK2 levels are not compensating the absence of DLK1 in *Dlk1* (-/-) mice. (A) (a, c) E13 SMG stained with DLK2 is positive for epithelial end bud cells and mesenchyme, (b, d) P1 SMG stained with DLK2 is positive for ductal and acni epithelial cells and mesenchymal cells. (a, c) Scale bar: 150 µm. (b, d) Scale bar: 50 µm. (B) RT-PCR amplified products show no differences. (C) qPCR for *Dlk2* mRNA expression levels for *Dlk1* (+/+) and *Dlk1* (-/-) E14 SMGs. The differences are not statistically significant.

4.7.2 SMG FUNCTION ANALYSIS

Taking into account that *Dlk1* (-/-) mice presented smaller salivary glands with no alterations in their histological structure, we carried out a functional analysis. We measured the total amount of secreted saliva in *Dlk1* (+/+) and (-/-) mice, after stimulation with a pilocarpine injection. We observed that the *Dlk1* (-/-) mice, both male and female, produced a smaller amount of saliva as a function of time (0-22 minutes) compared to *Dlk1* (+/+) mice. For instance, after 22 min *Dlk1* (+/+) males could reach a secretion rate of 12 mg of saliva per body weight (g). By contrast, *Dlk1* (-/-) males only produced an average of 8 mg/body weight (Fig 36.A,C). Likewise, WT females reached a saliva secretion rate of 8 mg/body weight and the KO female only an average of 5 mg/body weight (Fig 36.B, D). There was also a difference in the rate of secretion between normal *Dlk1* (+/+) males and females, females comparatively producing less saliva than males, what we attributed to sexual dimorphism.

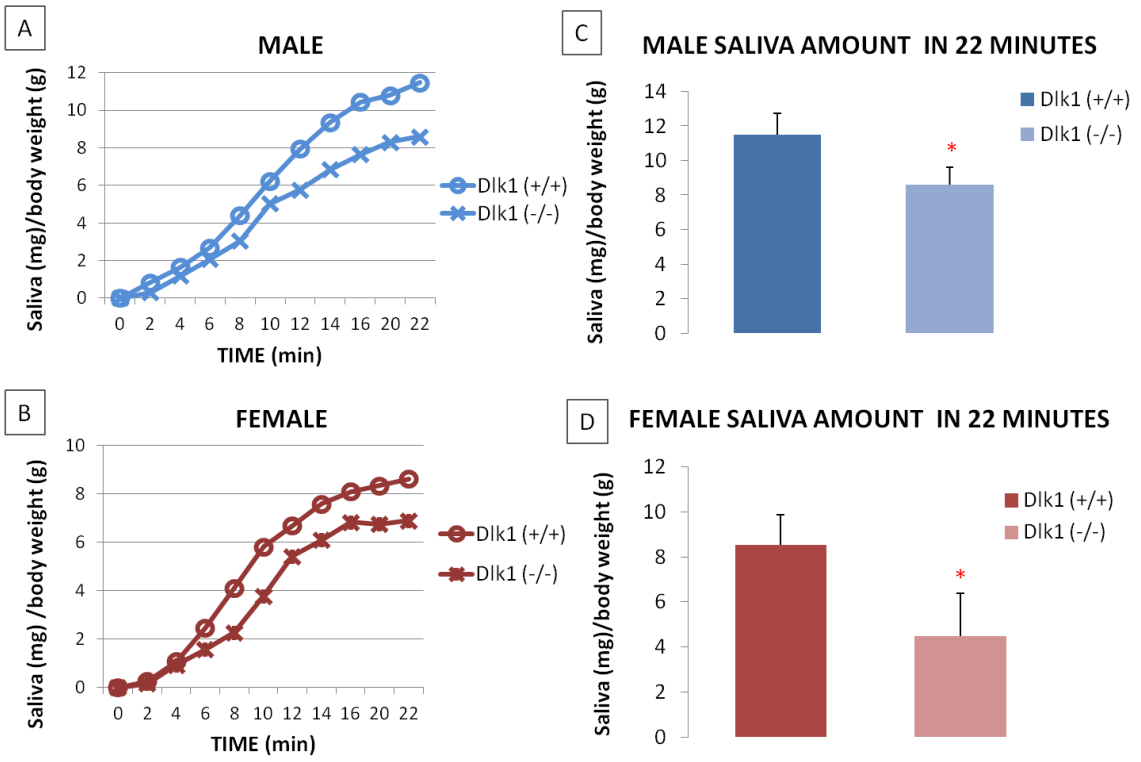

Figure 36. Saliva amount measurement. (A) After stimulation, produced saliva mg per body weight for the DLK1-/- and WT/WT males, (B) total saliva for the *Dlk1* (-/-) and *Dlk1* (+/+) males, (C) produced saliva mg per body weight for the DLK1-/- and WT/WT females, (D) total saliva *Dlk1* (-/-) and *Dlk1* (+/+) females. Paired T test * p≤0.05.

Considering this result, we wanted to determine why *Dlk1* (-/-) mice produced less saliva. The SMG is the gland which, in rodents, produces the biggest amount of saliva. Although we detected no histological anomalies in the acini and tubuli in H/E stained sections, it remained the possibility that SMG secretory units, especially acini and GCTs, would present some kind of ultrastructural defect, not detectable by H/E, which would relate with a reduced saliva secretion in *Dlk1* (-/-) mice. GCTs are the main histological feature that distinguishes the male and female SMG (Gresik E, 1980), as we corroborate with the toloudin blue staining (Fig 37).

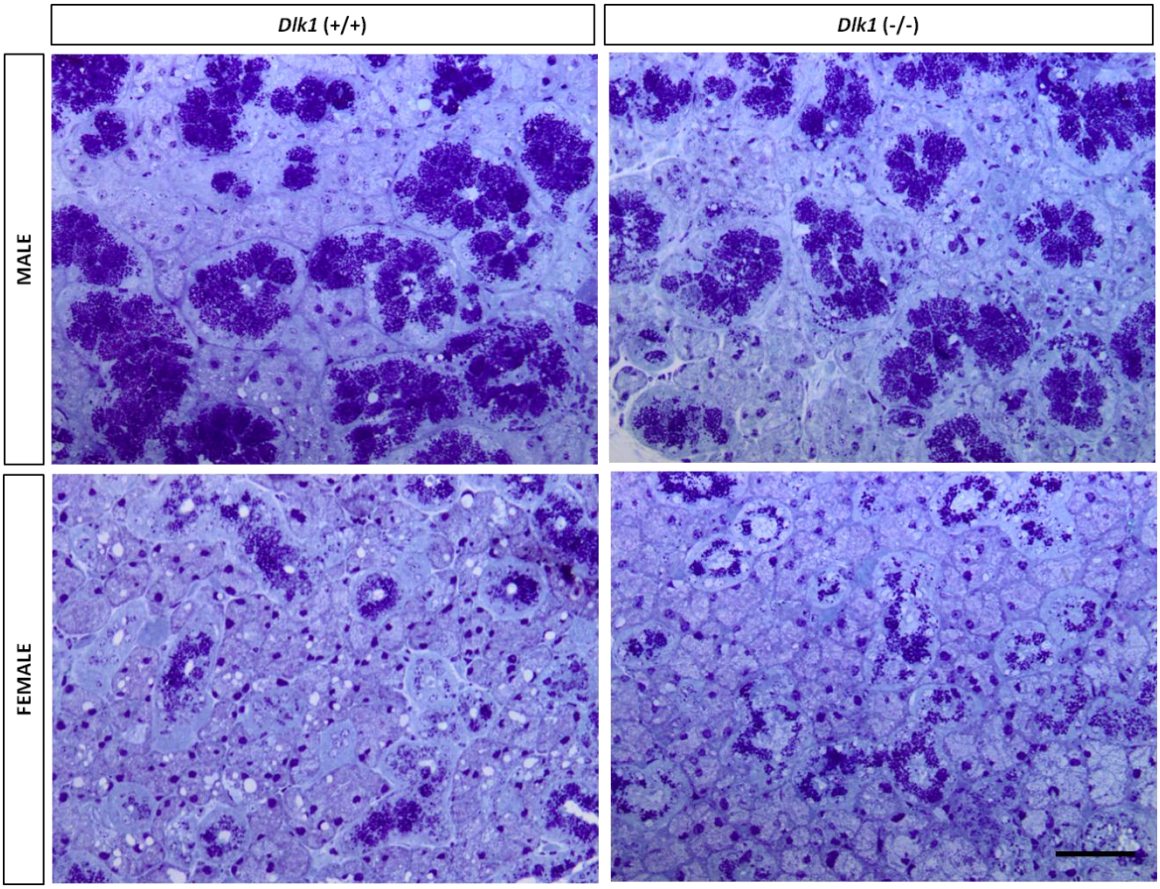

Figure 37. Sexual dimorphism in the SMG of both *Dlk1 (+/+)* and *Dlk1 (-/-)*. Toloudin blue staining for previsualating the samples before preparing for TEM. The biggest difference is in the number of CGT ducts between males and females. Scale bar: 50 µm.

As shown in Fig. 36, saliva secretion is significantly higher in males compared to females, which can be directly attributed to differences in GCT function. We wanted to assess if an alteration in GCT, the surrounding acini or the striated duct ultrastructure might be responsible for a similar decrease on saliva secretion in *Dlk1* (-/-) mice.

To address this question we visualized *Dlk1* (+/+) and (-/-) SMG by Transmission Electron Microscopy (TEM), which enabled us to visualize fine cellular details with a high magnification. As the sexual dimorphism is very marked in the mouse SMG, we examined males and females separately. TEM images revealed that sexual dimorphism involved changes in GCTs, which were bigger in males and had a higher amount of secretion vesicles (Fig 38.A, arrowheads), comparing to females. We also observed that the female SMG had bigger mitochondria accumulated in the basal side of striated duct cells, compared to the male SMG (Fig 38.B, arrowheads). Striated ducts on the male SMG still showed some secretory vesicles in the apical part of the cells, as these ducts are the continuation of GCT. However, we were not able to detect any difference by TEM, in the structure of neither acinar nor ductal cells, between *Dlk1* (-/-) and (+/+) SMG.

In males, the total amount of saliva produced after stimulation decreases 33.4% in the knock-out mice and the difference in the weight of the glands is 35.2% less for these animals, with respect to wild types. For the females, the reduction in saliva production is 37.5% and the difference in the weight of the glands is 25.5% less in *Dlk1* (-/-) mice.

We attribute the difference between *Dlk1* (+/+) and (-/-) mice in saliva secretion to a size difference in the salivary glands themselves. We assume that the bigger is the size of the glands, the higher will be their capacity to secrete saliva. Therefore, as salivary glands of *Dlk1* (-/-) mice are smaller than those of *Dlk1* (+/+), that seems to be the most likely explanation of why they produce less saliva.

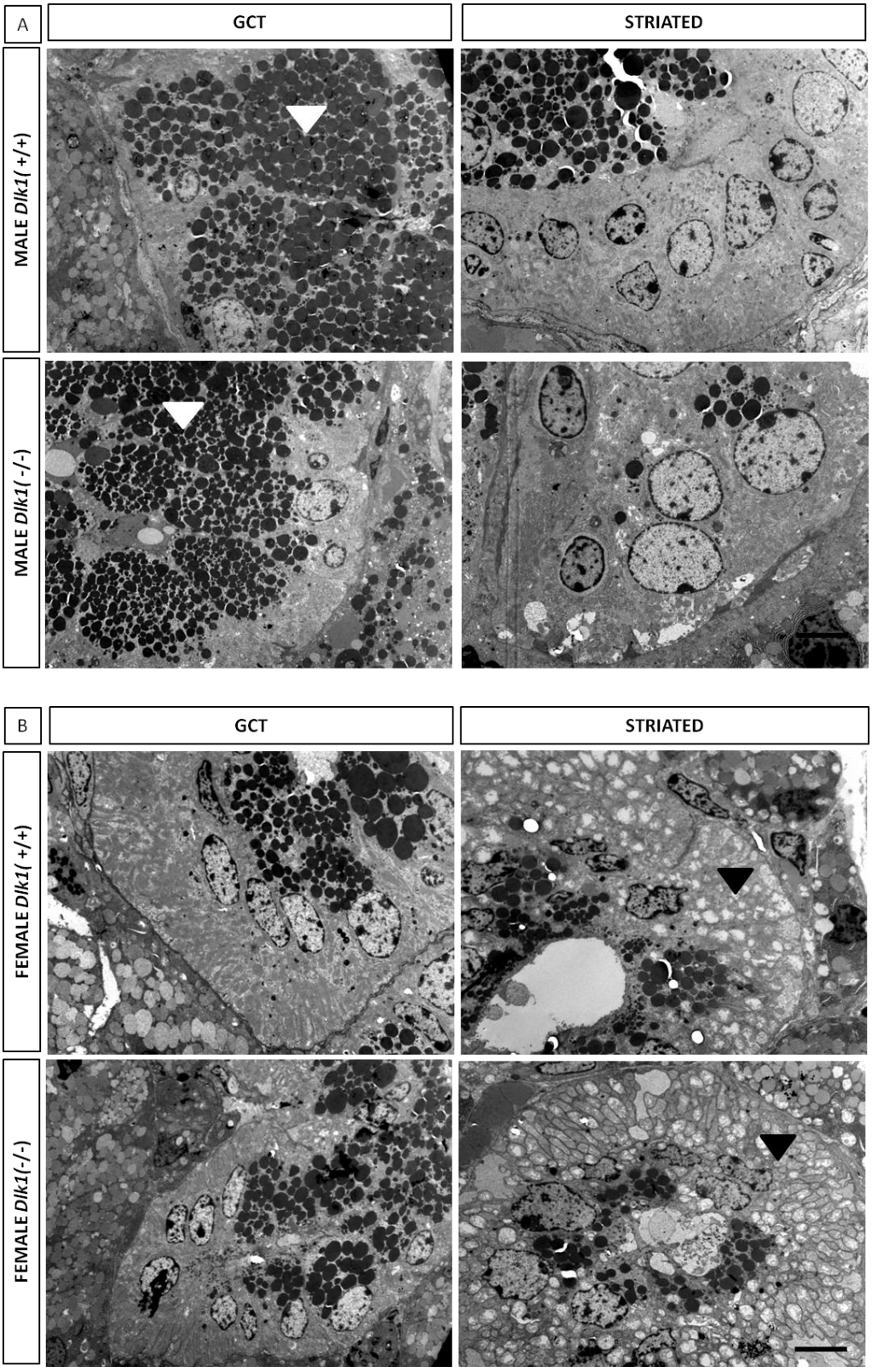

Figure 38. Transmission electron microscope images of the GCT and Striated ducts. (A) *Dlk1 (+/+)* and *Dlk1 (-/-*) GCT and striated ducts for the male. (B) *Dlk1 +/+* and *Dlk1 -/-* GCT and striated ducts for the female. Scale bar: 5 µm.

4.7.3 SALIVARY GLAND MARKERS

As DLK1 is a gene with genomic imprinting that it is important for SMG development and its function is related with the control of cell fate decisions, we thought that the absence of this protein in mice could be affecting the progenitor/stem population. Because of that we decided to check the levels of C*k5* and *Ck14*, two progenitor/stem cell markers of the salivary gland. CK5 and CK14 label different cell populations of salivary progenitors: whereas CK5 is predominantly a ductal marker, CK14 is more widespread and extends through both ducts and acini, with a peak of expression during the canalicular stage, around E15 (Lombaert and Hoffman, 2010).

Moreover, taken into account that the histology of the glands was not affected, the absence of *Dlk1* in the development of the gland could have being compensated by other pathways, so that is why we look for *Fgf10* that is one of the most important molecules which controls salivary gland development.

In addition, we considerate that maybe the histology could not be changing between WT and KO but for instance the molecular levels of a differentiation marker could be delayed or modified between these mice. So we check a differentiation marker of the salivary gland acini, *Aqp5*.

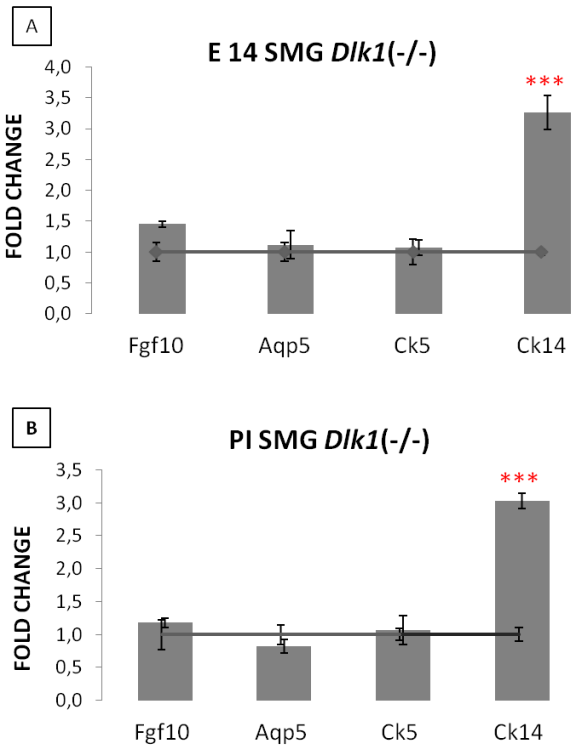

Figure 39. *Ck14* progenitor/stem cell marker is upregulated in *Dlk1 (-/-)* mice vs. *Dlk1 (+/+)*. qPCR analysis of gene expression in SMG at (A) E14 and (B) P1, there is no difference between *Fgf10*, *Aqp5* and *Ck5*, but *Ck14* is around three fold increase in both stages. Normalized to WT mice. Data plotted as mean ± SEM. Unpaired t Test;***p≤0.001.

To study these markers we used the qPCR at early in development, E14 SMG and late stages P1 SMG of *Dlk1* (-/-) and *Dlk1* (+/+) mice. The analysis of the qPCR levels reveals that *Fgf10*, *Aqp5* and *Ck5* remain unchanged. Nonetheless, *Ck14* was increased three fold in *Dlk1* (-/-) compared to the *DLK1* (+/+) (Fig 39). To corroborate these results we stained salivary gland sections with different antibodies.

Innervation is a crucial factor not only to regulate the physiology and secretion rate of the adult salivary gland, but also to regulate its proper organogenesis (Knox *et al*., 2013; Knosp *et al*., 2012). During embryo development, at branching morphogenesis stages, a communication is established between growing axon terminals from the PSG and the branching salivary epithelium. Moreover, as sDLK1 is blocking branching morphogenesis in the SMG, this came along with a loss of PSG innervation and a fall in CK5-positive epithelial cell numbers. We decided to analyze both these developmental features in the SMG of *Dlk1* (+/+) and (-/-) mice.

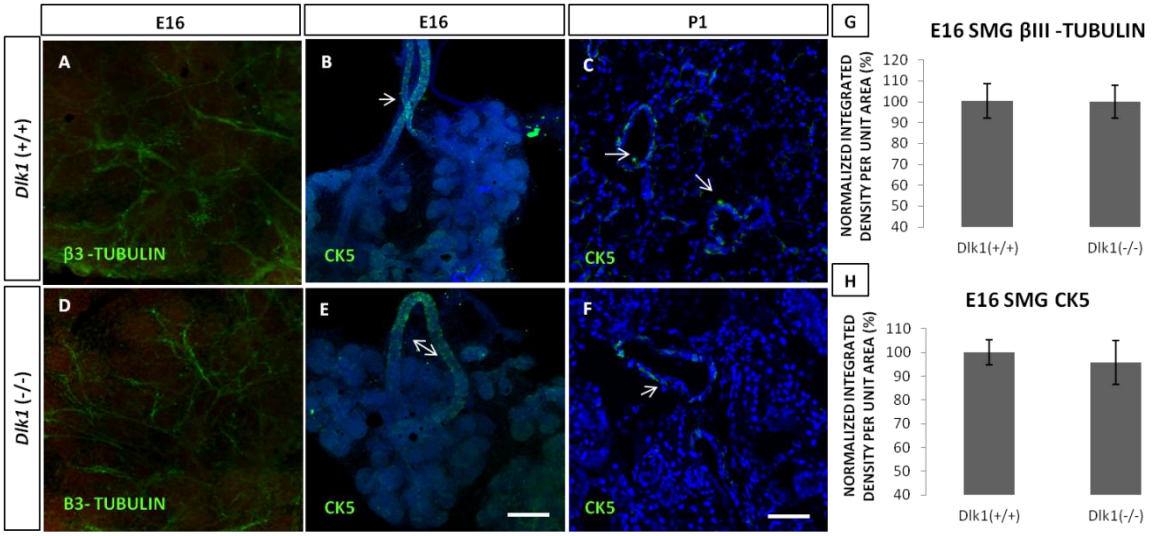

Figure 40. Immunostaining of PSG innervation and CK5+ progenitor cells in *Dlk1 (+/+)* vs. *Dlk1* (-/-) SMG. (A, D) Innervation staining against βIII-tubulin in green shows no differences between *Dlk1* (+/+) and *Dlk1* (-/-) E16 SMG (B,E) Epithelial progenitor cell marker CK5 staining in E16 SMG, for *Dlk1 (-/-)* and *Dlk1* (+/+) mice. These cells are located mainly in the excretory ducts. (C, F) CK5 marker staining in P1 SMG, mainly found in the basal epithelial cells of the ducts. (G,H) Fluorescent labeling density quantification of βIII-tubulin (A,D) and CK5 (B,E) staining, respectively. Data are represented as mean ± SEM.. Scale bar: 50 µm. (B,E) Scale bar: 150 µm.

E16 *Dlk1* (+/+) and (-/-) mouse SMGs were whole-mount immunostained for the PSG axonal marker βIII Tubulin. We saw that axons were properly extended through epithelial end buds at this stage (Fig 40.A, D). Besides, we made an inmunostaining for CK5+ epithelial progenitor cells at E16 (Fig 40.B, E) and P1 (Fig 40.C, F). These cells are typically and most abundantly located in the excretory ducts, as we found for both E16 and P1 SMG samples.

However, no differences were detected, neither in PSG innervation (βIII Tubulin) nor in epithelial CK5 progenitor cell populations, when we compared *Dlk1* (+/+) and (-/-) SMGs.

Indded we quantified the fluorescence density of these samples with Image J and no differences were detected, neither in PSG innervation (βIII Tubulin) nor in epithelial progenitor cell populations (CK5), when we compared the localization and the intensity of inmunostaining in *Dlk1* (+/+) and *Dlk1* (-/-) SMGs (Fig 5.G, H). So, we conclude that *Dlk1* absence does not affect these developmental characteristics of the SMG in genetically modified mice.

Acording to the qPCR results, mRNA levels for *Ck14* were increased three-fold in *Dlk1* (-/-) SMG, at both developmental stages, E14 and P1 (Fig 41). This striking result prompted us to examine CK14 protein expression by immunocytochemistry in SMG from *Dlk1* (+/+) and (-/-) mice. As expected, *Dlk1* (-/-) SMG showed more CK14-positive cells (Fig 39).

In the normal SMG at P1, CK14 labeling displays a characteristic grid-like pattern, showing the long and thin cytoplasms of myoepithelial cells surrounding round acinar and ductal structures. By contrast, in *Dlk1* (-/-) SMGs of same age, in addition to the typical myoepithelial labeling pattern, we also could identify many other CK14-positive cells, some of them intensely labeled, inside the ducts and the acini.

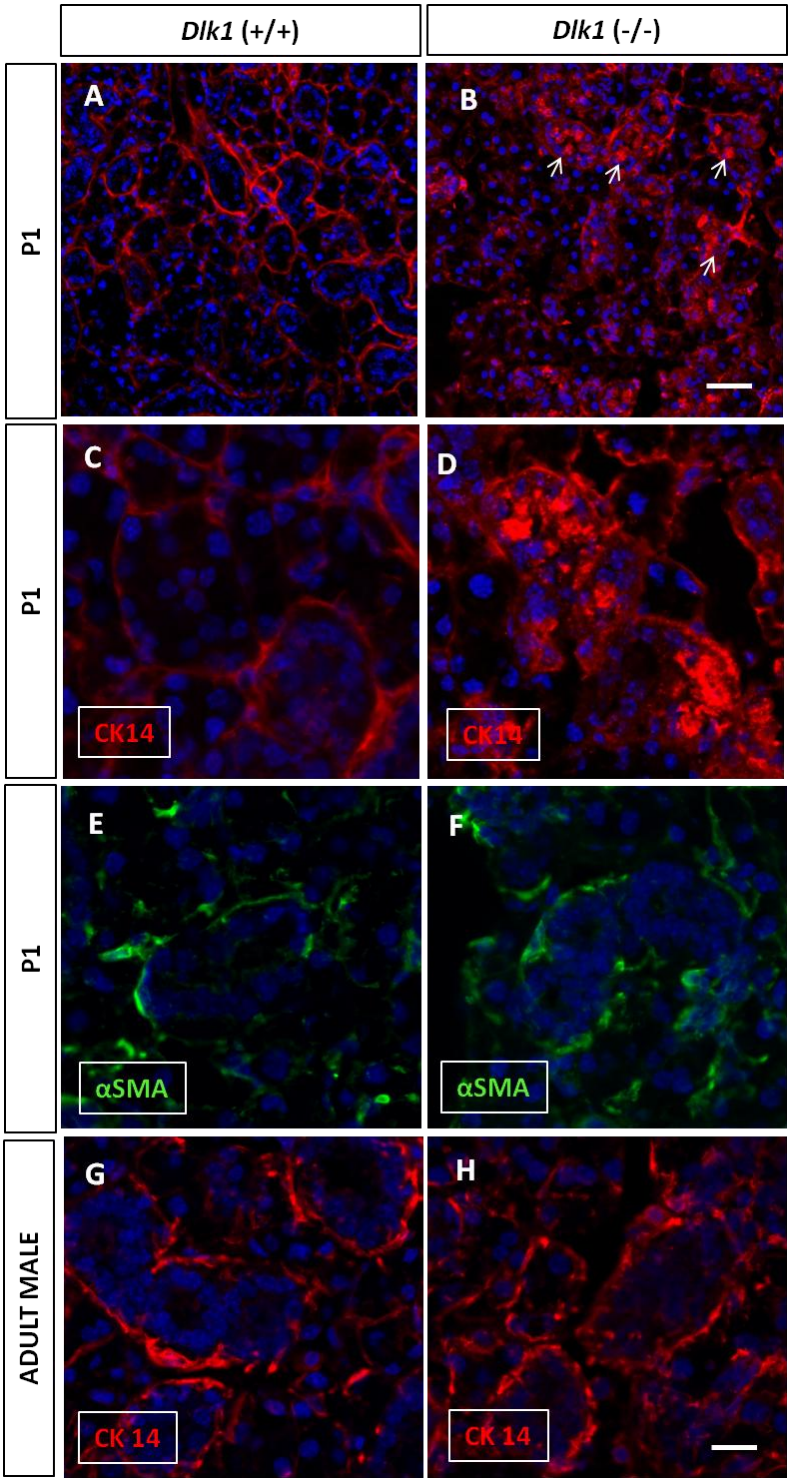

Figure 41. CK14 epithelial stem cell marker in *Dlk1 (-/-)* mice vs. *Dlk1 (+/+)*. (A,B) low magnification; (C,D) high magnification. There is an increased amount of CK14+ epithelial cells (arrows) inside the ducts and acini of *Dlk1* (-/-) SMG. (E,F) P1 SMG stained for αSMA highlights myoepithelial cells in green. No differences in αSMA immunoreactivity were found between SMG from *Dlk1* (-/-) and *Dlk1* (+/+) mice. (G,H) Adult male SMG immunostained for CK14 show the typical grid-like labeling pattern of the stellate myoepithelial cells surrounding the ducts and acini. No differences in CK14 immunoreactivity where found between adult SMG from *Dlk1* (-/-) and *Dlk1* (+/+) mice. (a,b) Scale bar: 50 µm. (c,d,e,f,g,h) Scale bar: 20 µm.

CK14, apart from being an epithelial progenitor marker, also labels adult myoepithelial cells surrounding the ducts and acini (Grandi *et al*., 2000). To verify whether the increase in CK14 protein and gene expression was restricted to progenitor cells or, alternatively, related to an expansion of the myoepithelial cell population, we performed immunostainings of SMG sections for α-smooth muscle actin (αSMA). Contrary to CK14, αSMA is a specific marker for myoepithelial cells in the salivary gland. We observed that αSMA immunostaining was restricted to the periphery of ducts and acini in SMGs at P1, generating a grid-like staining pattern characteristic of myoepithelial cells which was partly similar to the one found for CK14 in *Dlk1* (+/+) mice. However, in this case there was a complete absence of αSMA-positive labeled cells inside the ducts and acini, both in *Dlk1* (+/+) and *Dlk1* (-/-) samples (Fig 41. E,F), suggesting that the previously detected CK14+ cell population in Dlk1 (-/-) SMG was not related to myoepithelial cells. Thus, we confirm that the CK14+ epithelial progenitor cell pool is expanded in the SMG of *Dlk1* (-/-) mice.

We wanted to assess whether the expansion of salivary progenitor cells would persist and be maintained in the adult salivary gland. To this end, we performed CK14 immunostaining of adult *Dlk1* (+/+) and *Dlk1* (-/-) mouse SMG sections. Surprisingly, we found that the expanded non myoepithelial CK14+ cell population that was detected at P1 had dissapeared from adult SMG samples (Fig 41.G,H). CK14 immunostaining gave identical results for both *Dlk1* (+/+) and *Dlk1* (-/-) adult SMGs, showing a purely myoepithelial labeling pattern in both cases. No increased populations of CK14+ cells could be detected inside the ducts and acini in the SMG of adult *Dlk1* (-/-) mice, contrary to what found at P1.

Altogether, these results confirm that the CK14+ epithelial progenitor cell pool is expanded in the SMG of *Dlk1* (-/-) mice, but this effect is transient and restricted exclusively to embryonic development and early postnatal stages, and could not be detected in the adult salivary glands.

5. DISCUSSION

Morphogenesis and cell differentiation of submandibular salivary gland (SMG) several growth factors (such as FGFs or BMPs), signaling molecules (Shh and Eda among others), extracellular matrix components and parasympathetic innervation are fundamental. SMG development occurs by a process called branching morphogenesis, where the progenitor cells are expanded and the epithelia clefts to produce the acini while is branched to become a mature salivary gland after birth.

In this thesis work, we investigated SMG development, where the expression, location and function of DLK1 and DLK2, protein ligands that belong to NOTCH signaling pathway, are involved.

To investigate the role of these proteins we used *in vitro* organotypic culture of SMG rudiments treated with DAPT or sDLK1. DAPT is an inhibitor reagent of γ-secretase, that is downstream NOTCH signaling and releases N1ICD active domain of NOTCH receptor, therefore is the pharmacologic way to inhibit this signaling pathway. In the same way, we wanted to mimic the natural physiological conditions of inhibiting this signaling, for what we used sDLK1. This protein is a soluble ligand that is interacting with NOTCH and inhibiting NOTCH signaling, that cause a negative effect in SMG morphogenesis. Meanwhile, we also performed experiments with null-*Dlk1* mice. We analyzed the phenotype of these mice comparing to the wild-type mice.

5.1 DLK1 AND DLK2 ARE PRESENT IN SMG DEVELOMPENT

DLK 1 (Delta-like1, also named pG2, Pref1, FA-1, SCP-1 and ZOG) is a transmembrane and secreted protein belonging to the EGF-like repeat containing family, where NOTCH receptor and their ligands belong. In humans, DLK1 is located in the 14q32 chromosomic band (Gubina *et al.,* 1999). In 2007 a protein whose structural features were virtually identical to those of DLK1, and very similar to the NOTCH ligand DLL1 was described (Nueda *et al.,* 2007b; Nueda *et al.,* 2008), it was named as DLK2. Obviously it also belongs to the EGF-like family. The human gene of this protein is located in chromosome 6p21.1 and has six exons, one more than DLK1, the first exon is not coding and the sixth is the longest. The striking structural similarities between DLK1 and DLK2 point to a genetic duplication of the genes (Nueda *et al.,* 2007a).

In the adult *Dlk1 gene* is highly expressed by fetal liver, placenta, adrenal glands, brain, testicles, and ovaries, and in less proportion, in the kidneys, muscles, thymus and heart. However, all the tissues, except for fetal liver, and adult spleen, muscle and heart, express *Dlk2*. Both genes are expressed at different levels by placenta and adult adrenal glands, brain, testicles, kidneys, ovaries and thymus.

In this work, we provide evidence that both DLK1 and DLK2 are present during SMG development, from the initial to the terminal morphogenetic stages.

Interestingly, the expression pattern of DLK1 was completely different to that of DLK2. Thus, DLK1 showed strong expression in the mesenchyme and in myoepithelial cells, whereas it was weakly expressed on the acinar epithelial cells, and absent from the ducts. On the contrary, DLK2 was mainly expressed on the epithelial compartments, especially on the ducts. Although DLK1 had been previously detected in embryonic tissues, and particularly on the SMG, those studies were restricted to day E16.5 (canalicular-terminal bud stage) (Yevtodiyenko and Schmidt, 2006).

This inverse correlation of DLK1 and DLK2 expression levels has also been observed in other cell types. For instance, expression of DLK2 by fetal or adult mouse tissues appears more widespread than that of DLK1. Of particular interest is the fact that, in agreement with previous data (Laborda *et al.,* 1993) adult adrenal gland expresses high levels of *Dlk1*, but lacks expression of *Dlk2*. In addition, *Dlk1* is highly expressed by fetal liver, and it is absent in adult liver, but just the opposite situation is observed with *Dlk2*. Indeed, in the newborn mouse, after the 16th day of life, a decrease in *Dlk1* expression happened at the same time as an increase in *Dlk2* expression. This argues in favor of a mechanism of coordinated regulation of the expression of both genes, at least in some tissues (Nueda *et al.,* 2007b). However, the function of this opposite expression pattern in the SMG development is not well understood, so further investigation is need.

5.2 DLK1 AND DLK2 ARE NOTCH SIGNALING INHIBITORS

Nowadays no one has described a master or a unique receptor for these ligands. In addition, DLK2 has been much less studied. However, researchers are working hard to identify a number of binding partners for DLK1, and in consequence elucidate it mechanism of action and its function.

Among others, an interaction between DLK1 and the C-terminal region of fibronectin was reported to mediate the anti-adipogenic effect of DLK1 via activation of integrin signaling and MEK/ERK activation (Wang *et al.,* 2010). Additionally, the membrane bound DLK1 binds to insulin-like growth factor IGF-I and IGF binding protein 1 (IGFBP1) complex leading to the release of IGF-1 and enhanced IGF receptor signaling (Nueda *et al.,* 2008). Mitogen activated protein kinase (MAPK) and the MEK/ERK pathways are activated in the presence of DLK1 and mediate the inhibition of adipogenesis (Kim *et al.,* 2007). In addition, DLK1 inhibitory effects on chondrogenesis are associated with the inhibition of PI3K/AKT signaling (Chen *et al.,* 2011).

Other authors demonstrated the activation of NF-kB signaling as a potential mechanism underlying the inhibitory effect of DLK1 on MSC differentiation (Abdallah *et al.,* 2007). Constitutive expression of DLK1 or direct addition of FA1 to human bone stem cells (hBMSC) cultures, activate the NF-kB pathway leading to increased production of a number of cytokines and immune-related factors including IL-1α, IL-1β, IL-6, IL-8, CCL20 and COX-2 with known inhibitory effects on osteoblast and adipocyte differentiation (Chang *et al.,* 2013). A similar mechanism has been identified for DLK1 stimulated bone resorption in DLK1 transgenic mice. The association between DLK1 expression and the inflammatory response has been reported in other studies that demonstrate the presence of a relationship between DLK1 and pro-inflammatory cytokine production by adipose tissue (Chacon *et al.,* 2008) and by human skeletal muscle myotubes (Abdallah *et al.,* 2007).

In spite of all this possible partners that are important to understand the pleiotropic of DLK1 in the different tissues. However, the first evidences of DLK1 function

demonstrated, employing the yeast-two-hybrid systems, that NOTCH1 tandem EGF-like repeats 12/13 interact with the extracellular DLK1 EGF-like repeat region (Nueda *et al.,* 2007b). The interaction of DLK1 with NOTCH1 resulted in an inhibition of basal NOTCH signaling and its downstream target HES-1 expression and subsequently inhibition of adipogenesis (Sanchez-Solana *et al.,* 2011). More recently, using mice models of DLK1 loss and gain of function, DLK1 has been reported to inhibit angiogenesis via interaction with NOTCH receptors (Rodriguez *et al.,* 2012).

Since DLK1 and DLK2 were present in the gland, and they had the EGF-like repeats that classify these proteins into the NOTCH family, we used HSG salivary gland cell line and investigate whether DLK1 could interact with NOTCH receptor in the SMG.

We found that DLK1 and DLK2 acted as inhibitory non-canonical ligands of NOTCH1 in HSG cells, similarly to that previously shown in other systems (Nueda *et al.,* 2007b; Sanchez-Solana *et al.,* 2011). Both non canonical NOTCH ligands appear to inhibit the activation of NOTCH receptor in a luciferase assay. However, we cannot affirm that is the unique protein by which DLK proteins exert it function, as it has been said for other systems proteins like fibronectins, IGF or NF-kB can interact with DLK1 so it could also be happening in the salivary gland, we need further investigation.

In this way inhibition of NOTCH by this ligands would have effects in embryonic development (Iso *et al.,* 2003), stem cell maintenance (Yamamoto *et al.,* 2003; Chiba, 2006), adult tissue homeostasis (Schwanbeck *et al.,* 2008), and fate-specific differentiation (Apelqvist *et al.,* 1999; Zhu *et al.,* 2006).

Moreover, it is known that DLK1 maintains cells in the proliferative state, and it is a negative regulator of emerging progenitor/stem cells, in processes such as adipogenesis, angiogenesis, neurogenesis or hematopoyesis (Al Haj Zen and Maddedu, 2012; Ferron *et al.,* 2012; Mirshekar-Syahkal *et al.,* 2012). In this context, we wondered whether application of DLK protein in organotypic cultures may affect the initiation, growth and epithelial branching formation of SMGs.

5.3 NOTCH INHIBITION ON SMG DEVELOPMENT RESULTS IN REDUCED BRANCHING MORPHOGENESIS AND PSG IMPAIRED INNERVATION

The role of the NOTCH signaling pathway during SMG development is not completely understood yet. We have used purified, soluble DLK1 (sDLK1) protein for our experiments due to the fact that the extracellular domain of DLK1 has been described as an active protein, whereas at present nothing is known about the existence of a soluble form of DLK2. We wonder if DLK2 could also have function in SMG development.

We clearly show in this thesis that the addition of sDLK1 protein on SMGs cultures exerts a negative effect on branching morphogenesis and SMG growth, similarly to what happens after the addition of the pharmacological inhibitor of NOTCH pathway, DAPT. The fact that the expression of N1ICD is reduced in SMGs treated with sDLK1 clearly indicates a negative regulation of the NOTCH signaling pathway by sDLK1 during SMGs morphogenesis and branching formation. SMGs treated with NOTCH inhibitors show a reduced number of acini and wider en bud, with apoptotic progenitor cells inside of them (as it´s shown in the drawing).

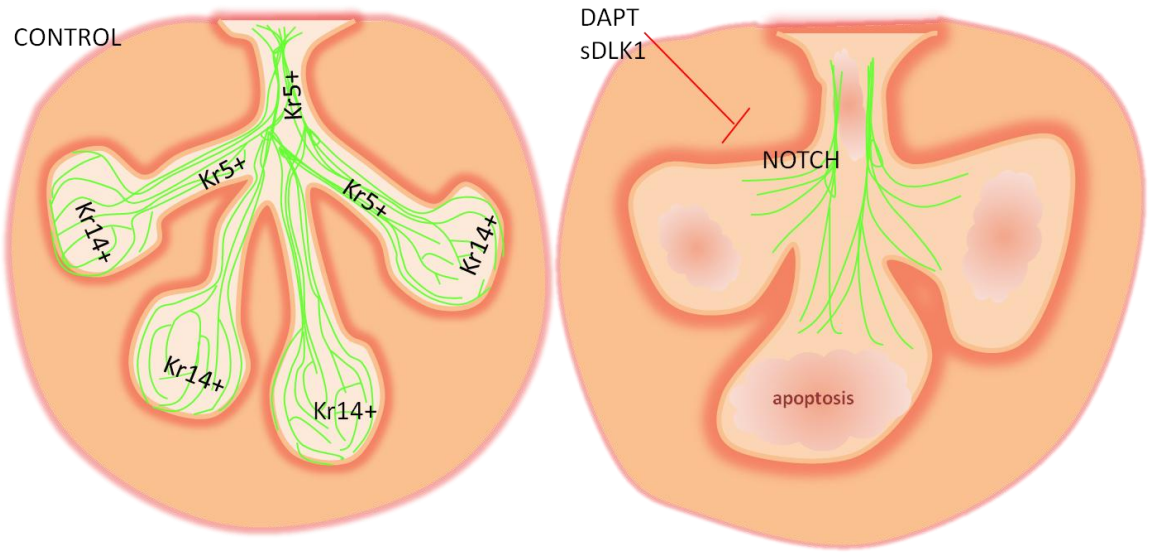

We also found that the alteration on branching by NOTCH inhibition correlated with reduced innervation, whose axons could not reach the epithelial end buds in *in vitro* SMGs (as is showed in green in the representation).

It is known that parasympathetic innervation occurs in parallel with salivary gland outgrowth. During early fetal stages, parasympathetic gangliogenesis and innervation occur along with the development of SMG epithelium (Coughlin, 1975; Knox *et al.,* 2010, Knox *et al.,* 2013). The epithelial morphogenesis of the SMG requires PSG innervation, acetylcholine and epithelial muscarinic receptor activity (Knox *et al.,* 2010). It is well known that NOTCH exerted profound effects on neuronal arborization (Berezovska *et al.,* 1999; Sestan *et al.,* 1999; Redmond *et al.,* 2000).

More recent experiments have shown that dendritic arborisation of newly generated neurons is modulated *in vivo* in a dosage-dependent manner based on the loss or gain of function of NOTCH receptor (Breunig *et al.,* 2007). In addition, NOTCH1 is required for the maintenance of adult hippocampal stem and progenitor cells, and importantly, it plays a critical role as a regulator of neurogenesis and gliogenesis in both central and peripheral nervous systems (Taylor *et al.,* 2007, Ables *et al.,* 2010, 2011). Besides NOTCH signaling is required for the generation of Schwann cells during mouse embryonic development (Woodhoo *et al.,* 2009) which may affect axonal extension of submandibular PSG neurons. Whereas the mechanisms whereby sDLK1 and DAPT inhibit SMG innervation still remain to be fully elucidated.

Our results demonstrate that the inhibition of NOTCH signaling pathway causes the interruption of salivary branching morphogenesis and impact dramatically on PSG axonal outgrowth, which translates into a remarkable decrease on the CK5+ salivary epithelial progenitor cells. This correlation between innervation and CK5+ SMG epithelial progenitors is consistent with previous reports, which described that parasympathetic innervation maintains the epithelial CK5+ progenitor cell population during SMGs development (Knox *et al.,* 2010).

Furthermore, our experiments also reveal a direct effect beyond the isolated epithelia, since dissected epithelium from the SMG and cultured for 48h with sDLK1 appeared to lose the control condition characteristic shape of the growing epithelia in 3D laminin with F10.HS. Thus, inhibition of NOTCH affects the PSG and the epithelium growing in the developing SMG.

5.4 CHOLINERGIC ACTIVATION RESTORES MORPHOGENESIS NOTCH INHIBITED SMG

According to our results, SMG normal development is dependent of sDLK1 action on the NOTCH pathway. Moreover, the inhibitory effect of DLK1 and DAPT on the axonal growth of PSG neurons can be partially rescued by cholinergic stimulation with CCh; however, branching morphogenesis was not completely restored when SMGs were treated at the same time with sDLK1 or DAPT and CCh. This demonstrates that other factors than innervation alone are also playing a role in the impaired SMG development induced by NOTCH signaling shutdown. In fact, the impaired morphogenesis could be due to the direct effect of NOTCH signaling inhibition upon the epithelia, as we show in the SMG isolated epithelia cultures.

We hypothesized that the reduced epithelial branching morphogenesis produced by the inhibition of NOTCH signaling by sDLK1 or DAPT could be based on an effect on bud clefting formation because cell proliferation is not affected. In fact, epithelial clefting formation has been shown to proceed independently of cell proliferation (Nakanishi *et al.,* 1987), but this question still remains to be completely clarified.

Another potential explanation lies in the extensive epithelial cell apoptosis that occurs following NOTCH inhibition in SMG. This apoptosis may be preventing newly formed CK5+ and CK14+ epithelial stem/progenitors cells to reach full maturity upon generation, (even in conditions of restored innervation with CCh).

Overall our data suggest that DLK1 regulates epithelial branching morphogenesis and PSG neuronal growth, through inhibition of the NOTCH signaling pathway. Besides, DLK1 could be a negative regulator of the maintenance of epithelial progenitors cells in the SMG. Inhibition of NOTCH in the SMG morphogenesis could be even an effect of combination affecting the epithelia and the innervation.

5.5 ADULT *Dlk1* (-/-) SALIVARY GLANDS ARE SMALLER AND THE EMBRYONIC SMG HAS THE PROGENITOR MARKER CK14 UPREGULATED

Dlk1 is a member of a cluster of imprinted genes which is only expressed from the paternally-inherited chromosome (Schmidt *et al.,* 2000; Takada *et al.,* 2000). Genes with genomic imprinting have an important role in the control of fetal growth and development (Murphy & Jirtle, 2003; Rand & Cedar, 2003; Wilkins & Haig, 2003) and DLK1 is not an exception.

Genetically modified mouse embryos to express a double dose of DLK1, which mimic the condition of loss of imprinting on the locus DLK1, did not thrive after birth despite the advantage that it could be assume for fetal and perinatal growth (da Rocha *et al.,* 2009).

It had been previously described that *Dlk1*-null mice, including the mouse strain tested here, had a reduced body weight (Moon *et al.,* 2002; Raghunandan *et al.*, 2008; Cheung *et al.,* 2013). We corroborated here that these mice are definitely smaller than their wild-type counterparts. However, this decrease appears to be particularly emphasized in the case of salivary glands, since their reduction in weight was significant even when referred to total body weight.

There are several possible explanations for this specific effect. In this context, we observed that *Dlk1* is highly expressed during salivary gland development. DLK1 is a regulator of the GH/IGF-1 somatotroph axis (Abdallah *et al.,* 2007), which has a key role in the regulation of *body size* in growing animals (Olney *et al.,* 2003; Ohlsson et al., 2000). DLK1 colocalizes with GH-secreting cells in the pituitary, where it has been proposed to play an inhibitory role over GH release (Ansell *et al.,* 2007). Accordingly, the same *Dlk1* (-/-) mouse strain that we used here was reported to present increased pituitary mRNA levels for GH (Puertas-Avendaño *et al.,* 2011). However, if increased levels of systemic GH were responsible for the salivary gland phenotype in these animals, it might be expected that these would be larger, rather than smaller, making it a very unlikely explanation.

Additionally, conditional *Dlk1* (-/-) mice in somatotroph cells present no growth alteration phenotype (Appelbe *et al.,* 2013). A more plausible scenario would be that DLK1 may also regulate IGF-1 binding proteins locally (Nueda *et al.,* 2008), making its growth-promoting or growth-repressing effect to be context-dependent. In this regard, it is interesting to note that IGF-1 is present through salivary gland branching morphogenesis stages (Jaskoll & Melnick, 1999), and its deregulation could lead to this organ size reduction. Furthermore, these mice have also been reported to present increased serum levels of other endocrine hormones, such as leptin (Puertas-Avendaño *et al.*, 2011), which may be reflecting a systemic metabolic alteration in these animals. It should be noted that salivary gland development is highly sensitive to endocrine action, in particular to sex hormones (Kontinnen *et al.,* 2010), and any perturbation of the global endocrine-metabolic balance at this level may affect salivary gland size.

In addition, the amount of saliva produced after stimulation was less for the KO. We attribute this difference in the function of the size gland. We chose mice of the same age (8 months) because researchers already know that morphological and functional changes are related with the age, such as dry mouth (Choi *et al.,* 2013). Thus, similarly to patients suffering Xerostomia (dry mouth syndrome) that loose ~40% of parotid volume (Teshima *et al.,* 2010), we hypothesize that our *Dlk1* (-/-) mice that have smaller glands would not be able to produce as much saliva as our *Dlk1* (+/+) mice.

In addition, we investigated the morphology of *Dlk1* (-/-) SMG, SLG and PG glands during some developmental stages and in the adult, by histology. We did not found any striking histological differences. We also decided to focus on the tubules, due to their function of changing the saliva while it travels through tubule diameter sections, converting saliva in a hypotonic solution (Catalán *et al.,* 2009). The GCT and the striated tubules are the biggest diameter in rodents. Under TEM, we did not find any difference between null and wild type mice. We also stained the salivary gland to visualize the amount of mucins, by alcian blue, but the quantity of mucins was similar for *Dlk1* (+/+) and *Dlk1* (-/-) mice. We thought that *Dlk2* could be compensating the absence of *Dlk1* in the salivary gland, but our results did not show any increase neither in the expression of *Dlk2* gene nor at the protein level, making this an unlikely mechanism for genetic compensation.

Considering all these data, we think that the difference between *Dlk1* (+/+) and (-/-) mice in saliva secretion is due to a size difference in the salivary glands themselves. These data suggest that both variables, salivary gland size and saliva secretion, are effectively related. Therefore, smaller salivary glands in *Dlk1* (-/-) mice will lead to a reduction in saliva production (Teshima *et al*., 2010). Salivary gland size / body weight ratio is a fundamental factor to explain why males produce more saliva after stimulation, and females less. Some other authors described also a gender-dependent difference in saliva flow rate in humans, which was attributed to a difference in salivary gland size (Inoue H *et al*., 2006).

Nevertheless, as we could not visualize any difference we thought it could be changes in a molecular level. We measured expression levels of different markers. No changes in the expression of differentiation markers such of *Aqp5* or *Fgf10*. However, the stem/progenitor cell marker *Ck14* was upregulated in *Dlk1* (-/-) P1 and adult SMG. This progenitor marker is localized in the ducts and in some epithelial cells of the acini as we detected in the inmunofluorescence.

In a healthy SMG, DLK1 has the highest levels at E12 coinciding with the moment of expansion of progenitor cells, then the concentration in the gland decreases at E14 until almost disappear after birth. During these developmental stages the epithelial progenitor cells, such as CK14+ cells, proliferate and the epithelia start the process of clefting. At E18 when the gland start to differentiate, DLK1 is down regulated until be expressed in a very little in the adult SMG, meanwhile the levels of the differentiation marker Aqp5 increase gradually until the SMG become mature in the adult.

Taken into account the relationship between DLK1 and the progenitor population CK14, increased levels of DLK1 in organotypic SMG cultures resulted in the inhibition of the morphogenesis of the gland. The progenitor cells die, as a result of the excessive stimulation of DLK1, because DLK1 maintain the cells in a proliferative state, without leading them to branch and cleft.

In contrast, in *Dlk1* (-/-) mice, we hypothesize that the stem progenitor cell population cannot be properly regulated and as a consequence the CK14 population is upregulated, just the opposite that happened with the addition of DLK1 in the organotypic cultures.

We could assume a failure in progenitor cell differentiation would negatively affect the final salivary gland size, and ultimately cause a reduction in saliva secretion, as we observed in *Dlk1* (-/-) animals, but this hypotheis remains yet unproven. It is known from other studies that DLK1 is an important regulator of stem-cell renewal, and changes on its expression levels are associated with processes such as adipogenesis, angiogenesis, neurogenesis or hematopoiesis (Al Haj Zen and Maddedu, 2012; Ferron *et al*., 2011; Mirshekar-Syahkal *et al*., 2013).

In our study, the absence of DLK1 in the SMG lead to an increase in the population of CK14+ progenitor cells, which again point to DLK1 as a regulator of the stemness balance.

6. CONCLUSIONS

Taken into account the results obtained in this project, we extract the following conclusions:

I. DLK1 and DLK2 are expressed through salivary gland development and present a complementary expression pattern that made us think that these proteins could play an important role in the morphogenesis of the salivary gland.

II. The non canonical ligands DLK1 and DLK2 negatively inhibit NOTCH signaling pathway. The inhibition of NOTCH, by either DLK1 or DAPT, is crucial for a correct morphogenesis of the developing SMG; affects the innervation, the epithelia branching and in the inner epithelia progenitor cells integrity.

III. Cholinergic activation, by the addition of CCh, can be used to recover the impaired morphogenesis caused by inhibition of NOTCH in cultured SMG.

IV. The increase of epithelial stem/progenitor cells in *Dlk1* (-/-) mice could be the result of a failure in progenitor cell differentiation during salivary gland development. This fact would negatively affect the final salivary gland size, and ultimately cause a reduction in saliva secretion.

Summarizing, this work describes the significance of the non-canonical NOTCH ligands, DLK1 and DLK2, in the morphogenesis and nervous system development of the mouse submandibular salivary gland. Moreover, the level of DLK1 in the development of the salivary gland needs a precise balance to control the mechanism between inhibiting and promoting stemness for cell proliferation and differentiation.

7. BIBLIOGRAPHY

Abdallah B.M., Jensen C.H., Gutierrez G., Leslie R.G., Jensen T.G. & Kassem M. (2004) Regulation of human skeletal stem cells differentiation by Dlk1/Pref-1. *Journal of bone and mineral research : the official journal of the American Society for Bone and Mineral Research,* **19,** 841-852.

Abdallah B.M., Ding M., Jensen C.H., Ditzel N., Flyvbjerg A., Jensen T.G., Dagnaes-Hansen F., Gasser J.A. & Kassem M. (2007) Dlk1/FA1 is a novel endocrine regulator of bone and fat mass and its serum level is modulated by growth hormone. *Endocrinology,* **148,** 3111-3121.

Ables J.L., Decarolis N.A., Johnson M.A., Rivera P.D., Gao Z., Cooper D.C., Radtke F., Hsieh J. & Eisch A.J. (2010) Notch1 is required for maintenance of the reservoir of adult hippocampal stem cells. *The Journal of neuroscience : the official journal of the Society for Neuroscience,* **30,** 10484-10492.

Ables J.L., Breunig J.J., Eisch A.J. & Rakic P. (2011) Not(ch) just development: Notch signalling in the adult brain. *Nature reviews.Neuroscience,* **12,** 269-283.

Al Haj Zen A. & Madeddu P. (2012) DLK1: a novel negative regulator of angiogenesis? *Cardiovascular research,* **93,** 213-214.

Andersen D.C., Laborda J., Baladron V., Kassem M., Sheikh S.P. & Jensen C.H. (2013) Dual role of delta-like 1 homolog (DLK1) in skeletal muscle development and adult muscle regeneration. *Development (Cambridge, England),* **140,** 3743-3753.

Ansell P.J., Zhou Y., Schjeide B.M., Kerner A., Zhao J., Zhang X. & Klibanski A. (2007) Regulation of growth hormone expression by Delta-like protein 1 (Dlk1). *Molecular and cellular endocrinology,* **271,** 55-63.

Apelqvist A., Li H., Sommer L., Beatus P., Anderson D.J., Honjo T., Hrabe de Angelis M., Lendahl U. & Edlund H. (1999) Notch signalling controls pancreatic cell differentiation. *Nature,* **400,** 877-881.

Appelbe O.K., Yevtodiyenko A., Muniz-Talavera H. & Schmidt J.V. (2013) Conditional deletions refine the embryonic requirement for Dlk1. *Mechanisms of development,* **130,** 143-159.

Artavanis-Tsakonas S., Rand M.D. & Lake R.J. (1999) Notch signaling: cell fate control and signal integration in development. *Science (New York, N.Y.),* **284,** 770-776.

Atkinson W.B., Wilson F. & Coates S. (1959) The nature of the sexual dimorphism of the submandibular gland of the mouse. *Endocrinology,* **65,** 114-117.

Avery J. (2002) Oral development and histology. *New York: Thieme,* .

Ayaz F. & Osborne B.A. (2014) Non-canonical notch signaling in cancer and immunity. *Frontiers in oncology,* **4,** 345.

Baladron V., Ruiz-Hidalgo M.J., Nueda M.L., Diaz-Guerra M.J., Garcia-Ramirez J.J., Bonvini E., Gubina E. & Laborda J. (2005) dlk acts as a negative regulator of Notch1 activation through interactions with specific EGF-like repeats. *Experimental cell research,* **303,** 343-359.

Berezovska O., McLean P., Knowles R., Frosh M., Lu F.M., Lux S.E. & Hyman B.T. (1999) Notch1 inhibits neurite outgrowth in postmitotic primary neurons. *Neuroscience,* **93,** 433-439.

Blanpain C., Lowry W.E., Pasolli H.A. & Fuchs E. (2006) Canonical notch signaling functions as a commitment switch in the epidermal lineage. *Genes & development,* **20,** 3022-3035.

Bouma I., Pijpe J. & Vissink A. (2003) Sjogren' syndrome: a progressive disease. *Nederlands tijdschrift voor tandheelkunde,* **110,** 316-320.

Breunig J.J., Arellano J.I., Macklis J.D. & Rakic P. (2007) Everything that glitters isn't gold: a critical review of postnatal neural precursor analyses. *Cell stem cell,* **1,** 612-627.

Catalan M.A., Nakamoto T. & Melvin J.E. (2009) The salivary gland fluid secretion mechanism. *The journal of medical investigation : JMI,* **56 Suppl,** 192-196.

Chacon M.R., Miranda M., Jensen C.H., Fernandez-Real J.M., Vilarrasa N., Gutierrez C., Naf S., Gomez J.M. & Vendrell J. (2008) Human serum levels of fetal antigen 1 (FA1/Dlk1) increase with obesity, are negatively associated with insulin sensitivity and modulate inflammation in vitro. *International journal of obesity (2005),* **32,** 1122-1129.

Chang J., Liu F., Lee M., Wu B., Ting K., Zara J.N., Soo C., Al Hezaimi K., Zou W., Chen X., Mooney D.J. & Wang C.Y. (2013) NF-kappaB inhibits osteogenic differentiation of mesenchymal stem cells by promoting beta-catenin degradation. *Proceedings of the National Academy of Sciences of the United States of America,* **110,** 9469-9474.

Chen L., Qanie D., Jafari A., Taipaleenmaki H., Jensen C.H., Saamanen A.M., Sanz M.L., Laborda J., Abdallah B.M. & Kassem M. (2011) Delta-like 1/fetal antigen-1 (Dlk1/FA1) is a novel regulator of chondrogenic cell differentiation via inhibition of the Akt kinase-dependent pathway. *The Journal of biological chemistry,* **286,** 32140-32149.

Cheung L.Y., Rizzoti K., Lovell-Badge R. & Le Tissier P.R. (2013) Pituitary phenotypes of mice lacking the notch signalling ligand delta-like 1 homologue. *Journal of neuroendocrinology,* **25,** 391-401.

Chiba S. (2006) Notch signaling in stem cell systems. *Stem cells (Dayton, Ohio),* **24,** 2437-2447.

Chillakuri C.R., Sheppard D., Lea S.M. & Handford P.A. (2012) Notch receptor-ligand binding and activation: insights from molecular studies. *Seminars in cell & developmental biology,* **23,** 421-428.

Choi J.S., Park I.S., Kim S.K., Lim J.Y. & Kim Y.M. (2013) Analysis of age-related changes in the functional morphologies of salivary glands in mice. *Archives of Oral Biology,* **58,** 1635-1642.

Coughlin M.D. (1975) Target organ stimulation of parasympathetic nerve growth in the developing mouse submandibular gland. *Developmental biology,* **43,** 140-158.

da Rocha S.T., Charalambous M., Lin S.P., Gutteridge I., Ito Y., Gray D., Dean W. & Ferguson-Smith A.C. (2009) Gene dosage effects of the imprinted delta-like homologue 1 (dlk1/pref1) in development: implications for the evolution of imprinting. *PLoS genetics,* **5,** e1000392.

Dang H., Lin A.L., Zhang B., Zhang H.M., Katz M.S. & Yeh C.K. (2009) Role for Notch signaling in salivary acinar cell growth and differentiation. *Developmental dynamics : an official publication of the American Association of Anatomists,* **238,** 724-731.

Dudek R. & Fix J. (1998) Embryology. *Baltimore: Williams and Wilkins,* .

Falix F.A., Aronson D.C., Lamers W.H., Hiralall J.K. & Seppen J. (2012) DLK1, a serum marker for hepatoblastoma in young infants. *Pediatric blood & cancer,* **59,** 743-745.

Ferron S.R., Charalambous M., Radford E., McEwen K., Wildner H., Hind E., Morante-Redolat J.M., Laborda J., Guillemot F., Bauer S.R., Farinas I. & Ferguson-Smith A.C. (2011) Postnatal loss of Dlk1 imprinting in stem cells and niche astrocytes regulates neurogenesis. *Nature,* **475,** 381-385.

Fiuza U.M. & Arias A.M. (2007) Cell and molecular biology of Notch. *The Journal of endocrinology,* **194,** 459-474.

Fleming R.J. (1998) Structural conservation of Notch receptors and ligands. *Seminars in cell & developmental biology,* **9,** 599-607.

Fleming R.J., Gu Y. & Hukriede N.A. (1997) Serrate-mediated activation of Notch is specifically blocked by the product of the gene fringe in the dorsal compartment of the Drosophila wing imaginal disc. *Development (Cambridge, England),* **124,** 2973-2981.

Floridon C., Jensen C.H., Thorsen P., Nielsen O., Sunde L., Westergaard J.G., Thomsen S.G. & Teisner B. (2000) Does fetal antigen 1 (FA1) identify cells with regenerative, endocrine and neuroendocrine potentials? A study of FA1 in embryonic, fetal, and placental tissue and in maternal circulation. *Differentiation; research in biological diversity,* **66,** 49-59.

Frise E., Knoblich J.A., Younger-Shepherd S., Jan L.Y. & Jan Y.N. (1996) The Drosophila Numb protein inhibits signaling of the Notch receptor during cell-cell interaction in sensory organ lineage. *Proceedings of the National Academy of Sciences of the United States of America,* **93,** 11925-11932.

Grandi D., Campanini N., Becchi G. & Lazzaretti M. (2000) On the myoepithelium of human salivary glands. An immunocytochemical study. *European journal of morphology,* **38,** 249-255.

Greenwald I. (1998) LIN-12/Notch signaling: lessons from worms and flies. *Genes & development,* **12,** 1751-1762.

Gresik E.W. (1994) The granular convoluted tubule (GCT) cell of rodent submandibular glands. *Microscopy research and technique,* **27,** 1-24.

Gresik E.W. (1980) Postnatal developmental changes in submandibular glands of rats and mice. *The journal of histochemistry and cytochemistry : official journal of the Histochemistry Society,* **28,** 860-870.

Gridley T. (2003) Notch signaling and inherited disease syndromes. *Human molecular genetics,* **12 Spec No 1,** R9-13.

Gubina E., Ruiz-Hidalgo M.J., Baladron V. & Laborda J. (1999) Assignment of DLK1 to human chromosome band 14q32 by in situ hybridization. *Cytogenetics and cell genetics,* **84,** 206-207.

Haara O., Fujimori S., Schmidt-Ullrich R., Hartmann C., Thesleff I. & Mikkola M.L. (2011) Ectodysplasin and Wnt pathways are required for salivary gland branching morphogenesis. *Development (Cambridge, England),* **138,** 2681-2691.

Hansson E.M., Lendahl U. & Chapman G. (2004) Notch signaling in development and disease. *Seminars in cancer biology,* **14,** 320-328.

Hartenstein A.Y., Rugendorff A., Tepass U. & Hartenstein V. (1992) The function of the neurogenic genes during epithelial development in the Drosophila embryo. *Development (Cambridge, England),* **116,** 1203-1220.

Heitzler P. & Simpson P. (1991) The choice of cell fate in the epidermis of Drosophila. *Cell,* **64,** 1083-1092.

Hermida C., Garces C., de Oya M., Cano B., Martinez-Costa O.H., Rivero S., Garcia-Ramirez J.J., Laborda J. & Aragon J.J. (2008) The serum levels of the EGF-like homeotic protein dlk1 correlate with different metabolic parameters in two hormonally different children populations in Spain. *Clinical endocrinology,* **69,** 216-224.

Hisatomi Y., Okumura K., Nakamura K., Matsumoto S., Satoh A., Nagano K., Yamamoto T. & Endo F. (2004) Flow cytometric isolation of endodermal progenitors from mouse salivary gland differentiate into hepatic and pancreatic lineages. *Hepatology (Baltimore, Md.),* **39,** 667-675.

Hosoi K., Kobayashi S. & Ueha T. (1978) Sex difference in L-glutamine D-fructose-6-phosphate aminotransferase activity of mouse submandibular gland. *Biochimica et biophysica acta,* **543,** 283-292.

Hukriede N.A., Gu Y. & Fleming R.J. (1997) A dominant-negative form of Serrate acts as a general antagonist of Notch activation. *Development (Cambridge, England),* **124,** 3427-3437.

Inoue H., Ono K., Masuda W., Morimoto Y., Tanaka T., Yokota M. & Inenaga K. (2006) Gender difference in unstimulated whole saliva flow rate and salivary gland sizes. *Archives of Oral Biology,* **51,** 1055-1060.

Iso T., Hamamori Y. & Kedes L. (2003) Notch signaling in vascular development. *Arteriosclerosis, Thrombosis, and Vascular Biology,* **23,** 543-553.

Jaskoll T. & Melnick M. (1999) Submandibular gland morphogenesis: stage-specific expression of TGF-alpha/EGF, IGF, TGF-beta, TNF, and IL-6 signal transduction in normal embryonic mice and the phenotypic effects of TGF-beta2, TGF-beta3, and EGF-r null mutations. *The Anatomical Record,* **256,** 252-268.

Jaskoll T., Zhou Y.M., Chai Y., Makarenkova H.P., Collinson J.M., West J.D., Hajihosseini M.K., Lee J. & Melnick M. (2002) Embryonic submandibular gland morphogenesis: stage-specific protein localization of FGFs, BMPs, Pax6 and Pax9 in normal mice and abnormal SMG phenotypes in FgfR2-IIIc(+/Delta), BMP7(-/-) and Pax6(-/-) mice. *Cells, tissues, organs,* **170,** 83-98.

Jaskoll T., Zhou Y.M., Trump G. & Melnick M. (2003) Ectodysplasin receptor-mediated signaling is essential for embryonic submandibular salivary gland development. *The anatomical record.Part A, Discoveries in molecular, cellular, and evolutionary biology,* **271,** 322-331.

Jaskoll T., Witcher D., Toreno L., Bringas P., Moon A.M. & Melnick M. (2004a) FGF8 dose-dependent regulation of embryonic submandibular salivary gland morphogenesis. *Developmental biology,* **268,** 457-469.

Jaskoll T., Leo T., Witcher D., Ormestad M., Astorga J., Bringas P.,Jr, Carlsson P. & Melnick M. (2004b) Sonic hedgehog signaling plays an essential role during embryonic salivary gland epithelial branching morphogenesis. *Developmental dynamics : an official publication of the American Association of Anatomists,* **229,** 722-732.

Joutel A., Corpechot C., Ducros A., Vahedi K., Chabriat H., Mouton P., Alamowitch S., Domenga V., Cecillion M., Marechal E., Maciazek J., Vayssiere C., Cruaud C., Cabanis E.A., Ruchoux M.M., Weissenbach J., Bach J.F., Bousser M.G. & Tournier-Lasserve E. (1996) Notch3 mutations in CADASIL, a hereditary adult-onset condition causing stroke and dementia. *Nature,* **383,** 707-710.

Kadoya Y., Nomizu M., Sorokin L.M., Yamashina S. & Yamada Y. (1998) Laminin alpha1 chain G domain peptide, RKRLQVQLSIRT, inhibits epithelial branching morphogenesis of cultured embryonic mouse submandibular gland. *Developmental dynamics : an official publication of the American Association of Anatomists,* **212,** 394-402.

Katsube K. & Sakamoto K. (2005) Notch in vertebrates--molecular aspects of the signal. *The International journal of developmental biology,* **49,** 369-374.

Kim K.A., Kim J.H., Wang Y. & Sul H.S. (2007) Pref-1 (preadipocyte factor 1) activates the MEK/extracellular signal-regulated kinase pathway to inhibit adipocyte differentiation. *Molecular and cellular biology,* **27,** 2294-2308.

Kim Y., Lin Q., Zelterman D. & Yun Z. (2009) Hypoxia-regulated delta-like 1 homologue enhances cancer cell stemness and tumorigenicity. *Cancer research,* **69,** 9271-9280.

Knosp W.M., Knox S.M. & Hoffman M.P. (2012) Salivary gland organogenesis. *Wiley interdisciplinary reviews.Developmental biology,* **1,** 69-82.

Knox S.M., Lombaert I.M., Reed X., Vitale-Cross L., Gutkind J.S. & Hoffman M.P. (2010) Parasympathetic innervation maintains epithelial progenitor cells during salivary organogenesis. *Science (New York, N.Y.),* **329,** 1645-1647.

Knox S.M., Lombaert I.M., Haddox C.L., Abrams S.R., Cotrim A., Wilson A.J. & Hoffman M.P. (2013) Parasympathetic stimulation improves epithelial organ regeneration. *Nature communications,* **4,** 1494.

Konttinen Y.T., Stegaev V., Mackiewicz Z., Porola P., Hanninen A. & Szodoray P. (2010) Salivary glands - "an unisex organ'? *Oral diseases,* **16,** 577-585.

Laborda J., Sausville E.A., Hoffman T. & Notario V. (1993) Dlk, a Putative Mammalian Homeotic Gene Differentially Expressed in Small Cell Lung Carcinoma and Neuroendocrine Tumor Cell Line. *The Journal of biological chemistry,* **268,** 3817-3820.

Lammel U. & Saumweber H. (2000) X-linked loci of Drosophila melanogaster causing defects in the morphology of the embryonic salivary glands. *Development genes and evolution,* **210,** 525-535.

Lee Y.L., Helman L., Hoffman T. & Laborda J. (1995) dlk, pG2 and Pref-1 mRNAs encode similar proteins belonging to the EGF-like superfamily. Identification of polymorphic variants of this RNA. *Biochimica et biophysica acta,* **1261,** 223-232.

Li L., Krantz I.D., Deng Y., Genin A., Banta A.B., Collins C.C., Qi M., Trask B.J., Kuo W.L., Cochran J., Costa T., Pierpont M.E., Rand E.B., Piccoli D.A., Hood L. & Spinner N.B. (1997) Alagille syndrome is caused by mutations in human Jagged1, which encodes a ligand for Notch1. *Nature genetics,* **16,** 243-251.

Liu F. & Wang S. (2014) Molecular cues for development and regeneration of salivary glands. *Histology and histopathology,* **29,** 305-312.

Lombaert I.M., Brunsting J.F., Wierenga P.K., Faber H., Stokman M.A., Kok T., Visser W.H., Kampinga H.H., de Haan G. & Coppes R.P. (2008) Rescue of salivary gland function after stem cell transplantation in irradiated glands. *PloS one,* **3,** e2063.

Lombaert I.M. & Hoffman M.P. (2010) Epithelial stem/progenitor cells in the embryonic mouse submandibular gland. *Frontiers of oral biology,* **14,** 90-106.

Louvi A., Arboleda-Velasquez J.F. & Artavanis-Tsakonas S. (2006) CADASIL: a critical look at a Notch disease. *Developmental neuroscience,* **28,** 5-12.

Makarenkova H.P., Hoffman M.P., Beenken A., Eliseenkova A.V., Meech R., Tsau C., Patel V.N., Lang R.A. & Mohammadi M. (2009) Differential interactions of FGFs with heparan sulfate control gradient formation and branching morphogenesis. *Science signaling,* **2,** ra55.

McMahon A.P., Ingham P.W. & Tabin C.J. (2003) Developmental roles and clinical significance of hedgehog signaling. *Current topics in developmental biology,* **53,** 1-114.

Mei B., Zhao L., Chen L. & Sul H.S. (2002) Only the large soluble form of preadipocyte factor-1 (Pref-1), but not the small soluble and membrane forms, inhibits adipocyte differentiation: role of alternative splicing. *The Biochemical journal,* **364,** 137-144.

Mirshekar-Syahkal B., Haak E., Kimber G.M., van Leusden K., Harvey K., O'Rourke J., Laborda J., Bauer S.R., de Bruijn M.F., Ferguson-Smith A.C., Dzierzak E. & Ottersbach K. (2013) Dlk1 is a negative regulator of emerging hematopoietic stem and progenitor cells. *Haematologica,* **98,** 163-171.

Mohr O.L. (1919) Character Changes Caused by Mutation of an Entire Region of a Chromosome in Drosophila. *Genetics,* **4,** 275-282.

Moon Y.S., Smas C.M., Lee K., Villena J.A., Kim K.H., Yun E.J. & Sul H.S. (2002) Mice lacking paternally expressed Pref-1/Dlk1 display growth retardation and accelerated adiposity. *Molecular and cellular biology,* **22,** 5585-5592.

Moore K.A., Pytowski B., Witte L., Hicklin D. & Lemischka I.R. (1997) Hematopoietic activity of a stromal cell transmembrane protein containing epidermal growth factor-like repeat motifs. *Proceedings of the National Academy of Sciences of the United States of America,* **94,** 4011-4016.

Morita K. & Nogawa H. (1999) EGF-dependent lobule formation and FGF7-dependent stalk elongation in branching morphogenesis of mouse salivary epithelium in vitro. *Developmental dynamics : an official publication of the American Association of Anatomists,* **215,** 148-154.

Mumm J.S. & Kopan R. (2000) Notch signaling: from the outside in. *Developmental biology,* **228,** 151-165.

Murphy S.K. & Jirtle R.L. (2003) Imprinting evolution and the price of silence. *BioEssays : news and reviews in molecular, cellular and developmental biology,* **25,** 577-588.

Mysliwiec P. & Boucher M.J. (2009) Targeting Notch signaling in pancreatic cancer patients--rationale for new therapy. *Advances in medical sciences,* **54,** 136-142.

Nakanishi Y., Morita T. & Nogawa H. (1987) Cell proliferation is not required for the initiation of early cleft formation in mouse embryonic submandibular epithelium in vitro. *Development (Cambridge, England),* **99,** 429-437.

Nedvetsky P.I., Emmerson E., Finley J.K., Ettinger A., Cruz-Pacheco N., Prochazka J., Haddox C.L., Northrup E., Hodges C., Mostov K.E., Hoffman M.P. & Knox S.M. (2014) Parasympathetic innervation regulates tubulogenesis in the developing salivary gland. *Developmental cell,* **30,** 449-462.

Nueda ML, Baladron V, Garcia-Ramirez JJ, Sanchez-Solana B, Ruvira MD, Rivero S, Ballesteros MA, Monsalve EM, Diaz-Guerra MJ, Ruiz-Hidalgo MJ, Laborda J (2007a) The novel gene EGFL9/Dlk2, highly homologous to Dlk1, functions as a modulator of adipogenesis. *Journal of Molecular Biology,* **367,**1270-1280

Nueda M.L., Baladron V., Sanchez-Solana B., Ballesteros M.A. & Laborda J. (2007b) The EGF-like protein dlk1 inhibits notch signaling and potentiates adipogenesis of mesenchymal cells. *Journal of Molecular Biology,* **367,** 1281-1293.

Nueda M.L., Garcia-Ramirez J.J., Laborda J. & Baladron V. (2008) dlk1 specifically interacts with insulin-like growth factor binding protein 1 to modulate adipogenesis of 3T3-L1 cells. *Journal of Molecular Biology,* **379,** 428-442.

Ogawa M., Oshima M., Imamura A., Sekine Y., Ishida K., Yamashita K., Nakajima K., Hirayama M., Tachikawa T. & Tsuji T. (2013) Functional salivary gland regeneration by transplantation of a bioengineered organ germ. *Nature communications,* **4,** 2498.

Ohlsson C., Jansson J.O. & Isaksson O. (2000) Effects of growth hormone and insulinlike growth factor-I on body growth and adult bone metabolism. *Current opinion in rheumatology,* **12,** 346-348.

Olney R.C. (2003) Regulation of bone mass by growth hormone. *Medical and pediatric oncology,* **41,** 228-234.

Osamu Amano, Kenichi Mizobe, Yasuhiko Bando, Koji Sakiyama (2012) Anatomy and Histology of Rodent and Human Major Salivary Glands. **45(5),** 241–250.

Patel N., Sharpe P.T. & Miletich I. (2011) Coordination of epithelial branching and salivary gland lumen formation by Wnt and FGF signals. *Developmental biology,* **358,** 156-167.

Patel V.N., Likar K.M., Zisman-Rozen S., Cowherd S.N., Lassiter K.S., Sher I., Yates E.A., Turnbull J.E., Ron D. & Hoffman M.P. (2008) Specific heparan sulfate structures modulate FGF10-mediated submandibular gland epithelial morphogenesis and differentiation. *The Journal of biological chemistry,* **283,** 9308-9317.

Patel V.N. & Hoffman M.P. (2014) Salivary gland development: a template for regeneration. *Seminars in cell & developmental biology,* **25-26,** 52-60.g

Pawson T. & Nash P. (2003) Assembly of cell regulatory systems through protein interaction domains. *Science (New York, N.Y.),* **300,** 445-452.

Pierfelice T.J., Schreck K.C., Dang L., Asnaghi L., Gaiano N. & Eberhart C.G. (2011) Notch3 activation promotes invasive glioma formation in a tissue site-specific manner. *Cancer research,* **71,** 1115-1125.

Puertas-Avendano R.A., Gonzalez-Gomez M.J., Ruvira M.D., Ruiz-Hidalgo M.J., Morales-Delgado N., Laborda J., Diaz C. & Bello A.R. (2011) Role of the non-canonical notch ligand delta-like protein 1 in hormone-producing cells of the adult male mouse pituitary. *Journal of neuroendocrinology,* **23,** 849-859.

Raghunandan R., Ruiz-Hidalgo M., Jia Y., Ettinger R., Rudikoff E., Riggins P., Farnsworth R., Tesfaye A., Laborda J. & Bauer S.R. (2008) Dlk1 influences differentiation and function of B lymphocytes. *Stem cells and development,* **17,** 495-507.

Rand E. & Cedar H. (2003) Regulation of imprinting: A multi-tiered process. *Journal of cellular biochemistry,* **88,** 400-407.

Rebustini I.T. & Hoffman M.P. (2009) ECM and FGF-dependent assay of embryonic SMG epithelial morphogenesis: investigating growth factor/matrix regulation of gene expression during submandibular gland development. *Methods in molecular biology (Clifton, N.J.),* **522,** 319-330.

Redmond L., Oh S.R., Hicks C., Weinmaster G. & Ghosh A. (2000) Nuclear Notch1 signaling and the regulation of dendritic development. *Nature neuroscience,* **3,** 30-40.

Rivero S., Diaz-Guerra M.J., Monsalve E.M., Laborda J. & Garcia-Ramirez J.J. (2012) DLK2 is a transcriptional target of KLF4 in the early stages of adipogenesis. *Journal of Molecular Biology,* **417,** 36-50.

Rodriguez P., Higueras M.A., Gonzalez-Rajal A., Alfranca A., Fierro-Fernandez M., Garcia-Fernandez R.A., Ruiz-Hidalgo M.J., Monsalve M., Rodriguez-Pascual F., Redondo J.M., de la Pompa J.L., Laborda J. & Lamas S. (2012) The non-canonical NOTCH ligand DLK1 exhibits a novel vascular role as a strong inhibitor of angiogenesis. *Cardiovascular research,* **93,** 232-241.

Rose S.L. (2009) Notch signaling pathway in ovarian cancer. *International journal of gynecological cancer : official journal of the International Gynecological Cancer Society,* **19,** 564-566.

Ferron SR, Charalambous M, Radford E, McEwen K, Wildner H, Hind E, Morante-Redolat JM, Laborda J, Guillemot F, Bauer SR, Farinas I, Ferguson-Smith AC (2011) Postnatal loss of Dlk1 imprinting in stem cells and niche astrocytes regulates neurogenesis. *Nature*,**475**,381-385

Sanalkumar R., Indulekha C.L., Divya T.S., Divya M.S., Anto R.J., Vinod B., Vidyanand S., Jagatha B., Venugopal S. & James J. (2010) ATF2 maintains a subset of neural progenitors

through CBF1/Notch independent Hes-1 expression and synergistically activates the expression of Hes-1 in Notch-dependent neural progenitors. *Journal of neurochemistry,* **113,** 807-818.

Sanchez-Irizarry C., Carpenter A.C., Weng A.P., Pear W.S., Aster J.C. & Blacklow S.C. (2004) Notch subunit heterodimerization and prevention of ligand-independent proteolytic activation depend, respectively, on a novel domain and the LNR repeats. *Molecular and cellular biology,* **24,** 9265-9273.

Sanchez-Solana B., Nueda M.L., Ruvira M.D., Ruiz-Hidalgo M.J., Monsalve E.M., Rivero S., Garcia-Ramirez J.J., Diaz-Guerra M.J., Baladron V. & Laborda J. (2011) The EGF-like proteins DLK1 and DLK2 function as inhibitory non-canonical ligands of NOTCH1 receptor that modulate each other's activities. *Biochimica et biophysica acta,* **1813,** 1153-1164.

Schmidt J.V., Matteson P.G., Jones B.K., Guan X.J. & Tilghman S.M. (2000) The Dlk1 and Gtl2 genes are linked and reciprocally imprinted. *Genes & development,* **14,** 1997-2002.

Schmittgen T.D. & Livak K.J. (2008) Analyzing real-time PCR data by the comparative C(T) method. *Nature protocols,* **3,** 1101-1108.

Schwanbeck R., Schroeder T., Henning K., Kohlhof H., Rieber N., Erfurth M.L. & Just U. (2008) Notch signaling in embryonic and adult myelopoiesis. *Cells, tissues, organs,* **188,** 91-102.

Sestan N., Artavanis-Tsakonas S. & Rakic P. (1999) Contact-dependent inhibition of cortical neurite growth mediated by notch signaling. *Science (New York, N.Y.),* **286,** 741-746.

Shirasuna K., Sato M. & Miyazaki T. (1981) A neoplastic epithelial duct cell line established from an irradiated human salivary gland. *Cancer,* **48,** 745-752.

Smas C.M., Green D. & Sul H.S. (1994) Structural characterization and alternate splicing of the gene encoding the preadipocyte EGF-like protein pref-1. *Biochemistry,* **33,** 9257-9265.

Smas C.M., Chen L. & Sul H.S. (1997a) Cleavage of membrane-associated pref-1 generates a soluble inhibitor of adipocyte differentiation. *Molecular and cellular biology,* **17,** 977-988.

Smas C.M. & Sul H.S. (1997b) Molecular mechanisms of adipocyte differentiation and inhibitory action of pref-1. *Critical reviews in eukaryotic gene expression,* **7,** 281-298.

Szebenyi G. & Fallon J.F. (1999) Fibroblast growth factors as multifunctional signaling factors. *International review of cytology,* **185,** 45-106.

Takada S., Tevendale M., Baker J., Georgiades P., Campbell E., Freeman T., Johnson M.H., Paulsen M. & Ferguson-Smith A.C. (2000) Delta-like and gtl2 are reciprocally expressed, differentially methylated linked imprinted genes on mouse chromosome 12. *Current biology : CB,* **10,** 1135-1138.

Talora C., Campese A.F., Bellavia D., Felli M.P., Vacca A., Gulino A. & Screpanti I. (2008) Notch signaling and diseases: an evolutionary journey from a simple beginning to complex outcomes. *Biochimica et biophysica acta,* **1782,** 489-497.

Tanimizu N., Nishikawa M., Saito H., Tsujimura T. & Miyajima A. (2003) Isolation of hepatoblasts based on the expression of Dlk/Pref-1. *Journal of cell science,* **116,** 1775-1786.

Taylor M.K., Yeager K. & Morrison S.J. (2007) Physiological Notch signaling promotes gliogenesis in the developing peripheral and central nervous systems. *Development (Cambridge, England),* **134,** 2435-2447.

Teshima K., Murakami R., Tomitaka E., Nomura T., Toya R., Hiraki A., Nakayama H., Hirai T., Shinohara M., Oya N. & Yamashita Y. (2010) Radiation-induced parotid gland changes in oral cancer patients: correlation between parotid volume and saliva production. *Japanese journal of clinical oncology,* **40,** 42-46.

Tucker A.S. (2007) Salivary gland development. *Seminars in cell & developmental biology,* **18,** 237-244.

van Es J.H. & Clevers H. (2005) Notch and Wnt inhibitors as potential new drugs for intestinal neoplastic disease. *Trends in molecular medicine,* **11,** 496-502.

Vissink A., Kallenberg C.G. & Bootsma H. (2010) Treatment approaches in primary Sjogren syndrome. *Jama,* **304,** 2015-6; author reply 2016.

Wang Y. & Sul H.S. (2006) Ectodomain shedding of preadipocyte factor 1 (Pref-1) by tumor necrosis factor alpha converting enzyme (TACE) and inhibition of adipocyte differentiation. **26,** 5421-5435.

Wang Y., Zhao L., Smas C. & Sul H.S. (2010) Pref-1 interacts with fibronectin to inhibit adipocyte differentiation. *Molecular and cellular biology,* **30,** 3480-3492.

Weng A.P. & Aster J.C. (2004) Multiple niches for Notch in cancer: context is everything. *Current opinion in genetics & development,* **14,** 48-54.

Wilkins J.F. & Haig D. (2003) What good is genomic imprinting: the function of parent-specific gene expression. *Nature reviews.Genetics,* **4,** 359-368.

Woodhoo A., Alonso M.B., Droggiti A., Turmaine M., D'Antonio M., Parkinson D.B., Wilton D.K., Al-Shawi R., Simons P., Shen J., Guillemot F., Radtke F., Meijer D., Feltri M.L., Wrabetz L., Mirsky R. & Jessen K.R. (2009) Notch controls embryonic Schwann cell differentiation, postnatal myelination and adult plasticity. *Nature neuroscience,* **12,** 839-847.

Wu F., Stutzman A. & Mo Y.Y. (2007) Notch signaling and its role in breast cancer. *Frontiers in bioscience : a journal and virtual library,* **12,** 4370-4383.

Yamamoto N., Tanigaki K., Han H., Hiai H. & Honjo T. (2003) Notch/RBP-J signaling regulates epidermis/hair fate determination of hair follicular stem cells. *Current biology : CB,* **13,** 333-338.

Yanai H., Nakamura K., Hijioka S., Kamei A., Ikari T., Ishikawa Y., Shinozaki E., Mizunuma N., Hatake K. & Miyajima A. (2010) Dlk-1, a cell surface antigen on foetal hepatic stem/progenitor cells, is expressed in hepatocellular, colon, pancreas and breast carcinomas at a high frequency. *Journal of Biochemistry,* **148,** 85-92.

Yevtodiyenko A. & Schmidt J.V. (2006) Dlk1 expression marks developing endothelium and sites of branching morphogenesis in the mouse embryo and placenta. *Developmental dynamics : an official publication of the American Association of Anatomists,* **235,** 1115-1123.

Zhu X., Zhang J., Tollkuhn J., Ohsawa R., Bresnick E.H., Guillemot F., Kageyama R. & Rosenfeld M.G. (2006) Sustained Notch signaling in progenitors is required for sequential emergence of distinct cell lineages during organogenesis. *Genes & development,* **20,** 2739-2753.

8. ANNEX